SERUM AMYLOID A (SAA) AND CHOLESTEROL EFFLUX --- A MECHANISTIC STUDY

LI HONGZHE
(Bachelor of Medicine, Capital University of Medical Sciences)
(Master of Science, National University of Singapore)

A THESIS SUBMITTED
FOR THE DEGREE OF DOCTOR OF PHILOSOPHY
DEPARTMENT OF PAEDIATRICS
NATIONAL UNIVERSITY OF SINGAPORE

2011

ACKNOWLEDGEMENTS

This project was generously supported by the National Medical Research Council, Singapore (Grant NMRC/1155/2008). I would like to express my utmost gratitude to my supervisor, Prof. Heng Chew-Kiat, for his advice, support and invaluable mentoring of my scientific and personal development. I am very grateful for the opportunity to have worked with him for my dissertation. It has been my privilege to learn from him. He has been very patient and understanding as well as encouraging, guiding me through this wonderful journey of discovery and learning.

I gratefully acknowledge the precious comments and advices from Prof. Samuel S Chong, Prof. Lai Poh San and Prof. Teresa Tan.

Sincere gratitude also goes to Dr Zhang Yulan for her effort in initiating the project as well as her valuable suggestions in my postgraduate study. I would also like to express my utmost appreciation to all working under Prof. Hengôs group at one time or another, for their friendship, the camaraderie spirit and many stimulating and enjoyable lively discussions: Ms. Zhou Shuli, Ms. Karen Lee, Ms. Lye Hui Jen, Mr. Leow Koon Yeow, Ms. Goh June Mei, Ms. Yang Ennan, Ms. Tan Si Zhen and Ms. Ke Tingjing and many others.

A financial support from National University of Singapore is gratefully acknowledged.

This work is dedicated to my family and my dear friends for their continuous encouragement and support during my Ph.D study. Without their support, completing a PhD study would be a far-fetch dream for me. Words cannot express how much I

appreciate you for sparking my creativity in various aspects of my life and for just being around for me.

PUBLICATIONS

The major part of this work has been published in:

Serum Amyloid A Activates Peroxisome Proliferator-Activated Receptor ↄ through Extracellularly Regulated Kinase 1/2 and COX-2 Expression in Hepatocytes. **Hongzhe Li,** Yulan Zhao, Shuli Zhou and Chew-Kiat Heng. *Biochemistry* (2010) (In press)

Manuscript in preparation:

The role of NF-ϞB in SAA-induced PPARↄ activation. **Hongzhe Li** and Chew-Kiat Heng (2011)

SUMMARY

Coronary artery disease (CAD) is one of the leading causes of mortality in developed countries. It most often results from atherosclerosis, a progressive condition characterized by the accumulation of lipids and fibrous elements in the large arteries. Many inflammatory proteins are elevated in this process and correlated with future coronary events. One of such inflammatory proteins is serum amyloid A (SAA). SAA is an acute phase protein whose level of expression increases markedly during bacterial infection, tissue damage, and inflammation. The potential beneficial roles of SAA include its involvement in reverse cholesterol transport and possibly extracellular lipid deposition at sites of inflammation and tissue repair. It is an attractive therapeutic target for the treatment of atherosclerosis. Peroxisome proliferator-activated receptor ↄ (PPARↄ) plays a major regulatory role in adipogenesis and in the expression of genes involved in lipid metabolism. Activation of PPARↄ leads to multiple changes in gene expression, some of which are believed to be atherogenic while others are antiatherogenic. In this study, we investigated the effects of SAA on PPARↄ activation and its downstream target gene expression profiles in HepG2 cells. We demonstrated that SAA could activate PPARↄ transcriptional activity. Preincubation of HepG2 cells with SAA enhanced the efflux of cholesterol to HDL and apoA-I. In addition, SAA increased the level of intracellular 15-deoxy-ϕ^{12,14}-prostaglandin J_2 (15d-PGJ_2), which is a potent natural ligand for PPARↄ. Our data suggested that SAA activated PPARↄ through extracellular signal-regulated kinase 1/2 (ERK1/2) and NF-ϟB dependent COX-2 expression. Furthermore, SAA-induced cholesterol efflux was suppressed when the ERK1/2 pathway or COX-2 was inhibited. Overall, our study has established, for the first time, a relationship between

SAA and PPARↃ. Additionally, the data from our study has also provided new insights into the role of SAA in cholesterol efflux.

TABLE OF CONTENTS

	Page
ACKNOWLEDGEMENTS	1
PUBLICATIONS	3
SUMMARY	4
TABLE OF CONTENTS	6
LIST OF FIGURES	13
LIST OF TABLES	16
LIST OF ABBREVIATIONS	17
CHAPTER I INTRODUCTION	22
1.1 Coronary artery disease and atherosclerosis	23
1.2 Atherosclerosis development	23
1.3 Inflammatory factors in atherosclerosis	25
1.4 Serum amyloid A (SAA)	27
1.4.1 The SAA family	27
1.4.2 Structure of human SAA proteins	29
1.4.3 Expression and induction of SAA	30
1.4.4 Functions of SAA	32
1.4.4.1 Immune-related functions	33
1.4.4.2 Anti-inflammatory roles	33
1.4.4.3 SAA, amyloid A protein and amyloidosis	34
1.4.4.4 Lipid-related functions	35
1.4.5 Receptors for SAA	38

1.4.5.1 SR-BI 38

1.4.5.2 FPRL-1 39

1.4.5.3 RAGE 40

1.4.5.4 TLRs 40

1.4.5.5 TANIS 41

1.4.6 SAA and cardiovascular disease 42

1.5 Peroxisome proliferator-activated receptor ɔ (PPARɔ) 43

1.5.1 PPAR family 43

1.5.2 PPARɔ activation 45

1.5.3 Functions of PPARɔ 46

1.6 Mitogen-activated protein kinases (MAPKs) 50

1.6.1 General features and biological functions of MAPK 50

1.6.1.1 MAPK in cancer 51

1.6.1.2 MAPK in cell cycle 52

1.6.1.3 MAPK in apoptosis 53

1.6.2 SAA and MAPK 54

1.6.2.1 Endothelial cells 56

1.6.2.2 Monocytes 57

1.6.2.3 Fibroblasts 58

1.7 NF-ʏB 59

1.7.1 General features and biological functions of NF-HB 59

1.7.2 SAA and NF-ʏB 62

1.8 Reverse cholesterol transport 63

1.8.1 ABCA1-mediated cholesterol efflux 65

1.8.2 ABCG1-mediated cholesterol efflux 67

1.9 Objectives of the project 67

CHAPTER II MATERIALS AND METHODS 69

2.1 Materials 70

2.2 Routine cell line maintenance 72

2.2.1 Cells lines 72

2.2.2 Cells culture media 72

2.2.3 General cells culture procedures 73

2.3 SAA treatment 76

2.4 Measurement of endotoxin activity 77

2.5 RNA isolation 77

2.6 Quantitative real-time PCR (qRT-PCR) 78

2.7 Protein extraction 80

2.8 Membrane protein extraction 81

2.9 SDS-PAGE and Western blot 81

2.10 Nuclear protein extraction 83

2.11 Cholesterol efflux assay 84

2.12 PPARↃ activity assay 85

2.13 Electrophoretic mobility shift assay 86

2.14 Transfection and luciferase assay 87

2.15 EIA for 15d-PGJ_2 88

2.16 NF-ⱡB (p50) transcription factor assay 89

2.17 SAA-HDL association 89

2.18 siRNA mediated gene silencing 90

2.19 Bacterial work 92

2.19.1 Media 92

2.19.2 Competent cell preparation 92

2.19.3 Isolation of plasmid DNA from *E.coli* 93

2.19.3.1 Small scale preparation of plasmid DNA 93

2.19.3.2 Large scale preparation of plasmid DNA 93

2.20 Cloning 95

2.20.1 Cloning of SAA1 in the pcDNAÊ 3.1(+) vector 95

2.20.1.1 Reverse transcriptase-PCR and purification 95

2.20.1.2 Digestion 96

2.20.1.3 Gel purification 97

2.20.1.4 Ligation 97

2.20.1.5 Transformation 98

2.20.1.6 Selection and DNA sequencing 98

2.20.2 Other subclonings 99

2.20.2.1 Generation of pcDNA3.1-SAA1-NLS 99

2.20.2.2 Generation of pcDNA3.1-SAA1-G8D 99

2.20.2.3 Generation of pcDNA3.1-SAA1φ1-11 99

2.20.2.4 Generation of pcDNA3.1-PPARɔ 100

2.21 Plasmid DNA transfection 100

2.22 Detection of SAA secretion 100

2.23 Statistical analysis 101

CHAPTER III RESULTS 102

3.1 SAA activates peroxisome proliferator-activated receptor ↄ through extracellular-regulated kinase 1/2 and COX-2 expression in hepatocytes 103

3.1.1 SAA induces PPARↄ and its target genes expression in HepG2 cells 103

3.1.2 SAA facilitates cholesterol efflux in HepG2 105

3.1.3 SAA enhances PPARↄ activativity in HepG2 108

3.1.4 SAA-induced PPARↄ activation is suppressed by HDL 113

3.1.5 *De novo* protein synthesis is required for the SAA-induced PPARↄactivation 114

3.1.6 SAA-induced PPARↄ activation and cholesterol efflux in HepG2 is partially mediated by SR-BI 116

3.1.7 SAA increases intracellular 15d-PGJ_2 level 118

3.1.8 SAA induces COX-2 expression 119

3.1.9 SAA-induced PPARↄ activation is mediated by ERK1/2 dependent COX-2 expression 121

3.1.10 AA has the same PPARↄ activation effect in HCAEC and THP-1 cell lines 125

3.2 SAA activates PPARↄ through FPRL1 and TLRs-mediated NF-ϞB activation 126

3.2.1 SAA stimulates NF-ϞB activity 126

3.2.2 SAA-induced COX-2 expression and PPARɔ activation is through NF-ʏB pathway 129
3.2.3 SAA-induced PPARɔ activation is completely blocked by the combination of ERK1/2 and NF-ʏB inhibitors 132
3.2.4 SAA-induced NF-ʏB activation is suppressed by HDL 132
3.3 SAA-induced effects are mediated by different receptors 134
3.3.1 FPRL-1 and TLR4 are involved in SAA-induced PPARɔ and NF-ʏB activation 134
3.3.2 SAA- enhanced cholesterol efflux is partially through SR-BI 136
3.3.3 NF-ʏB and PPARɔ activation via FPRL-1 is SAA-selective 138
3.4 The N-terminal is essential for SAA protein expression, secretion and cholesterol efflux 139
3.4.1 mutSAA protein expression and secretion are impaired in HEK293 cells 139
3.4.2 Cholesterol efflux is impaired in HEK293 cells transfected with mutSAA constructs 142
3.4.3 PPARɔ activity is impaired in HEK293 cells transfected with mutSAA constructs 143
CHAPTER IV DISCUSSION 144
4.1 SAA induces PPARɔ activation 146
4.2 SAA induces the expression of ABCA1, ABCG1 and enhances cholesterol efflux 149
4.3 The effect of SAA is not due to bacterial contamination in recombinant

SAA protein 151

4.4 Lipid--free SAA and HDL-conjugated SAA have different effects 152

4.5 SAA induces COX-2 expression and subsequently increases the intracellular 15d-PGJ_2 level 154

4.6 SAA-induced COX-2 expression could be mediated through ERK1/2 and NF-ϞB 156

4.7 The receptors involved in SAA-induced effects 158

4.8 The essential role of N-terminal SAA in protein expression, secretion, cholesterol efflux and PPARↃ activation 161

CHAPTER V CONCLUSIONS AND FUTURE WORK 165

5.1 Main findings 166

5.2 Summary of major contributions of this study 166

5.3 Suggestions for future work 167

CHAPTER VI REFERENCES 169

LIST OF FIGURES

Figure No.		Page
1.	Schematic representation of the atherosclerotic lesion development.	25
2.	The structure of human SAA protein.	30
3.	Induction of SAA during the acute-phase response.	32
4.	Classical structure of PPAR with the zinc fingers which interact with specific response elements located in the target genes.	44
5.	Regulation of cholesterol efflux pathways in macrophages by PPARɔ and LXRŬ. LXRŬagonists stimulate the expression of ABCA1, which facilitates the efflux of cholesterol to lipid-poor apolipoprotein A-I (apoA-I), and ABCG1, which facilitates the efflux of cholesterol to HDL.	49
6.	Model of the generic NF-ʕB activation pathway.	61
7.	Mechanisms of cholesterol efflux from the arterial wall.	65
8.	Figure 8. Map of pcDNAÊ 3.1(+).	96
9.	SAA induces PPARɔ, LXRŬ, ABCA1 and ABCG1 gene expression in HepG2 cells.	103
10.	SAA facilitates cholesterol efflux in HepG2 cells.	105
11.	SAA-facilitated cholesterol efflux in HepG2 cells was mediated by ABCA1 and ABCG1.	107
12.	SAA enhances PPARɔ activation and SAA-induced PPARɔ target genes expressions are inhibited by PPARɔ antagonist.	110
13.	SAA-induced PPARɔ activity is suppressed in the presence of HDL.	113

14. *De novo* protein synthesis is required for the SAA-induced PPARɔ activation. 115
15. SAA-induced PPARɔ activation and cholesterol efflux in HepG2 is partially mediated by SR-BI. 117
16. SAA induces intracellular 15d-PGJ_2 in HepG2. 119
17. SAA-induced COX-2 gene expression is involved in PPARɔ activation in HepG2 cells. 120
18. SAA-induced PPAR activation is mediated by ERK1/2. 122
19. SAA enhances PPARɔ activity in HCAEC and THP-1 cell lines. 126
20. SAA stimulates NF-ʕB activation. 128
21. SAA-induced COX-2 expression and PPARɔ activation is through NF-ʕB pathway. 130
22. SAA-induced PPARɔ activation is completely blocked by the combination of ERK1/2 and NF-ʕB inhibitors. 132
23. SAA-induced NF-ʕB activity is inhibited by HDL association. 133
24. FPRL-1 and TLR4 are involved in SAA-mediated effects. 135
25. SAA-enhanced cholesterol efflux is partially through SR-BI. 137
26. NF-ʕB and PPARɔ activation via FPRL-1 is SAA-selective. 138
27. The SAA mRNA levels are similar after transfection with different constructs. 140
28. Cholesterol efflux is impaired in HEK293 cells transfected with mutSAA constructs. 142
29. PPARɔ activity is impaired in HEK293 cells transfected with mutSAA

constructs. 143

30. Schematic diagram of the proposed mechanism of cholesterol efflux through SAA-induced PPARↃ activation of its target genes. 146

LIST OF TABLES

Table No.		Page
1.	SAA-induced signaling and cellular responses	55
2.	Characteristics of the inhibitors mentioned in Table 1	56
3.	Cell lines used in this study	72
4.	Primer sequences for qRT-PCR analysis	79
5.	Compositions of SDS-PAGE	82
6.	siRNA sequences for gene silencing	90
7.	ELISA measurement of SAA in transfected HEK293 cells	141

LIST OF ABBREVIATIONS

15d-PGJ_2	15-deoxy-$\Delta^{12,14}$-prostaglandin J_2
AA	arachidonic acid
ABCA1	ATP-binding cassette, sub-family A (ABCA), member 1
ABCG1	ATP-binding cassette, sub-family G (ABCG), member 1
ACAT	acyl-CoA cholesteryl acyl transferase
AMI	acute myocardial infarction
Amp	ampicillin
AP-1	activator protein 1
APP	acute phase protein
apo	apolipoprotein
BAY 11-7082	(E)-3-(4-Methylphenylsulfonyl)-2-propenenitrile
CAD	coronary artery disease
CAM	cellular adhesion molecule
CLA-1	CD36 and LIMPII analogous-1
CMV	Cytomegalovirus
COX-2	cyclooxygenase-2
CRP	C-reactive protein
CSF	colony stimulating factor
DMSO	dimethyl sulfoxide
DTT	1,4-Dithiothreitol
EC	endothelial cell

ECM	extracellular matrix
EDTA	ethylene diamine tetra-acetic acid
EGFR	epidermal growth factor receptor
EIA	enzyme immunoassay
ELISA	enzyme-linked immunosorbent assay
EMSA	electrophoretic mobility shift assay
ERK1/2	p44/42 MAP kinase
E-selectin	endothelial cell-derived selectin
EU	endotoxin unit
FBS	fetal bovine serum
FCS	fetal calf serum
FGF	fibroblast growth factor
FPRL-1	formyl peptide receptor like 1
GAPDH	glyceraldehydes-3-phosphate dehydrogenase
GPCR	G-protein coupled receptor
HCAEC	human coronary artery endothelial cell
HDL	high density lipoprotein
HEK	human embryonic kidney
HRP	horseradish peroxidase
HUVEC	human umbilical vein endothelial cell
ICAM	intercellular adhesion molecule 1
IKK	IŁB kinase
IL	interleukin

IϞB	inhibitor of NF-ϞB
JNK	c-jun terminal NH_2 kinase
LB	Luria Broth
LCAT	lecithin-cholesterol acyltransferase
LDL	low density lipoprotein
LDLR	low density lipoprotein receptor
LPS	lipopolysaccharide
LXR	liver X receptor
MAPK	mitogen-activated protein kinase
MCP-1	monocyte chemotactic protein 1
MMP	matrix metalloproteinsease
MSK	mitogen- and stress-activated protein kinase
nCEH	neutral cholesterol ester hydrolase
NF-ϞB	nuclear factor kappa B or nuclear factor of kappa light polypeptide gene
NO	nitric oxide
NS-398	N-[2-(Cyclohexyloxy)-4-nitrophenyl]methanesulfonamide (NS-398)
p38	p38 MAP kinase
PBS	phosphate buffered saline
PCR	polymerase chain reaction
PD98059	2-(2-Amino-3-methoxyphenyl)-4H-1-benzopyran-4-one
PDGF	platelet-derived growth factor
PECAM-1	platelet-endothelial-cell adhesion molecule 1
PG	prostaglandin

PMB	polymyxin B
PPAR	peroxisome proliferator-activated receptor
PPRE	peroxisome proliferators response element
PTX	pertussis toxin
qRT-PCR	quantitative real-time polymerase chain reaction
RAGE	receptor for advanced glycation end products
ROS	reactive oxygen species
RXR	retinoid X receptor
SAA	serum amyloid A
SAF	SAA-activating factor
SDS	sodium dodecyl sulphate
siRNA	synthetic interfering RNA
SMC	smooth muscle cell
$sPLA_2$-IIa	group-IIa secretory phospholipase A_2
SR-BI	scavenger receptor class B type I
T0070907	2-Chloro-5-nitro-N-4-pyridinyl-benzamide
TBS	tris-buffered saline
TdT	terminal deoxynucleotidyl transferase
TEMED	tetramethylethylenediamine
TF	tissue factor
TFPI	tissue factor pathway inhibitor
TGF	transforming growth factor
TLR	toll-like receptor

TNFŬ	tumor necrosis factor-alpha
TXA_2	thromboxane A_2
TZD	thiazolidinedione
VCAM-1	vascular cell adhesion molecule 1
VEGF	vascular endothelial growth factor

CHAPTER I

INTRODUCTION

1.1 CORONARY ARTERY DISEASE AND ATHEROSCLEROSIS

Coronary arteries deliver oxygen-rich blood to the myocardium. Coronary artery disease (CAD) is the end result of the accumulation of atheromatous plaques within the walls of the coronary arteries that supply the myocardium with oxygen and nutrients. It is sometimes also called coronary heart disease (CHD). CAD is the most common form of heart disease. It is one of the leading causes of mortality in developed countries [1]. It most often results from atherosclerosis, a progressive condition characterized by the accumulation of lipids and fibrous elements in the large arteries.

1.2 ATHEROSCLEROSIS DEVELOPMENT

Our views of the pathophysiology of atherosclerosis have evolved substantially over the past century. The link between lipids and atherosclerosis dominated our thinking based on strong experimental and clinical relationships between hypercholesterolaemia and atheroma [2]. More recently, a prominent role of inflammation was discovered for the development of atherosclerosis and its complications [3-5]. In fact, the lesions of atherosclerosis represent a series of highly specific cellular and molecular responses that can best be described, in aggregate, as an inflammatory disease [6].

The earliest changes that precede the formation of lesions of atherosclerosis take place in the endothelium. These changes include increased endothelial permeability to lipoproteins and other plasma constituents, up-regulation of leukocyte adhesion molecules, up-regulation of endothelial adhesion molecules, and migration of leukocytes into the artery wall (Fig. 1a). Then the fatty streaks start to build up in the arteries. Fatty

streaks initially consist of lipid ï laden monocytes and macrophages (foam cells) together with T lymphocytes. Later they are joined by various numbers of smooth-muscle cells (Fig. 1b). The steps involved in this process include smooth-muscle migration, T-cell activation, foam cell formation, and platelet adherence and aggregation. As fatty streaks progress to intermediate and advanced lesions, they tend to form a fibrous cap that walls off the lesion from the lumen (Fig. 1c). This represents a type of healing or fibrous response to the injury. The fibrous cap covers a mixture of leukocytes, lipid, and debris, which may form a necrotic core. Continuing influx and activation of macrophages could increase metalloproteinases and other proteolytic enzymes at the advanced lesion, which results in the thinning of the fibrous cap (Fig. 1d). Finally, rupture of the fibrous cap can rapidly lead to thrombosis and occlusion of the artery. It usually occurs at sites of thinning of the fibrous cap that covers the advanced lesion.

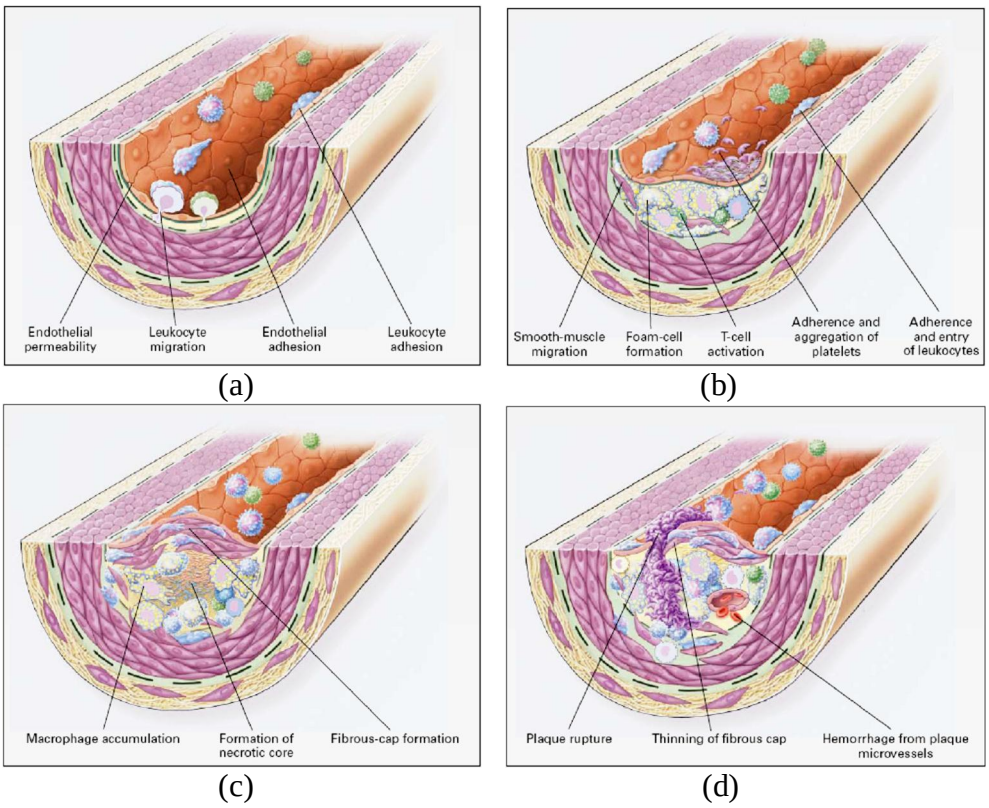

Figure 1. Schematic representation of the atherosclerotic lesion development.
(a) Endothelial dysfunction in atherosclerosis. (b) Fatty-streak formation in atherosclerosis. (c) Formation of an advanced, complicated lesion of atherosclerosis. (d) Unstable fibrous plaques in atherosclerosis (Adapted from Ref. [3]).

1.3 INFLAMMATORY FACTORS IN ATHEROSCLEROSIS

In the past decades, an increasing number of inflammatory factors were revealed to play a role in atherosclerosis [7]. The effectors of the immune system are involved directly in all stages of atherogenesis [3]. Endothelial dysfunction takes place before the formation of lesions of atherosclerosis. The endothelial permeability is increased, which is mediated by nitric oxide (NO), prostacyclin, platelet-derived growth factor (PDGF), angiotension II, and endothelin. The leukocyte adhesion molecules are up-regulated, including L-selectin, integrins, and platelet-endothelial-cell adhesion molecule 1 (PECAM-1). The endothelium-derived cellular adhesion molecules (CAMs) are also up-

regulated, which include endothelial cell-derived selectin (E-selectin), intercellular adhesion molecule 1 (ICAM-1), and vascular-cell adhesion molecule 1 (VCAM-1). The leukocytes finally enter into the artery wall, which is mediated by oxidized low density lipoprotein (ox-LDL), monocyte chemotactic protein 1 (MCP-1), interleukin-8 (IL-8), PDGF, macrophage colony-stimulating factor (CSF), and osteopontin. Subsequently, fatty streaks begin to build up, which is mediated by PDGF, fibroblast growth factor 2 (FGF-2), transforming growth factor ß (TGF-ß). T-cell activation is mediated by tumor necrosis factor Ŭ (TNFŬ), interleukin-1 (IL-1), interleukin-2 (IL-2), and granulocyte-macrophage CSF. Foam cell formation is mediated by ox-LDL, macrophage CSF, TNFŬ, and IL-1. Platelet adherence and aggregation are stimulated by integrins, P-selectin, fibrin, thromboxane A_2 (TXA_2), and tissue factor (TF). As fatty streaks progress to advanced lesion, the principal factors associated with macrophage accumulation include macrophage CSF, monocyte chemotactic protein 1 (MCP-1), and ox-LDL. Thinning of the fibrous cap is apparently due to matrix metalloproteinsease (MMPs) and other proteolytic enzymes released from vaso-related cells at these sites. These enzymes can cause matrix degradation and plaque rupture, and eventually result in acute coronary events.

Histological studies have shown immune cells accumulating in the atherosclerotic lesions, including monocuclear phagocytes, lymphocytes and mast cells. Inflammatory proteins such as cytokines, chemokines, adhesion molecules, and acute phase proteins have been found to be highly expressed in atheroma as well. In addition, many inflammatory proteins have also been shown to be elevated in CAD [8]. The Womenôs Health Study showed that 4 inflammatory markers, C-reactive protein (CRP), serum

amyloid A (SAA), IL-6 and ICAM-1, were significant predictors of CAD risk [9, 10]. Among them, CRP and SAA were the strongest predictors of CAD risk. Interestingly, both CRP and SAA are major acute phase proteins which can be induced 100-1000 folds during acute phase responses.

In vitro studies have shown that CRP activates the entire recruitment cascade of white blood cells via inducing the release of ICAM-1, VACM-1, selectin E, and MCP-1 [11, 12]. In such a case, endothelium enters into a ñproinflammatoryò state and initiates atherogenesis. In another study, CRP was implicated in endothelial dysfunction, characterized by impaired NO production and vasoreactivity [13]. In addition, CRP could also induce TF expression which is the key molecule in the coagulation cascade [14]. Furthermore, CRP was recently reported to induce MMP-1 and MMP-10 which could cause plaque instability [15]. To date, CRP is accepted as a direct risk factor of CAD because of its wide effects on atherogenesis. As another acute phase protein, SAA shares many characters with CRP. Both of them could be highly induced under inflammatory stimuli and in acute myocardial infarction (AMI) patients [9]. However, compared to CRP, SAA was less studied, especially its effects in atherosclerosis.

1.4 SERUM AMYLOID A (SAA)

1.4.1 The SAA family

The serum amyloid A (SAA) family is known to contain a number of differentially expressed apolipoproteins which are synthesized primarily by the liver and can be divided into two main classes based on their responsiveness to inflammatory stimuli. Acute-phase serum amyloid A (A-SAA) is the archetypal vertebrate major acute

phase protein (APP). Acute-phase proteins are a class of proteins whose plasma concentrations increase (positive acute-phase proteins) or decrease (negative acute-phase proteins) by at lease 25 percent in response to inflammation [16]. A-SAA is induced from resting levels by more than 1000-folds during bacterial infection, tissue damage and inflammation. The plasma concentration of A-SAA can exceed 1 mg/ml [17-19]. Constitutive SAA (C-SAA) has been described in two species, human [20] and mouse [21]. Unlike the A-SAAs, the C-SAAs are at most minimally induced during the acute-phase response. Multiple SAA genes and proteins have been described for several mammalian species including human, mouse, hamster, rabbit, dog, mink, cow, sheep and horse [22-24]. The high degree of conservation of the SAA genes and proteins implies that they are likely to have important biological functions.

The human SAA family comprises four members, which have been subject to the most comprehensive analyses. The human SAA1 and SAA2 genes encode A-SAAs. These two genes have almost identical sequences and organizations, suggesting that the A-SAA genes have been subjected to recent gene conversion (i.e. homogenizing) events within each evolutionary lineage [22]. They are coordinately induced during the acute-phase response and their mature protein sequences share greater than 90% identity. Among the two human A-SAAs, SAA1 is the dominant isotype, which consists of at least five allelic variants, while less have been reported for SAA2 [25]. The human SAA3 gene is a pseudogene because of a single base insertion in exon 3 which produces a frameshift and, consequently, generates a down-stream stop signal at codon 43 [26, 27]. No mRNA or protein product specified by human SAA3 has been identified. The human SAA4 gene is the only constitutively expressed gene in human SAA family. The human SAA4

protein sequence shares only 53% and 55% identities with human SAA1 and SAA2, establishing that the C-SAA constitute a distinct branch of the SAA family.

1.4.2 Structure of human SAA proteins

All of the SAA genes described to date share a four-exon three-intron organization which is characteristic of many other apolipoproteins [28]. The mature SAA proteins range in size from 104 to 112 amino acids and are derived from primary translation products with 18-amino acid leader peptides (Fig. 2). Early work based on predictive methods suggested that SAA is likely to contain two regions of Ǔ helix and ɓ-sheet [29]. In addition, several regions of mammalian A-SAA proteins that are important in facilitating the beneficial roles of SAA during inflammation have been identified. *In vitro* study indicated that the amyloidogenic region is within the first 10-15 N-terminal amino acids [30]. The lipid binding region of SAA resides within the first 11 N-terminal amino acids [31]. The region between residues 29 and 42 is the extracellular matrix (ECM)-like binding region, which suggests a role of SAA in inhibiting immune cell migration towards inflammatory sites and, perhaps, metastatic processes *in vivo* [32]. Evidence of A-SAA involvement in platelet aggregation is provided by its modulation of the induction of prostaglandin I_2 (PGI_2), a potent antiaggregation agent; this is mediated by the first 14 N-terminal amino acids of SAA [33]. A putative calcium-binding sequence, GPGG, between residues 48 and 51, is conserved in all SAA sequences identified to date [29]. Although relatively few functional studies of the C-terminus of SAA have been performed, there is evidence that it may facilitate binding to neutrophils [34].

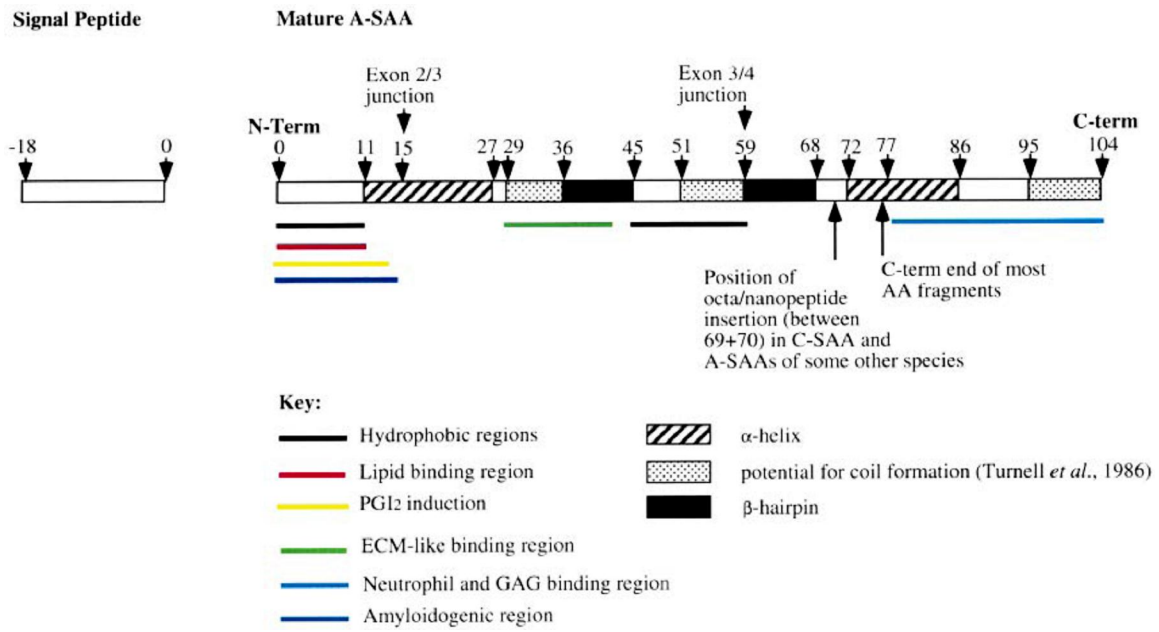

Figure 2. The structure of human SAA protein. The 18-amino acid signal peptide is shown (-18 to 0) together with the 104 mature protein (1-104). The most frequently observed C-terminus of the amyloid A protein is indicated at residue 76. Regions of potential functional importance are indicated by underlining in color, while structurally important regions are indicated by shading/hatching; both are discussed in the text. Sites delimiting sequences encoded by exons 2/3 and 3/4 are indicated (exon 1 contains only 5ô untranslated region) (Adapted from Ref. [35]).

1.4.3 Expression and induction of SAA

SAA is mainly synthesized in the liver following inflammatory stimuli, although induction of SAA synthesis has also been reported in adipocytes, intestinal epithelial cells, myocytes and macrophages [36-39]. Within the first 24 to 36 hours after infection or injury, the blood concentration of SAA can increase by as much as 1000-fold over basal level, reaching a concentration of 80 µM or 1 mg/ml [40]. SAA is also catabolized in the liver [41], has a much shorter half-life of 1 day [42] and is cleared from the plasma more rapidly than other high density lipoprotein (HDL) apoproteins such as apolipoprotein A-I (ApoA-I) which has a half-life of 4-6 days [43, 44]. During an acute-phase response or chronic inflammation, the capacity of the liver to degrade SAA

decreases, by 14% and 31% respectively [45], thereby contributing to the elevated circulating SAA levels observed under these conditions.

SAA mRNA and protein synthesis are induced *in vivo* during the inflammatory response to challenges such as tissue injury, infection and trauma in all vertebrate species (Fig. 3). These challenges induce the pro-inflammatory cytokine cascade. Expression of SAA is primarily regulated at the transcriptional level. Cytokines such as IL-1, IL-6, and tumor-necrosis factor Ŭ (TNFŬ), alone or in combination, act by binding to their respective receptors. As a consequence, induction of a series of transcription factors (CCAAT/enhancer binding proteins, NF-ʏB, and SAF-1), either by activation of resident pools of inactive factors in the cytoplasma and/or by increased factor biosynthesis, occurs. Alternatively, post-transcriptional regulation of human SAA genes has been reported [36]. Glucocorticoids, which are also released during inflammation, have been shown to enhance cytokine-induced SAA expression in several studies [46-48].

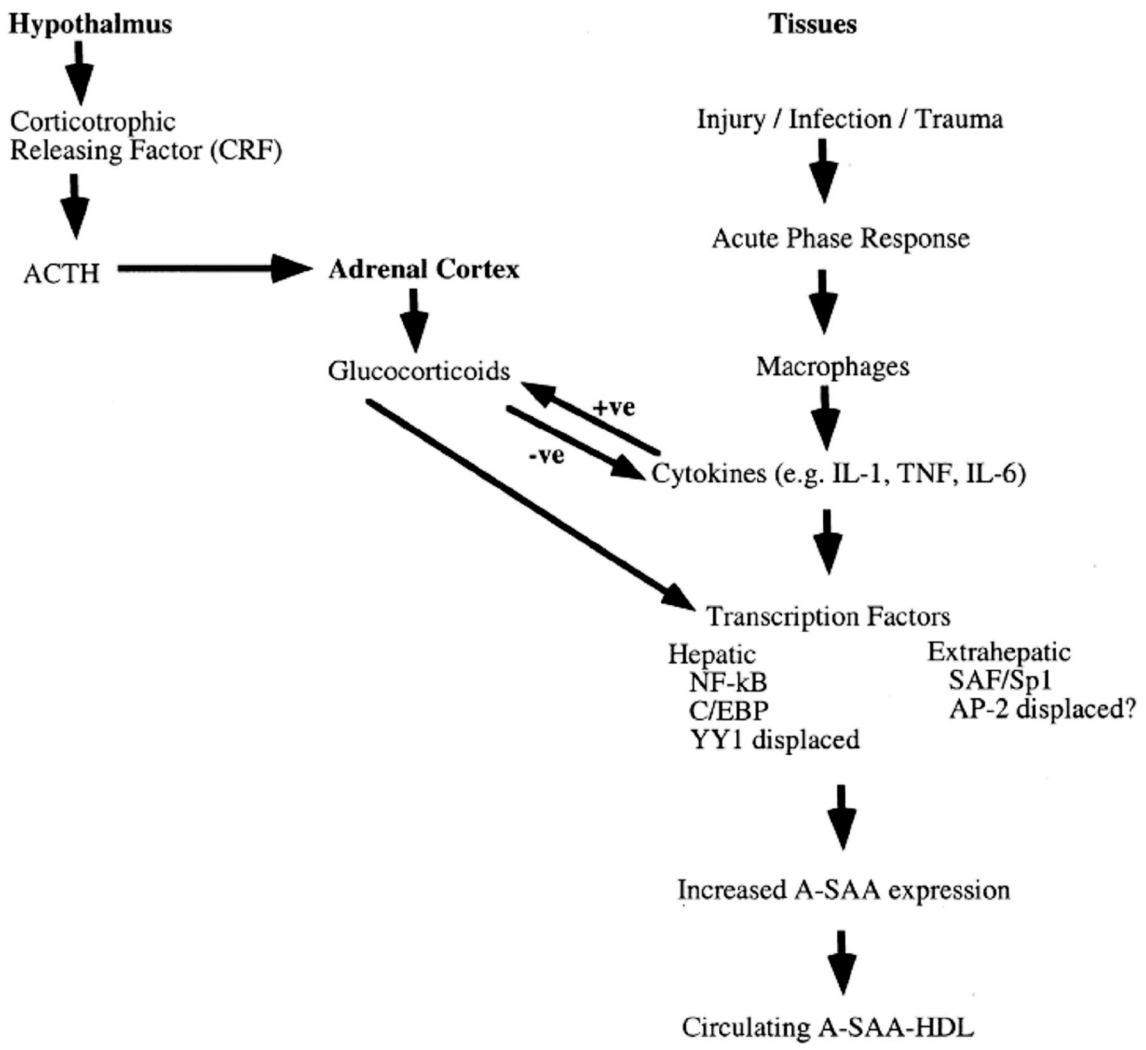

Figure 3. Induction of SAA during the acute-phase response. The flow diagram represents the induction of the acute-phase response in tissues by inflammatory stimuli leading to recruitment of macrophages and subsequent cytokine production. These cause changes in transcription factor availability in different tissues which result in increased SAA expression and consequently increased protein concentrations. The production of glucocorticoids by the adrenal cortex is upregulated by inflammatory cytokines and enhances SAA synthesis. ACTH, corticotropin (Adapted from Ref. [35]).

1.4.4 Functions of SAA

The SAA proteins have been highly conserved through evolution [22-24], and this, together with the dramatic induction of SAA expression in response to potentially

life-threatening physiological challenges, indicates a critical protective role in the acute-phase response.

1.4.4.1 Immune-related functions

SAA has been reported to induce ECM-degrading enzymes, such as collagenase, stromelysin, matrix metalloproteinases 2 and 3. These proteins are important for repair processes after tissue damage [49-51]. However, prolonged expression of SAA, and the consequent long-term production of these enzymes, may contribute to degenerative diseases such as rheumatoid arthritis. *In vivo* studies have provided convincing evidence that SAA can act as a chemoattractant for immune cells such as monocytes, polymorphonuclear leukocytes, mast cells and T lymphocytes [52-56]. If SAA has this property *in vivo*, its local production would result in the active recruitment of these cell types to inflammatory sites and the augmentation of local inflammation. Furthermore, several studies have reported induced expression and secretion of pro-inflammatory cytokines by SAA [55, 57]. Taken together, the above suggest that SAA may have cytokine-like properties.

1.4.4.2 Anti-inflammatory roles

During an acute phase response, SAA constitutes 2.5% of the total protein produced in liver, and its plasma levels could be increased by as much as 1000- fold over the basal level, suggesting a beneficial role of SAA in host defense. SAA was implicated in the suppression of *in vitro* immune responses to antigens by affecting T cell-macrophage interactions and helper T lymphocyte function [58-60]. Human SAA was

subsequently found to be a potent inhibitor of lymphocyte, HeLa and MRC5 cell function [61]. A potential feedback relationship between SAA and immunoregulatory cytokines was proposed based on the observation that SAA inhibits IL-1-induced and TNF-induced fever in mice [62]. Platelet aggregation has also been reported to be inhibited by SAA [63, 64]. SAA modestly induces prostaglandin I_2 which is also an anti-aggregation agent [33]. As both platelets and the range of mediators released by them upon activation are involved in inflammatory and thrombotic processes, these findings suggest that SAA may act to down-regulate such pro-inflammatory events during the acute-phase response. SAA has also been reported to bind to neutrophils and, like other apolipoproteins such as ApoA-I, inhibit the oxidative burst response, suggesting that it may help prevent oxidative tissue damage during inflammation [65, 66].

1.4.4.3 SAA, amyloid A protein and amyloidosis

SAA is the serum precursor of amyloid A protein [67, 68], which is the principal component of the amyloid deposits found in the heterogeneous group of disorders, the amyloid A amyloidosis [69]. The predominant amyloid A protein type found in amyloidotic tissues corresponds to the N-terminal two thirds of SAA, the first 76 residues of mature human SAA [67]. However, both smaller and larger amyloid A protein types, 45-95 residues, have also been found [70-73]. Multiple proteolytic cleavage events could be involved in the processing of SAA as it appears to be degraded first into an intermediate product with the same size and antigenic properties as amyloid A protein and is subsequently processed further. Amyloid A amyloidosis may therefore be the result of the incomplete digestion, and consequent accumulation, of amyloidogenic

intermediate peptides of SAA. A large number of cell-associated and serum proteases have been implicated in the degradation of SAA, which include serum serine proteases, elastase, collagenase, stromelysin and cathepsin B, D, G [74-79]. SAA is probably degraded after its disassociation from HDL, as full-length SAA can be found in amyloid fibrils [80-82]. Furthermore, lipid-free SAA can be degraded *in vitro* to form fibris [83]. In addition, SAA degradation *in vivo* is inhibited by lipoproteins, in particular HDL [41, 74], and different plasma clearance rates of SAA and ApoA-I also suggest that SAA is not associated with HDL when it is degraded [44, 74].

1.4.4.4 Lipid-related functions

SAA exists predominantly in the plasma HDL fraction (>90%) [84], which is the class of lipoproteins particles that play an important role in the prevention of atherosclerosis by both mediating reverse cholesterol transport and inhibiting the lipid (LDL) oxidation that promotes foam cell formation [84, 85]. As a result, the association of SAA with HDL during acute inflammation may alter HDL metabolism and cholesterol transport and promote a pro-atherogenic phenotype [86-88]. Several enzymes involved in cholesterol metabolism, including lecithin-cholesterol acyltransferase (LCAT), group-IIa secretory phospholipase A_2 ($sPLA_2$-IIa) and neutral cholesterol ester hydrolase (nCEH), are affected by induction of SAA during the acute-phase response. Under normal physiologic conditions, ApoA-I is the main apolipoprotein of HDL [89]. However, during the acute-phase response, SAA becomes the major HDL-associated apolipoprotein and the particle becomes depleted of ApoA-I [90]. As HDL is the site of cholesterol esterification which occurs through the action of LCAT, which in turn, requires ApoA-I

as an activating cofactor [91]. The relative lack of ApoA-I on SAA-enriched HDL (acute-phase HDL) during inflammation may account for the positive correlation observed between plasma SAA and unesterified cholesterol levels, and the negative correlation with LCAT activity [88]. $sPLA_2$ is made by vascular smooth muscle cells [92] and is also found in human atherosclerotic lesions [93]. Human acute-phase HDL (SAA-enriched HDL) was found to be two to three folds more susceptible to hydrolysis by $sPLA_2$ than normal HDL [94]. Furthermore, SAA enhances the activity of $sPLA_2$ [95] and overexpression of $sPLA_2$ in transgenic mice can suppress HDL levels by 30% [96]. Consequently, the enhanced hydrolysis of acute-phase HDL by $sPLA_2$ appears to be mediated by SAA itself.

Two main hypotheses have been proposed regarding the role of SAA in modulating cholesterol transport during inflammation based on the experimental data. SAA, as part of HDL, substantially increases the binding affinity of HDL for macrophages. Macrophages from animals with inflammation had a 5-fold increase in the number of binding sites for HDL/SAA relative to macrophages obtained from normal mice [86]. These observations suggest that SAA alters reverse cholesterol transport to allow delivery of lipid, particularly cholesterol, via HDL to peripheral cells that may have an increased requirement for cholesterol to facilitate tissue regeneration at inflammatory sites. On the other hand, SAA enhances the uptake of HDL/SAA by macrophages [97] and rapidly prompts the export of cellular cholesterol from macrophages laden with cholesterol [98, 99]. At sites of tissue injury, macrophages are cholesterol-laden because they would have ingested cell membrane debris, which is rich in cholesterol [100]. Thus,

SAA is indicated to facilitate removal of the large quantities of cholesterol liberated at sites of tissue damage during inflammation.

The ability of SAA to promote cholesterol efflux resides in SAA and not in other apolipoproteins [98, 99, 101, 102]. Increased efflux appears to result from the ability of SAA, or peptides derived from SAA, to regulate the intracellular activities of both acylCoA:cholesterol acyl transferase (ACAT) and neutral cholesterol esterase (CEH) [98, 99]. ACAT esterifies cholesterol for storage and CEH de-esterifies cholesterol for export. SAA inhibits ACAT and enhances CEH activities, thereby driving the balance from stored to transportable free cholesterol. Regulation of ACAT and CEH by SAA was also observed in postnuclear homogenates and with purified pancreatic neutral CEH, indicating SAA or SAA peptides act directly within cells and not through a cell signaling pathway [101, 102]. SAA has also been shown to promote cholesterol as well as phospholipids efflux in an ABCA1-dependent manner [103]. Lipid-poor or lipid-free apolipoproteins function as cholesterol acceptors for ABCA1-dependent efflux in a manner requiring their binding to cells, probably through direct interactions with ABCA1, which initiates cholesterol efflux [104]. It is thus likely that in ABCA1-dependent cholesterol efflux, SAA functions similarly to other apolipoprotein acceptors that contain amphipathic helices, which are thought to be crucial for acceptor function. Thus, SAA may enhance cholesterol efflux both by functioning as an acceptor and increasing the availability of cellular free cholesterol.

1.4.5 Receptors for SAA

The mechanisms responsible for SAA-induced effects require SAA uptake into cells. SAA uptake into macrophages and a slow delivery to lysosomes has been described but the uptake mechanisms and receptors involved have not been defined [105, 106]. Several potential receptors for SAA have been postulated, including scavenger receptor B-I (SR-BI) and its human orthologue CLA-1, receptor for advanced glycation end products (RAGE), formyl peptide receptor-like 1(FPRL-1), toll-like receptors (TLRs) and hepatic expressed Tanis receptor.

1.4.5.1 SR-BI

Scavenger receptor SR-BI, is an HDL receptor that mediates cellular uptake of cholesterol ester from HDL by a mechanism known as selective lipid uptake [107, 108]. SR-BI-dependent selective lipid uptake in the liver plays a key role in HDL cholesterol clearance, thereby facilitating reverse cholesterol transport from the periphery cells to the liver. The receptor exhibits a broad ligand binding specificity and binds low density lipoprotein, very low density lipoprotein, and oxidized lipoproteins in addition to HDL [108]. SR-BI also binds anionic phospholipids as well as the apolipoproteins A-I, A-II, C-III, and E, either as lipid-bound or as free apolipoproteins. In addition to mediating selective uptake, SR-BI facilitates the efflux of cellular free cholesterol to HDL. It has been reported that SAA is a high affinity ligand for SR-BI that exerts an inhibitory effect on HDL binding and selective lipid uptake [109]. SAA has been reported to promote cellular cholesterol efflux via SR-BI [110]. However, the lipidation status of SAA seems to be a critical factor governing its cholesterol acceptor properties [111].

1.4.5.2 FPRL-1

In vitro studies have provided compelling evidence that SAA can act as a chemoattractant for such immune cells as monocytes, polymorphonuclear leukocytes, mast cells, and T lymphocytes [52, 53, 56]. Chemoattractants, such as N-formyl-methionyl-leucyl-phenylalanine (fMetLeuPhe) and the chemokines, act by binding seven-transmembrane-spanning G-protein-coupled receptors [112]. The first clue to the identity of the SAA receptor came from experiments in which SAA selectively induced calcium mobilization and a migratory response in human embryonic kidney (HEK) cells overexpressing FPRL-1, thus establishing SAA as the first naturally occurring chemotactic ligand for the earlier orphan FPRL-1 [113]. Since then, several papers have presented evidence that SAA binds to such a receptor [114, 115]. The hallmark of the interaction between chemokine and their receptors via G-protein-dependent pathways is Ca^{2+} mobilization and protein kinase C activation. SAA binding is characterized by some of the same phenotypic effects. Protein kinase C appears to be involved in the SAA signaling pathways that result in monocyte recruitment, and, on binding, SAA transiently induces monocyte intracellular Ca^{2+} levels from extracellular sources. Therefore, it is probable that a G-protein is involved in SAA chemotaxis [114]. Furthermore, as the chemotactic effects mediated by SAA are pertussis toxin sentsitive, they probably involve the G_i subset of G-protein. The participation of a G_i-protein in SAA chemotaxis has subsequently been confirmed in human mast cells, which are normally resident in tissues but can accumulate at inflammatory sites [56].

1.4.5.3 RAGE

Recently, the receptor for advanced glycation end products (RAGE) has been identified to bind SAA [116]. This multiligand receptor of the immunoglobulin superfamily also binds, in addition to nonenzymatically glycated adducts, the ßï sheet fibrils characteristic of amyloid, pro-inflammatory cytokine-like mediators of the S100/calgranulin family, and amphoterin, a nuclear protein sometimes found in the extracellular matrix [117]. Activation of cell-surface expressed RAGE by extracellular ligands results in a specific signaling cascade ultimately leading to the activation of NF-ʏB and MAPK. Increased expression of RAGE is associated with a number of pathological conditions with high SAA concentrations. RAGE has been reported to bind human SAA1 and to promote expression of monocyte tissue factor via activation of NF-ʏB through ERK and p38 MAPK pathway [116]. SAA also binds to sRAGE [116], the soluble and extracellular form of RAGE. Thus, sRAGE may be a promising therapeutic target to prevent vascular damage as a consequence of chronic inflammatory conditions by acting as a decoy for circulating RAGE ligands [117]. Indeed, preincubation of SAA with sRAGE prevented SAA-induced IʏBŬ degradation. Most importantly, incubation of murine microglial BV2 cells with SAA fibrils resulted in nuclear translocation of NF-ʏB [118].

1.4.5.4 TLRs

Recent findings revealed that SAA could act as an endogenous agonist for the toll-like receptor 4 (TLR4) [119]. SAA stimulated macrophage production of nitric oxide radical in a TLR4-dependent manner that requires phosphorylation of ERK and p38

MAPK pathway [119]. Macrophages from C3H/HeJ and C57BL/10ScCr mice lacking this functional receptor complex (associated with innate immunity) did not respond to SAA stimulation. TLR2 has also been reported to involve in NF-ϞB activation, a process that promotes phosphorylation of all three major MAPK, ERK, p38 and JNK, respectively [120]. A neutralizing antibody against TLR2 significantly reduced SAA-stimulated NF-ϞB activation in TLR2 overexpressing HeLa cells. SAA-induced expression of the two anti-inflammatory cytokines IL-10 and IL-1 receptor antagonist was completely abrogated in bone marrow-derived macrophages from *tlr2*$^{-/-}$ mice. SAA was shown to induce NO production through ERK1/2 and p38 pathway and this induction was dependent on functional TLR4 [119]. The researchers from another group also reported that SAA-induced G-CSF expression and neutrophilia were critically dependent on TLR2 [121]. All these data supported that SAA might be an endogenous ligand to TLRs.

1.4.5.5 TANIS

Another SAA binding receptor, identified by yeast two-hybrid screening, is TANIS [122]. TANIS, a membrane selenoprotein predicted to have a single transmembrane region close to its N-terminus, was shown to be regulated by glucose and is differentially expressed in type-2 diabetes. Therefore, it provides a link among inflammatory response, cardiovascular disease and diabetes.

1.4.6 SAA and cardiovascular disease

The characterization of SAA as both an inflammatory protein and an apolipoprotein generate increased interest in CAD research as both are involved in atherogenesis. SAA is implicated to have both beneficial and harmful effects in the inflammatory process. Accumulating clinical evidence shows that SAA is associated with CAD. Plasma SAA levels increase in response to tissue damage, causing consequent inflammation. It is therefore, not surprising that SAA concentration is elevated (100- to 500-fold) in patients who have suffered a myocardial infarction [123]. It has been observed that modestly elevated SAA (4- to 8-fold) is an indication of a poor prognosis in patients with unstable angina prior to objective evidence of a myocardial infarction [124]. SAA levels also increase with age, when cardiovascular disease increases with frequency [125]. Long-standing histological observations of atherosclerotic plaques indicate that inflammation is an ongoing process in these lesions. Therefore, active atherosclerotic lesion could be the stimulus for raised plasma SAA levels, but the increase is a fraction of that seen during significant tissue injury (4- to 8-fold versus 100- to 1000-fold, respectively). It is in this context that very modestly elevated plasma SAA serves as a prognostic indicator of cardiovascular disease. Elevated plasma SAA may identify patients with more active vascular disease, even in those individuals in whom the process is clinically silent. Thus, acute-phase SAA may be a product of the inflammation caused by atherosclerotic lesions, rather than a cause of the plaques. The potential beneficial roles of SAA include its involvement in the reverse cholesterol transport and possibly extracellular lipid deposition at sites of inflammation and tissue repair [97]. Reverse cholesterol transport involves the removal of excess cholesterol from peripheral tissues,

including foam cells of the arterial wall, and its delivery to the liver for biliary excretion. Cholesterol efflux is a crucial process regulating the cholesterol homeostasis of an organism and is thus an important therapeutic target for the prevention and reversal of atherosclerosis [126]. Cholesterol efflux is the only mechanism by which cells can limit or reverse the cellular cholesterol accumulation [127]. Therefore, the physiological role of SAA in atherosclerosis is not conclusive.

1.5 PEROXISOME PROLIFERATOR-ACTIVATED RECEPTOR ɔ (PPARɔ)

1.5.1 PPAR family

The peroxisome proliferator-activated receptors (PPARs) are a group of nuclear receptor proteins that serve as transcription factors regulating the expression of genes. PPARs possess a conserved DNA binding domain and a ligand binding domain which are characteristics of nuclear receptors [128-130]. The central DNA binding domain consists of two zinc finger motifs that mediate sequence-specific recognition of hormone response elements in direct target genes (Fig. 4). PPARs heterodimerize with retinoid X receptors (RXRs) and bind to specific PPAR response elements (PPRE) of the target genes. The C-terminal ligand binding domain (LBD) determined the ligand specificity of each receptor and mediates ligand-regulated interactions with other proteins that act as effectors of transcription activation and/or repression.

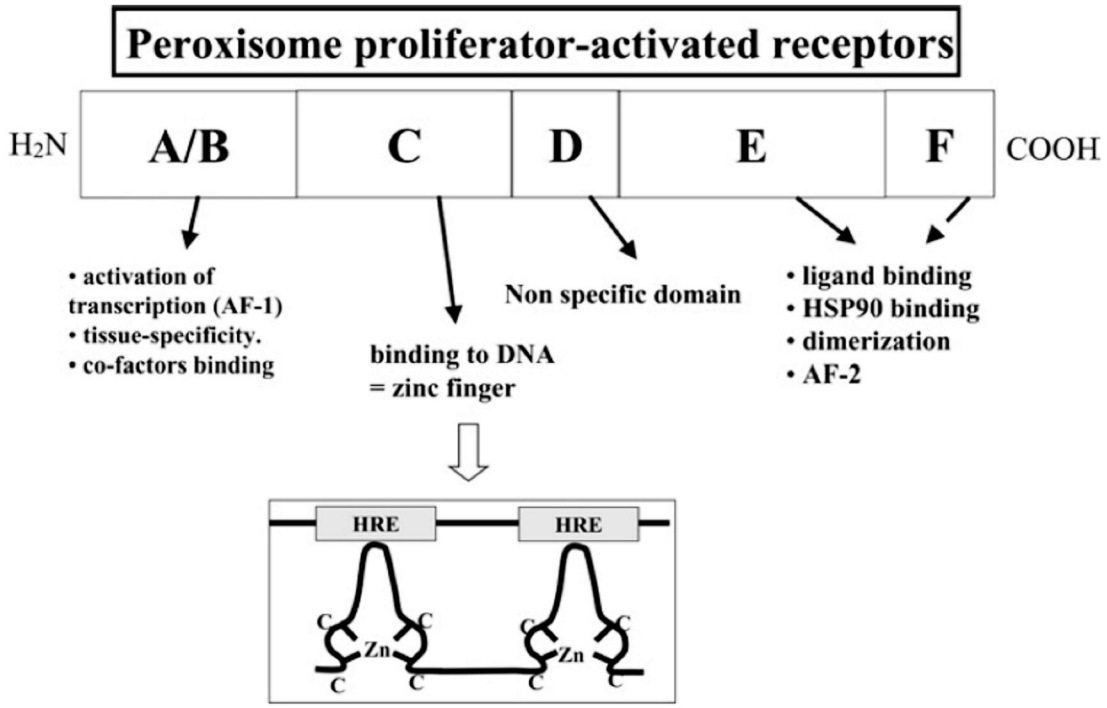

Figure 4. Classical structure of PPAR with the zinc fingers which interact with specific response elements located in the target genes (Adapted from Ref. [131]).

Three isoforms of PPARs (Ǔ, ɓ/ŭ, ɔ) have been identified, displaying distinct physiological and pharmacological functions depending on their target genes and their tissue distribution [132, 133]. Indeed, the activation of PPARǓ by both natural ligands such as fatty acids and eicosanoid derivatives or synthetic ligands (lipid-lowering fibrates), regulates lipid homeostasis [134]. PPARǓ is highly expressed in liver, kidney, heart and skeletal muscle and has been shown to be the biological target for the fibrate class of lipid-lowering drugs. PPARɓ/ŭ is one of the most widely expressed members of the PPAR family [128]. Until recently, the function of PPARɓ/ŭ remained elusive, but recent results have shown that PPARɓ/ŭ also plays a key role in lipid metabolism, as it regulates serum lipid profiles and fatty acid ɓ-oxidation in muscle and adipose tissue [135]. Synthetic ligands of PPARɓ/ŭ are at the moment in preclinical phases of

development [135]. As PPARɔ is a very important subject in my study, I will discuss its activation and functions in separate sections.

1.5.2 PPARɔ activation

Nuclear receptors can be activated in ligand-dependent and ligand-independent mechanisms. PPARɔ, like other nuclear receptors, binds lipophylic ligands and regulates transcription upon ligand binding. PPARɔ could be activated by endogenous ligands such as a number of naturally occurring unsaturated fatty acids, arachidonic acid metabolites, fatty acid-derived components of oxLDL, and synthetic ligands. Endogenous PPARɔ ligands include 15-deoxy-$\Delta^{12,14}$-prostaglandin J_2 (15d-PGJ_2) [136, 137] and 15-HETE [138], 9- and 13-HODE [139]. All of these endogenous ligands can activate PPARɔ *in vitro*. Synthetic ligands include thiazolidinedione (TZD), a group of compounds comprising troglitazone, rosiglitazone, pioglitazone and ciglitazone, and phenylacetic acid derivatives [140].

Peroxisome proliferators response elements (PPREs) are usually located upstream of PPARɔ target genes. PPREs consist of a direct repeat of the nucleotide sequence TGA(A/C)CT separated by a single nucleotide. PPARɔ binds to PPREs as heterodimers with retinoid X receptor (RXR). PPARɔ/RXR heterodimers recruit a protein complex that consists of co-activators or co-repressors to direct transcriptional activation or repression, respectively. In the absence of ligands, PPARɔ/RXR heterodimers bind to PPREs in a conformation that favors the binding of co-repressor molecules leading to the inhibition of transcriptional activity. Potential co-repressor candidates include NCoR and SMRT [141-144]. Upon ligand binding, the heterodimers are activated and undergo

conformational changes that promote co-activator recruitment and positive regulation of gene expression. The term ñactivationò represents an alteration in the three dimensional structure of the receptor complex such that it is able to regulate gene expression. The physical alteration that is initiated by ligand binding may include events such as loss of heat shock proteins and chaperones, nuclear translocation, and protein turnover. Conformational changes of PPARɔ have been observed using limited proteolysis [145]. Activation of PPARɔ is closely related with its functions.

1.5.3 Functions of PPARɔ

In the decades since it was first cloned [146], an extensive body of literature has evolved relating to the biology of PPARɔ. Differential promoter usage and alternative splicing of the gene generate three mRNA isoforms: PPARɔ1 and PPARɔ3 mRNA encode the same protein product; the PPARɔ2 isoform contains an additional 28 amino acids at its N-terminus that confers a tissue-specific transactivation function.

PPARɔ1 exhibits widespread expression, albeit at low levels, whilst PPARɔ2 and PPARɔ3 are highly expressed in adipose tissue. Systemic deletion of the PPARɔ gene results in embryonic lethality attributable to essential roles in adipose, kidney, and placental development [147]. Indeed, the receptor plays a critical role in fat cell differentiation, inducing the expression of adipocyte-specific genes, and promoting the formation of mature lipid-laden adipocytes [148-150]. Recent studies with mice genetically engineered to lack PPARɔ have confirmed its critical role in the development of both white and brown adipocytes *in vivo* [147, 151, 152], and the clinical phenotypes

of subjects with PPARɔ gene mutations suggest a similar role in the regulation of human adipose tissue mass [153, 154].

PPARɔ plays a crucial role in glucose homeostasis and is the molecular target of a class of insulin-sensitive drugs referred to as thiazolidinediones [155]. Consistent with this, a number of PPARɔ polymorphisms are linked with features of the metabolic syndromes including insulin resistance, hypertension, and obesity. Dominant-negative mutations in PPARɔ have been shown to cause severe insulin resistance [156]. The analysis of mice with deletions of PPARɔ in specific tissues indicates major roles in controlling insulin resistance in adipose tissue, with contributions also observed in liver and skeletal muscle [57, 157-159]. The mechanisms by which PPARɔ influences insulin action have been intensively studied, and several potentially important targets of regulation have been established. Activation of PPARɔ induces the expression of the insulin-dependent glucose transporter GLU4 [160], enhances the release of free fatty acids from chylomicrons and VLDL [161], upregulates genes involved in intracellular fatty acid transport, synthesis, and esterification [148, 162], and increases the expression of adiponectin [163, 164].

A role for PPARɔ in the regulation of inflammation and immunity was initially proposed by the findings that it is expressed in macrophages and inhibits the expression of a number of proinflammatory genes, including TNFŰ, IL-1ɓ, iNOS, and gelatinase B [165, 166]. A large number of inflammatory responses have been shown to be subject to negative regulation by PPARɔ agonists [167, 168]. PPARɔ ligands inhibited transcriptional responses of primary macrophages to bacterial lipopolysaccharide in a PPARɔ-dependent manner [169].

The results from *in vitro* studies of the effects of PPARɔ agonists on cholesterol homeostasis suggested both atherogenic and anti-atherogenic influences. PPARɔ was found to stimulate transcription of the CD36 gene [139, 170], which is a macrophage scavenger receptor that involves in macrophage foam cell formation and the development of atherosclerosis in mice [171]. In conjunction with the discovery that PPARɔ can be activated by 9- and 13-HODE present in oxLDL, oxLDL lipids would induce the activity of PPARɔ, leading to increased expression of CD36, which in turn would increase the uptake of oxLDL [139, 170]. This cycle would potentially promote foam cell formation and atherosclerosis. With respect to cholesterol efflux pathways, PPARɔ was shown to induce the expression of liver X recptor Ŭ (LXRŬ) and thereby enhance ABCA1-dependent cholesterol efflux to apoA-I and ABCG1-dependent cholesterol efflux to HDL [172-174] (Fig. 5). The cytochrome P450 enzyme Cyp27, which catalyzes production of the LXR agonist 27-hydroxy-cholesterol, has been demonstrated to be activated by PPARɔ [175]. Cyp27 may therefore serve as an integrator of the PPARɔ cholesterol efflux pathway in macrophages by generating ligands that activate LXR (Fig. 5).

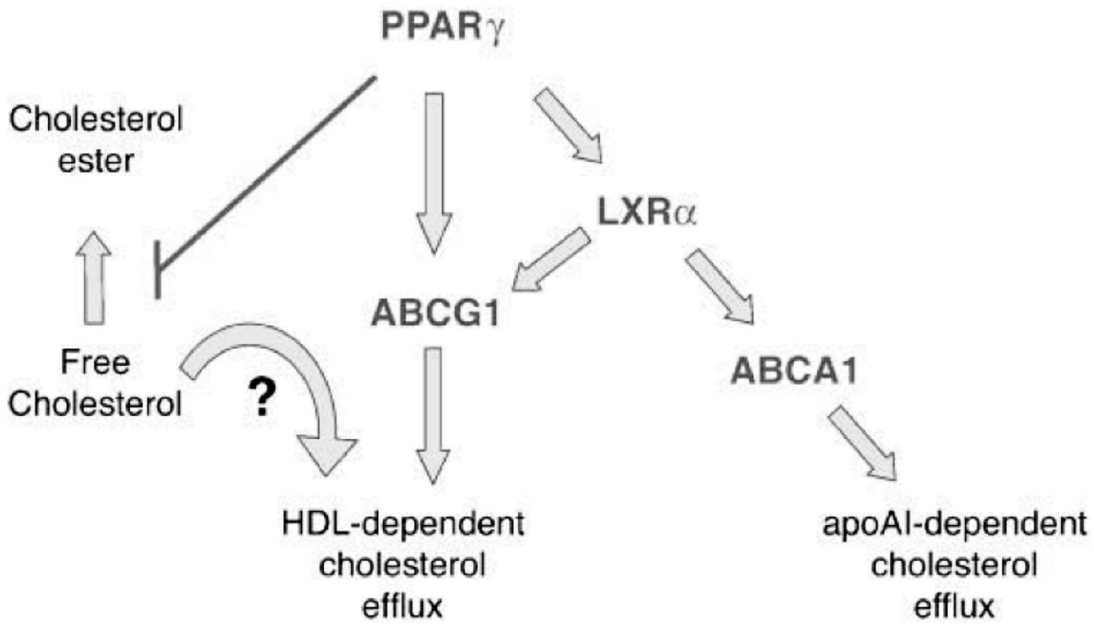

Figure 5. Regulation of cholesterol efflux pathways in macrophages by PPARɔ and LXRŬ. LXRŬ agonists stimulate the expression of ABCA1, which facilitates the efflux of cholesterol to lipid-poor apolipoprotein A-I (apoA-I), and ABCG1, which facilitates the efflux of cholesterol to HDL. PPARɔ agonists can induce the expression of LXRŬ, therefore stimulating cholesterol efflux to apoA-I in an LXR-dependent manner. PPARɔ ligands also directly activate ABCG1, enabling LXR-independent efflux to HDL. PPARɔ has also been shown to inhibit cholesterol esterification in cholesterol-loaded macrophages. This effect is not attributed to changes in ACAT expression and may result from altered cholesterol trafficking within the cell (Adapted from Ref. [176]).

Clinical studies found that treatment of diabetic patients with thiazolidinediones inhibited carotid intimal thickening [177, 178]. Investigations of the effects of PPARɔ agonists in hypercholesterolemic male mice have consistently demonstrated anti-atherogenic effects despite an increased expression of CD36 in atherosclerotic lesions [179-181]. PPARɔ agonists improved insulin sensitivity in these studies and inhibited the expression of inflammatory markers in the artery wall. Interestingly, in the one study using female mice, PPARɔ agonists were not effective at inhibiting the development of atherosclerosis [179]. These data are consistent with the idea that PPARɔ agonists can act

to promote both atherogenic and anti-atherogenic effects, with the net outcome being influenced by additional factors such as hormonal status.

PPARɔ is an important transcription factor that plays roles in an ever increasing list of regulatory mechanisms in metabolism, inflammation, endothelial function, cancer, atherosclerosis, and bone morphogenesis. Additionally, PPARɔ has gained instant medical relevance through the fortuitous discovery that members of the TZD class of drugs can be used to improve insulin sensitivity in type 2 diabetic patients and are high-affinity ligands for PPARɔ [137]. PPARɔ can also be used as a model transcription factor to study mechanisms of transcriptional regulation. For these reasons PPARɔ has always been in the spotlight of intense research.

1.6 MITOGEN-ACTIVATED PROTEIN KINASES (MAPKs)

1.6.1 General features and biological functions of MAPK

Mitogen-activated proteins kinase (MAPK) signal transduction pathways are among the most wide-spread mechanisms of eukaryotic cell regulation. All eukaryotic cells possess multiple MAPK pathways that are activated by distinct set of stimuli, allowing the cells to respond coordinately to multiple and divergent inputs. These signaling pathways control essential processes in all eukaryotic cells, including gene transcription, protein translation, cytoskeletal remodeling, endocytosis, cell metabolism, cell proliferation and survival. MAPKs are serine/threonine protein kinases that can phosphorylate their target proteins [182]. To date, six major subfamilies have been identified: extracellular-signal regulated kinases 1/2 (ERK1/2), p38 MAPKs, Jun N-terminal kinases/stress-activated protein kinases (JNKs/SAPKs), ERK7/8, ERK3/4 and

ERK5 [182-187]. There are splice variants for several of the MAPK proteins that increase the diversity of the cascade. The most extensively studied groups are ERK1/2, JNKs and p38 kinases.

Although each MAPK is unique, they share some common features, and have thus been grouped together in one family. A three-tiered signaling cascade is typical of these pathways. It consists of a set of three evolutionarily conserved, sequentially acting kinases: MAPK, MAPK kinase (MAPKK), and MAPK kinase kinase (MAPKKK), which is also called MAP3K or MEKK. MAP3Ks are Ser/Thr kinases that are activated by phosphorylation and/or their interaction with small GTP proteins of Ras/Rho family in response to extracellular stimuli. MAP3K activation results in phosphorylation and activation of downstream MAPKK, which is a dual specificity kinase and can phosphorylate MAPK. Once activated, MAPKs phosphorylate the target substrates on serine or threonine residues only if the amino acid residues are followed by proline [188]. These substrates could be transcription factors, other kinases or proteins like cytoskeletal proteins. The cellular responses regulated by MAPK pathways are very diverse, ranging from proliferation to differentiation, from apoptosis to cell survival.

1.6.1.1 MAPK in cancer

Carcinogenesis and the development of cancer can be said to be a disorder of the signaling system. The ERK pathway is deregulated in approximately one third of all human cancers. Many components of this signaling pathway have been linked to cell proliferation. In the ERK pathway, the key point seems to be the Ras/Raf motif. The involvement of Ras in cancer has been known for a very long time [189]. Aberration

spans the whole pathway beginning from an aberrant receptor like epidermal growth factor receptor (EGFR) overexpression, Ras and Raf mutation to amplification of nuclear targets, most notably myc and activator protein 1 (AP-1) [189]. ERK signaling also plays a role in the disrupting the anti-proliferative effects of ligands such as transforming growth factor-ϐ (TGF-ϐ). Accumulating evidence also suggests that the expression of different feedback inhibitors of the ERK pathway is deregulated in cancer [190-192]. A role for the JNK pathway in tumorigenesis is supported by the high levels of JNK activity found in several cancer cell lines. JNK activity and phosphorylation of c-jun has been reported to play a critical role in Ras-induced tumorigenesis and Ras and c-jun cooperate in cellular transformation [193, 194]. Another important function of c-jun appears to be transcription repressor of p53 [195, 196]. Some studies showed that p38 functions as a tumor suppressor. These tumorsuppressive effects have been demonstrated to be mediated by activation of p53 and p53-dependent apoptosis [197].

1.6.1.2 MAPK in cell cycle

The ERK1/2 pathway has emerged as a central regulator of cell proliferation by controlling both cell growth and cell cycle progression. Various mechanisms have been proposed to explain the role of ERK1/2 pathway in cell cycle progression. The most important targets are D-type cyclins and c-myc. Activation of the ERK pathway induces the D-type cyclins by up-regulating and activating the transcription factors involved in its synthesis. ERK1/2 may also control its expression at post-transcriptional level [198, 199]. c-myc is a transcription factor of the Myc family. It plays an important role in regulating cell growth, cell progression and apoptosis [200], exerts its functions by up-regulation of

certain genes involved in cell growth such as cyclin D [201] and p21 [202], ribosomal proteins and translation factors [203]. Activation of ERK stabilizes c-myc by phosphorylation [204-206]. p38 was reported to involve in cell cycle arrest and this effect is probably mediated by mitogen- and stress-activated protein kinases (MSKs) [207].

1.6.1.3 MAPK in apoptosis

Although the ERK pathway is attributed to survival in most cell types, its activation is now also thought to contribute to apoptosis. ERK activation has been shown to be involved in death induced by many factors such as reactive oxygen species (ROS) [208], *E. coli* toxins [209], and zinc [210], and also by deprivation of survival factors [211]. The mechanism by which the ERK pathway mediates apoptosis remains poorly understood and seems to occur at different level of signaling. Previous study showed that promotion of cell death by ERK activation may result through suppression of Akt-mediated survival signaling [211]. A role for JNK in apoptosis is well established [212]. One potential target of pro-apoptotic JNK signaling is the tumor suppressor p53. Binding to JNK was reported to destabilize p53 by promoting ubiquitin-mediated degradation [213]. Activation of p38 was observed in cells undergoing apoptosis induced by variety of agents. Studies showing the inhibition of p38 by caspase inhibitors suggested the role of p38 downstream of caspase activation.

Other than the functions mentioned above, MAPK pathway is also related to cell survival, development and differentiation and inflammation.

1.6.2 SAA and MAPK

Recent studies have shown that SAA could activate MAPK pathways in cells from the vessel wall [119, 120, 214-220]. The receptors involved in the SAA-induced MAPKs activation are different. Toll-like receptor 2 (TLR2), human orthologue of the scavenger receptor class B type I (SR-BI), CD36 and LIMPII analogous-1 (CLA-1) and G-protein coupled receptor such as formyl peptide receptor-like 1 (FPRL1) were indicated to play a role in SAA-induced MAPKs activation [119, 120, 215-217, 219, 220]. They are presented in Table 1 together with the possible cellular functions regulated by the MAPKs. Many of these studies have used inhibitors to assess the signaling and functions of SAA-induced MAPK activation. Therefore, to facilitate reading of Table 1, the inhibitors used are described in Table 2.

Table 1 SAA-induced signaling and cellular responses

Study	Cell line	SAA Conc.	MAPKs activation	Receptors involved	Molecular and cellular effects
Endothelial cells					
Jijon 2005 [214]	Caco-2	5 μM (~60 μg/ml)	ERK1/2, p38, JNK	----	IL-8 expression and secretion (Blocked by PD98059, SB203580 and SP600125)
Baranova 2005 [215]	HeLa	25 μg/ml	ERK1/2, p38	CLA-1	IL-8 production (Blocked by PD98059 and SB203580)
Jo 2007 [216]	WISH	2 μM (~24 μg/ml)	ERK1/2, p38	FPRL1	Apoptosis (Blocked by PD98059 and SB203580)
Zhao 2007 [217]	HUVEC	20 μg/ml	ERK1/2, p38, JNK	FPRL1	Procoagulation, TF expression and TFPI inhibition (Blocked by PD98059, SB203580 and SP600125)
Cheng 2008 [120]	HeLa	1 μM (~12 μg/ml)	ERK1/2	TLR2	NF- ϞB activation (Blocked by anti-TLR2 Ab)
Monocytes					
He 2006 [218]	THP-1	1 μM (~12 μg/ml)	p38	----	IL-12p40 expression (Blocked by SB202190)
Lee 2006 [219]	Human monocytes	2 μM (~24 μg/ml)	ERK1/2, p38	FPRL1	TNFŬand IL-10 production (Blocked by PD98059 and SB203580)
Sandri 2008 [119]	THP-1	10 μg/ml	ERK1/2, p38	GPCR	CCL20 production (Blocked by PD98059 and SB203580)
Fibroblast					
Koga 2008 [220]	RA-FLS	1 μM (~12 μg/ml)	p38, JNK	FPRL1	IL-6 production (Blocked by SB203580 and SP600125)

SAA 1 μM = 12 μg/ml

Caco-2, human epithelial colorectal adenocarcinoma cells; CCL20, Chemokine (C-C motif) ligand 20; CLA-1, CD36 and LIMPII analogous-1; ERK 1/2, extracellular-signal regulated kinases 1/2; FPRL1, formyl peptide receptor-like 1; GPCR, G-protein coupled

receptor; HeLa, human cervical adenocarcinoma cell line; HUVEC, primary human umbilical vein endothelial cell; IL, interleukin; JNK, Jun N-terminal kinases/stress-activated protein kinases; MAPK, mitogen-activated protein kinase; NF- ʏB, nuclear factor-kappa B; RA-FLS, rheumatoid arthritis fibroblasts; SAA, serum amyloid A; TF, tissue factor; TFPI, tissue factor pathway inhibitor; THP-1, human acute monocytic leukemia cell line; TLR-2, toll-like receptor 2; TNFŬ, tissue necrosis factor alpha; WISH, human amnion cell line. Information concerning the inhibitors mentioned here can be found in Table 2.

Table 2 Characteristics of the inhibitors mentioned in Table 1

Inhibitors	Targets
ERK MAPK pathway	
PD98059	MKK1/2 activation
p38 MAPK pathway	
SB203580	p38Ŭand p38ƀ MAPKs
SB202190	p38Ŭand p38ƀ MAPKs
JNK MAPK pathway	
SP600125	JNK1,2 and 3
Others	
anti-TLR2 Ab	TLR2 antibody

ERK 1/2, extracellular-signal regulated kinases 1/2; JNK, Jun N-terminal kinases/stress-activated protein kinases; MAPK, mitogen-activated protein kinase; MKK, MAPK kinase; TLR-2, toll-like receptor 2.

1.6.2.1 Endothelial cells

Endothelial cells were used to investigate the effects of SAA on the MAPKs activation in several studies [120, 214-217]. SAA-induced ERK1/2 and p38 activation were reported in most of these studies. However, evidence that the JNKs were activated by SAA was scarce, suggesting that the JNK MAPK pathway may not be an important target of SAA in endothelial cells. SAA-induced MAPKs activation in endothelial cells leads to the expression and secretion of the inflammatory cytokines [120, 214, 215], initiation of the procoagulation [217] and apoptosis [216].

As an acute-phase protein, SAA secretion is a host response to dangerous signals and a clinical indication of inflammation. Some recent reports suggest that the biological functions of SAA might induce inflammatory cytokine expression and secretion. The experimental data showed that SAA could induce IL-8 expression and secretion, which was dependent on ERK1/2 and p38 activation [214, 215]. SAA-dependent IL-8 expression was inhibited by ERK1/2 and p38 inhibitors in these studies. NF-ʢB transcriptional activity was also enhanced by SAA through ERK1/2 pathway [120], which would further lead to the expression and secretion of some other inflammatory cytokines.

SAA was involved in the procoagulation by inducing the expression of tissue factor (TF) and inhibiting the tissue factor pathway inhibitor (TFPI) [217]. The inhibition study confirmed that such effects were dependent on MAPKs activation. Surprisingly, all the three subfamilies of MAPKs were activated and contributed to such effects. One study has reported that SAA-dependent ERK1/2 and p38 phosphorylation in WISH induced apoptosis, which is a risk factor of atherogenesis and myocardial infarction [216].

1.6.2.2 Monocytes

ERK1/2 and p38 MAPK pathway have been clearly demonstrated to be activated by SAA in monocytes [119, 218, 219]. Most of the cellular effects associated with their activation have been related to the expression and secretion of the inflammatory cytokines such as IL-10, IL-12, TNFŬ and CCL20. These data indicate that SAA

potentially participates in the inflammatory process by virtue of its ability to activate inflammatory signaling in monocytes.

1.6.2.3 Fibroblasts

As observed in endothelial cells and monocytes, SAA also induces the production of pro-inflammatory cytokine, IL-6, in fibroblasts through the activation of p38 and JNK [220]. However, in this case, the implication of MAPK pathways is still not confirmed as there is only one study reported the involvement of p38 and JNK in fibroblasts.

Plasma SAA levels increase dramatically in response to tissue damage or inflammation. Evidence from recent studies has shown that increased SAA will stimulate the production and secretion of pro-inflammatory as well as inflammatory cytokines in endothelial cells, monocytes and fibroblasts [119, 120, 214, 215, 218-220]. Chronic production of such cytokines may result in pro-atherogenic inflammatory conditions and excessive proliferation and angiogenesis would participate in the development of atherosclerotic plaques, leading to vessel wall thickening and accelerate the atherogenic process. The observation that the thickening of blood vessels can be inhibited by MAPK inhibitors is consistent with the notion that SAA-induced MAPK activation participates in the development of atherosclerosis [221]. Accumulating evidence indicates that SAA potentially participate in the atherosclerosis by its ability to activate inflammatory signaling through MAPKs activation. Recent studies have also demonstrated that tissue factor (TF) could be markedly induced by some atherosclerosis risk factors such as tumor necrosis factor Ŭ (TNFŬ) and SAA. Conversely, native tissue factor pathway inhibitor (TFPI) degradation after thrombolysis may enhance procoagulation and leads to early

reocclusion after thrombolysis in myocardial infarction (MI). The data that SAA induces TF and inhibits TFPI expression in a MAPKs-dependent manner indicate that SAA may play a role in the initiation of coagulation, which is the major cause of atherosclerosis, based on the MAPKs activation. One study also linked SAA and MAPKs activation with endothelial cell apoptosis. Apoptosis occurs in all cells of the atherosclerotic plaque, becoming increasingly frequent and important as the plaque develops. Apoptosis contributes to plaque growth, lipid core development, plaque rupture and thrombosis. As there is only one study reporting such relationship among SAA, MAPKs and apoptosis, the possible impact of SAA on apoptosis remains obscure.

1.7 NF-HB

1.7.1 General features and biological functions of NF-HB

Nuclear factor ʏ B (NF-ʏB) signaling pathway regulates immune responses and is implicated in the pathogenesis of many inflammatory diseases. NF-ʏB induction is essential for the expression of a wide variety of immune-response genes. These include pro-inflammatory cytokines (TNFŬ, IL-1 and IL-6), chemokines (macrophage inflammatory protein-1Ŭ) and adhesion molecules (E-selectin and vascular cell adhension molecule-1), which collectively regulate the recruitment of immune cells to sites of infection [222]. TNFŬ and IL-1 stimulation of their respective receptors in turn strongly activates NF-ʏB, which plays an important role in amplifying and extending the duration of the innate immune response [223, 224]. Dysregulation of NF-ʏB can lead to the constitutive over-production of pro-inflammatory cytokines, which is associated with a number of chronic inflammatory disorders, including rheumatoid arthritis and Crohnôs

disease [225, 226]. NF-ϟB also plays an important role in regulating the expression of anti-apoptotic proteins and the cell-cycle regulator cyclin D1, which increase cellular survival and proliferation respectively [227, 228]. Consequently NF-ϟB has been implicated in cell transformation [228], and persistent NF-ϟB activation may explain the known causative link between chronic inflammation and certain types of cancer [229, 230].

The NF-ϟB family of transcription factors consists of five members in mammalian cells: RELA (also known as p65), REL (also known as c-REL), RELB, p50 and p52, which can form homodimers or heterdimers. In unstimulated cells, NF-ϟB dimmers are inactive, since they are sequestered in the cytoplasm by interaction with inhibitory proteins termed IϟBs [231]. Following cell stimulation, the IϟB kinase complex phosphorylates IϟB proteins on specific serine residues, which are proteolytically degraded by the proteasome, releasing associated NF-ϟB dimmers to translocate into the nucleus and modulate gene expression (Fig. 6).

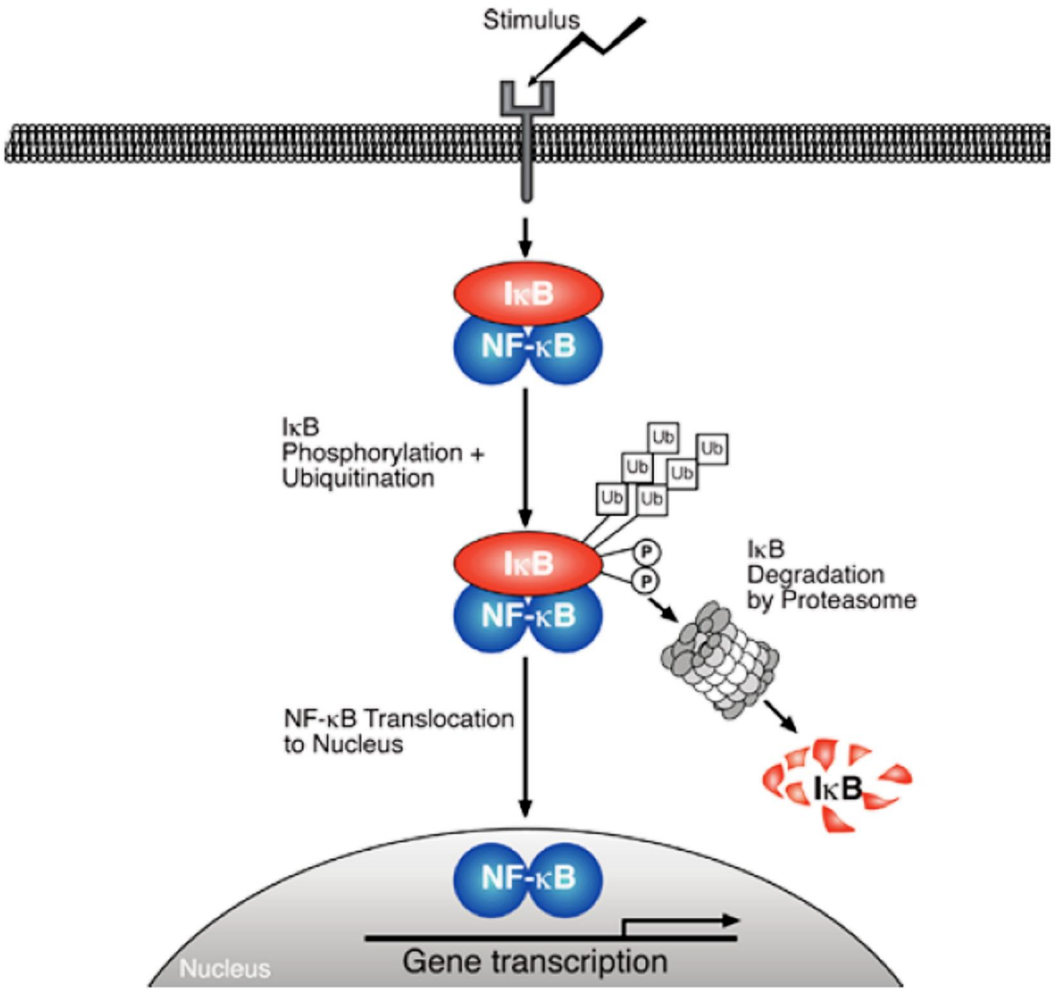

Figure 6. Model of the generic NF-ʁB activation pathway. Various stimuli induce the phosphorylation (P) and subsequent polyubiquitination (Ub) of IʁBs, which are then targeted for degradation by the 26 S proteasome. Associated NF-ʁB dimmers are thereby released to translocate into the nucleus, where they bind to the promoter regions of NF-ʁB-responsive genes to modulate their expression. The transactivating capacity of nuclear NF-ʁB dimmers can also be regulated by phosphorylation (Adapted from Ref. [232]).

Three distinct NF-ʁB activation pathways have been described. The canonical (classical) pathway is activated by a large number of stimuli, including proinflammatory cytokines, bacterial and viral products, and also stress-inducing stimuli such as ɔ-radiation, ultraviolet light and oxidative stress. Activation of this pathway depends on the IKK complex, which phosphorylates IʁB to induce its rapid degradation. This pathway is

essential for immune responses, inflammation and promoting cell survival. The alternative NF-ϟB pathway is activated by a limited number of agonists and is important for secondary lymphoid organogenesis, maturation of B-cells and adaptive humoral immunity. This pathway requires NF-ϟB binding kinase and IKK and induces the slow processing of p100 to p52, resulting in nuclear translocation of p52/RELB heterodimers. The p105 pathway is specifically involved in immune and inflammatory responses. Agonist activation of this pathway induces phosphorylation of the p105 PEST region by the classical IKK complex. This triggers p105 polyubiquitination and subsequent degradation, releasing p50 homodimers which undergo unclear translocation and positively or negatively regulate gene transcription [232].

1.7.2 SAA and NF-ϟB

Previous studies have shown that SAA could activate NF-ϟB in various cell types. Earlier studies found that SAA might play a role in inducing proinflammatory genes such as IL-8, IL-12 and IL-23 [214, 218]. Recent data showed that SAA could induce the expression of MMP-9, TNFǗ, IL-6, IL-10, TF and Chemokine (C-C motif) ligand 2 (CCL2) in a NF-ϟB-dependent manner [115, 116, 219, 220, 233]. A latest study demonstrated that SAA induced IKK phosphorylation as well as the movement of p65, a component of NF-ϟB, from the cytoplasm to the nucleus. The EMSA experiment results indicated that the binding of NF-ϟB to the identified binding site on the $sPLA_2$ (secretory phospholipase A2, group IIA) gene promoter was increased upon SAA stimulation [234]. SAA had also been suggested to stimulate angiogenesis, leukocyte recruitment and

matrix degradation in rheumatoid arthritis through a NF-ϰB-dependent signal transduction pathway [235].

Many bacterial products can activate NF-ϰB. The identification of toll-like receptors (TLRs) as specific pattern recognition molecules and the finding that stimulation of TLRs leads to activation of NF-ϰB improved our understanding of how different pathogens activate NF-ϰB. TLRs recognize invariant microbial molecules, including components of the bacterial cell wall such as lipopolysaccharide (LPS) and microbial nucleic acids [236]. SAA has been postulated to be a ligand of TLRs. Therefore, there is a potential link among SAA, TLRs and NF-ϰB. However, the receptors between SAA and NF-ϰB activation remain obsecure. Some data supported that SAA-induced effects were through FPRL-1 [115, 217, 219, 233]. Some studies provided evidence that SAA-induced NF-ϰB was mediated by other receptors such as RAGE and TLR [116, 121]. Whether these receptors are essential or dispensable for SAA-induced NF-ϰB activation in hepatocytes remains to be determined. A wide range of microbial pathogens could activate NF-ϰB through TLRs and SAA was identified to be a potential endogenous ligand for TLRs [119]. Whether SAA could activate NF-ϰB through TLRs also need to be explored.

1.8 REVERSE CHOLESTEROL TRANSPORT

An early hallmark of atherosclerosis is the accumulation of cholesterol-loaded macrophages (foam cells) in the intima of arteries. Numerous epidemiological studies have also demonstrated that plasma levels of high-density lipoproteins (HDL), and their major protein constituent apolipoprotein A-I (apoA-I) are inversely correlated with the

risk of atherosclerosis [237]. HDL and apoA-I could exert diverse potentially atheroprotective functions. Previous evidence showed that they reduced oxidative damage, corrected endothelial dysfunction, inhibited inflammation and mediated reverse cholesterol transport [127]. The latter process involves the removal of excess cholesterol from peripheral tissues including foam cells of the arterial wall and its delivery to the liver for biliary excretion. The efflux of cholesterol mediated by HDL and its apolipoproteins is both a crucial process regulating the cholesterol homeostasis of the organism and an important therapeutic target for the prevention and reversal of atherosclerosis.

For many years, the efflux of cholesterol was thought to occur primarily by passive aqueous diffusion from the cell surface onto various extracellular acceptors including HDL, LDL, albumin and protein-free unilamellar phospholipid vesicles. Net cholesterol efflux by this process requires a concentration gradient between the donor cell membrane and the various extracellular acceptor particles. Recently it has become clear that cholesterol efflux is a highly regulated process that is mediated by specific molecules, including ATP-binding cassette (ABC) transporters. ABC transporters form a large family of proteins involved in the cellular export or import of a wide range of substrate including ions, lipids, cyclic nucleotides, peptides and proteins. Two of them, ABCA1 and ABCG1, play a pivotal role in mediating cellular efflux of phospholipids and cholesterol to lipid-free apoA-I and HDL, respectively (Fig. 7).

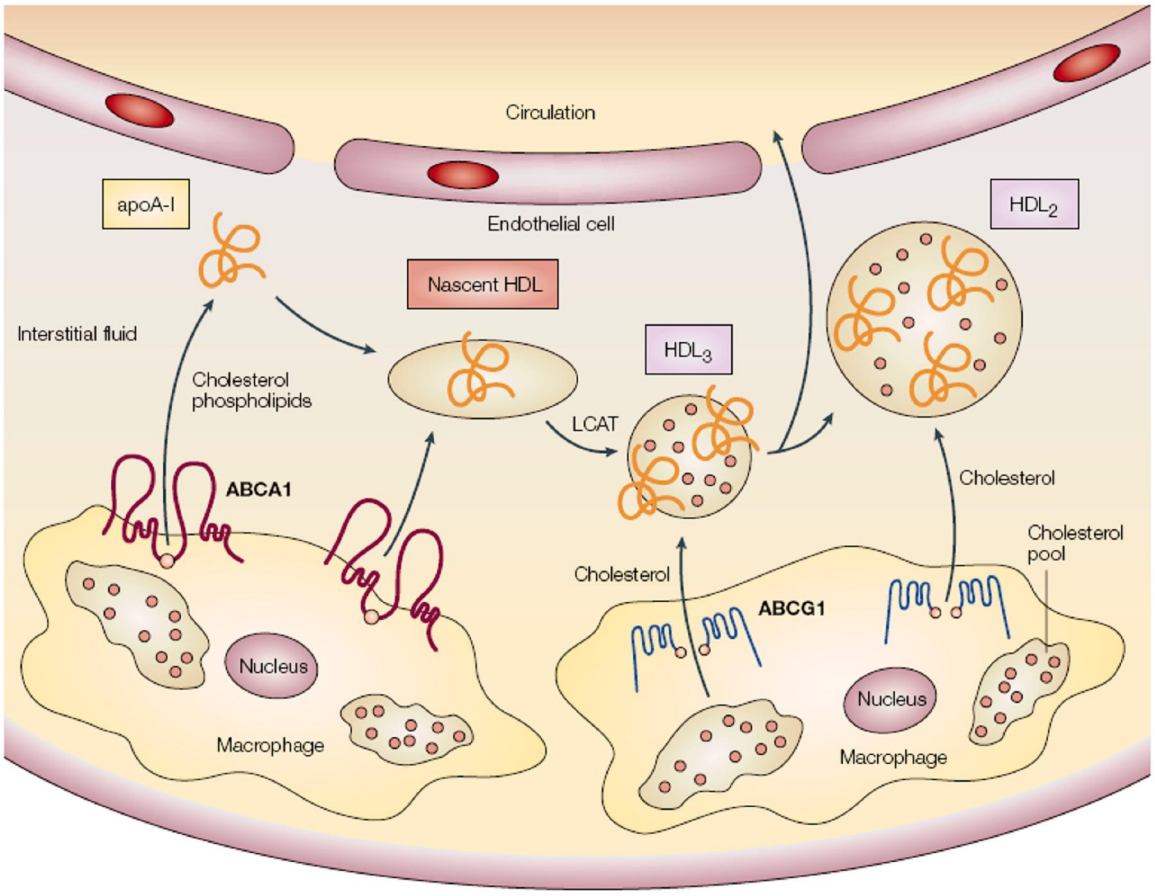

Figure 7. Mechanisms of cholesterol efflux from the arterial wall. On entering the sub-endothelial space, lipid-free or lipid-poor apolipoprotein A-I (apoA-I) can bind to the ABC transporter A1 (ABCA1) on the cell surface of macrophages in the arterial wall and promote efflux of free cholesterol and phospholipids from these cells. This results in the formation of nascent high-density lipoprotein (HDL) particles, which undergo further modification by the lecithin-cholesterol acyltransferase (LCAT) enzyme and develop into spherically shaped HDL_2 (larger, less dense particles) or HDL_3 (smaller, more dense particles), which, in turn, can act as acceptors for ABCG1-mediated cholesterol efflux from macrophages, resulting in further cholesterol enrichment of HDL, before returning to the circulation. Although inter-conversion of HDL subspecies is depicted as occurring in the arterial wall, it probably also occurs in the plasma (Adapted from Ref. [238]).

1.8.1 ABCA1-mediated cholesterol efflux

The human ABCA1 gene has been mapped to chromosome 9q31 and is composed of 50 exons, which encode 2261-amino-acid residues [239]. The ABCA1 protein is a full-size ABC transporter containing two transmembrane domains of six alpha-helices and

two intracellular nucleotide binding domains. The ABCA1 has been identified as the cause of Tangierôs disease [240-242], a rare disease characterized by very low levels of plasma HDL due to rapid catabolism and accumulation of cholesterol and cholesteryl esters in macrophage foam cells in various tissues such as tonsils, liver and spleen. Patients with Tangierôs disease seem to experience moderately accelerated atherosclerosis. ABCA1 promotes the efflux of free cholesterol and phospholipids from cells to lipid-poor apoliprotein A-I (apoA-I) to generate nascent HDL particles. Lipid-poor apoA-I interacts directly with ABCA1, possibly by binding to the two large extracellular domains of this transporter. This binding seems to constitute an essential step in the efflux of phospholipids and cholesterol to apoA-I. However, ABCA1 does not interact with the main forms of HDL that are present in plasma: it shows no interaction with HDL_2 (larger, less dense particles) and minimal interaction with HDL_3 (smaller, more dense particles).

ABCA1 is tightly regulated both transcriptionally and posttranscriptionally to maintain intracellular lipid homeostasis. In cholesterol-loaded cells, the oxysterol-activated nuclear receptor liver X receptor (LXR), in partnership with retinoid X receptor (RXR), targets the ABCA1 promoter, leading to increased ABCA1 gene expression and enhanced cholesterol efflux from foam cells, similarly, ABCA1 is induced by synthetic LXR agonists [243, 244]. Interestingly, the expression of the LXRs is modulated on the transcriptional level by agonists of peroxisome proliferators-activated receptor (PPAR) [245, 246]. Both systemic and selective hepatic overexpression of ABCA1 in mice results in an increase of HDL plasma levels [247, 248]. Conversely, apoA-I and HDL plasma levels are dramatically reduced in mice with a liver-specific deletion of ABCA1 [249].

By contrast, the selective inactivation or expression of ABCA1 in macrophages had little or no effect on the plasma concentration of HDL [250]. Therefore, hepatic ABCA1 expression plays an essential role in plasma HDL production and the maintenance of HDL levels in plasma. Macrophage ABCA1, although not contributing significantly to the maintenance of plasma HDL levels, is a crucial factor in the prevention of excessive cholesterol accumulation in macrophages of the arterial wall and their transformation in foam cells [250-252].

1.8.2 ABCG1-mediated cholesterol efflux

The human ABCG1 gene has been mapped to chromosome 21q22.3. It is composed of 23 exons and has multiple transcripts. Two major transcripts were described to encode proteins with alternative amino-termini [253]. ABCG1 is a half-transporter, which forms homodimers and is highly expressed in macrophages. Like ABCA1, ABCG1 mRNA levels are highly increased when macrophages are either incubated with LXR agonists or converted to cholesterol ester-loaded foam cells [254]. Activation of PPARↃ also induces the expression of ABCG1 [174]. In contrast to ABCA1, ABCG1 mediates the transport of cholesterol from cells only to the major HDL factions HDL_2 and HDL_3 but not to lipid-free apoA-I [254, 255]. Although the mechanism of action of ABCG1 is poorly understood, it seems that ABCG1 redistributes cholesterol to cell surface domains where it becomes accessible for removal by HDL [256].

1.9 OBJECTIVES OF THE PROJECT

The objectives of this project are:

1. To investigate the effect of SAA on PPARɔ activation
2. To investigate the mRNA and protein expression level of PPARɔ target genes after SAA stimulation
3. To investigate the underlying mechanisms of SAA induced PPARɔ activation (involvement of MAPK and NF-HB pathway)
4. To examine the effect of SAA on promoting cholesterol efflux
5. To examine the membrane receptors involved in SAA induced effects
6. To identify the functional domains of SAA responsible for cholesterol efflux, receptor binding and PPARɔ activation

The findings from this study would provide insights on the effects of SAA in atherosclerosis development and hopefully lead to development of novel therapies to combat atherosclerosis and coronary heart disease.

CHAPTER II

MATERIALS AND METHODS

2.1 MATERIALS

Recombinant synthetic human apolipoprotein SAA was purchased from PeproTech (Rocky Hill, NJ, USA). SAA is a hybrid molecule corresponding to human SAA1Ŭ except for the N-terminal methionine and substitution of asparagine for aspartic acid as position 60 and arginine for histidine at position 71. The latter two substituted residues are present in SAA2ƃ. The SAA protein was expressed in *Escherichia coli*, and following folding and purification by ion exchange chromatography, the lyophilized proteins or aliquots were stored at -80°C until used for cell stimulation. According to the supplier, the amount of endotoxin contaminant is less or equal to 0.1 ng/1 µl protein. Limulus amebocyte lysate (LAL) assay kit was purchased from Lonza (Walkerswille, USA). [^{3}H] Cholesterol was purchased from PerkinElmer (Waltham, MA, USA). 2-hexyl-1-cyclopentanone thiosemicarbazone (BLT-1) was purchased from ChemBridge (San Diego, CA, USA). Pertussis toxin (PTX), lipopolysaccharide (LPS), 2-(2-Amino-3-methoxyphenyl)-4H-1-benzopyran-4-one (PD98059), (E)-3-(4-Methylphenylsulfonyl)-2-propenenitrile (BAY 11-7082), cycloheximide (CHX), mouse anti-ƃ-actin antibody, mouse anti-ABCG1 antibody and anti-mouse secondary antibody coupled to horseradish peroxidase were from Sigma-Aldrich (St Louis, MO, USA). Lipofectamine 2000 reagent, Opti-MEM medium and fetal bovine serum (FBS) were purchased from Invitrogen (Carlsbad, CA, USA). Penicillin and Streptomycin was purchased from Gibco. Human HDL, apoA-I and polymyxin B (PMB) were obtained from Calbiochem (San Diego, CA, USA). 2-Chloro-5-nitro-N-4-pyridinyl-benzamide (T0070907), N-[2-(Cyclohexyloxy)-4-nitrophenyl]methanesulfonamide (NS-398), 4-(4-Fluorophenyl)-2-(4-methylsulfinylphenyl)-5-(4-pyridyl)-1H-imidazole (SB203580), 1,9-Pyrazoloanthrone,

Anthrapyrazolone (SP600125), cisglitazone, mouse anti-COX-2 antibody, and NF-ϞB (p50) Transcription Factor Assay Kit were purchased from Cayman Chemical (Ann Arbor, MI, USA). Mouse anti ERK1/2 antibody, anti-phospho-ERK 1/2 (Thy202/Tyr204) antibody, mouse anti-phospho-p38 MAPK (Thr180/Thr182) and mouse anti-phospho-JNK (Thr183/Thr185) antibody were from Cell Signaling Technology (Beverly, MA, USA). Mouse anti-ABCA1 antibody was from Millipore (Billerica, MA, USA). Mouse anti-LXRŬantibody and anti-PPARↄ were from Abcam (Cambridge, MA, USA). Mouse anti-IϞB antibody was from R&D Systems (Minneapolis, MN, USA). Anti-mouse TLR2 and anti-mouse TLR4 antibodies were from eBioscience (San Diego, CA, USA). Cignal^{TM} PPAR Reporter Assay Kit was from SABiosciences (Frederick, MD, USA). RNeasy Mini Kit, Gel Extraction kit and Midipreparation kit were purchased from Qiagen (Hilden, Germany). The LightCycler RNA Master SYBR Green I kit and Mini proteinase inhibitor cocktail tablet were obtained from Roche (Penzberg, Germany). Nuclear Extract Kit and TransAM PPARↄ kit were purchase from Active Motif (Carlsbad, CA, USA). Biotin 3ô-End DNA Labeling Kit, light shift chemiluminesencent EMSA kit, Chemiluminescent Nucleic Acid Detection Module, SuperSignal West Pico Chemiluminescent Substrate, Biodyne precut nylon membranes, and Clear Blue X-ray film were purchased from Pierce (Rockford, IL, USA). 30% acrylamide and bis-acrylamide solution and Bradford protein assay reagent was purchased from Bio-Rad Laboratories (Hercules, CA, USA). Plasma membrane protein extraction kit was from BioVision (Mountain view, CA, USA). THP-1 was purchased from ATCC. HCAEC cell line and EGM-2MV Bulletkit were obtained from clonetics. BCA protein Assay Kit was purchased from Pierce. The primers, synthetic peptides, WKYMVM, MMK-1, HFYLPM,

F-peptide, and WRW4 were synthesized by 1st Base (Singapore). The 96-well white plates used for luciferase activity assay were obtained from NUNC (Denmark). SAA enzyme-linked immunosorbent assay (ELISA) kit was from Biosource (Belgium). The vector pcDNAÊ 3.1(+), One-step RT-PCR Kit, Dual-Luciferase Reporter Gene Assay system were obtained from Promega (Madison, WI, USA). BigDye™ Terminator Cycle Sequencing Ready Reaction kit was from Applied Biosystems.

2.2 ROUTINE CELL LINE MAINTENANCE

2.2.1 Cells lines

Cell lines used in this project were listed in Table 3.

Table 3 Cell lines used in this study

Name	Details	Source
HepG2	Hepatocellular carcinoma cells	Lab stock ATCC No. HB-8065
THP-1	Human acute monocytic leukemia cell line	Lab stock ATCC No. TIB-202
HCAEC	Human Coronary Artery Endothelial Cells	Lab stock Lonza No. CC-2585

2.2.2 Cells culture media

Culture medium for HepG2:

Dulbecco's Modified Eagle Medium (DMEM)

10% (v/v) fetal bovine serum (FBS)

2 mM L-glutamine

100 units/ml penicillin/streptomycin

Culture medium for THP-1:

RPMI-1640

10% (v/v) fetal bovine serum (FBS)

2 mM L-glutamine

100 units/ml penicillin/streptomycin

0.05 mM ϐ-mercaptoethanol

1 mM sodium pyruvate

10 mM HEPES

Culture medium for HCAEC:

Endothelial cell basal medium-2 (EGM-2)

5% (v/v) fetal bovine serum (FBS)

GA-1000 (Gentamicin, Amphotericin-B)

Growth supplements: hEGF, hydrocortisone, VEGF, hFGF-B, R^3-IGF-1, ascorbic acid

Freezing media:

90% (v/v) FBS

10% (v/v) Dimethyl sulfoxide (DMSO)

2.2.3 General cells culture procedures

Culture procedures for HepG2 and HCAEC:

In setting up a culture, an appropriate amount of medium (1 ml/5 cm^2) was added to the tissue-culture grade flasks (Nunc) and equilibrated in a 37°C humidified incubator

(Thermo Forma, Marietta, OH) with 5% CO_2 for at least 30 minutes. The cryovial containing cells was incubated in a 37°C water bath until the frozen contents were almost fully thawed and then added drop-wise to 10 ml of culture media in a class II biological safety cabinet (Gelman). Cells were centrifuged at 1,000 rpm for 5 minutes to remove the freezing buffer containing DMSO. Cells were resuspended with medium and seeded into the culture flasks at a concentration of 2,500-5,000 cells/ cm^2. After overnight incubation, cells were attached to the wall and started to grow. The culture medium was changed to remove the cell debris. Subsequently, the cells were cultured with a change of medium every other day. Upon obtaining 90% confluence, the cells were detached from the surface by 0.025% trypsin-ethylenediaminetetraacetic acid (EDTA) and split at a 1-to-4 ratio into tissue culture flasks. Briefly, a culture flask was washed twice with 1x PBS and added with appropriate amount of 0.025% trypsin (1 ml/25 cm^2). The trypsinization was continued for 5 minutes at 37°C. After gentle rapping, cells were detached and 10 ml of full-supplemented medium was added to neutralize the trysin. Cells were transferred to a 15 ml tube and centrifuged at 1000 rpm for 5 min to obtain a cell pellet. After removing the supernatant, cells were resuspended with the appropriate volume of medium to obtain a concentration of between 0.5-2 x 10^6 cells/ml and plated out on new tissue-culture dishes/flasks.

These cells lines were frozen via the standard slow cooling protocol. Briefly, cultures were centrifuged at 1,000 rpm for 5 minutes after trypsinization and neutralization. The pellet was then resuspended in freezing media and split into cryovials (Nalgene; 1 ml per vial). The vials were placed into a Mr. Frosty freezing aid (Nalgene)

and incubated at -80°C overnight. The next day, the vials were transferred to a liquid nitrogen tank.

Culture procedures for THP-1:

In setting up a culture, an appropriate amount of medium (1 ml/5 cm^2) was added to the tissue-culture grade flasks (Nunc) and equilibrated in a 37°C humidified incubator (Thermo Forma, Marietta, OH, USA) with 5% CO_2 for at least 30 minutes. The cryovial containing cells was incubated in a 37°C water bath until the frozen contents were almost fully thawed and then added drop-wise to 10 ml of culture media in a class II biological safety cabinet (Gelman). Cells were plated into the culture flasks at a concentration of 2 x 10^5 cells/ cm^2. After overnight incubation, cells were centrifuged at 1,000 rpm for 5 minutes to remove the DMSO and resuspended in 10 ml of fresh media. The cells were subcultured when the cell concentration reached 1 x 10^6 cells/ml and split at a 1-to-4 ratio into tissue culture flasks. Cells were transferred to a 15 ml tube and centrifuged at 1000 rpm for 5 minutes to obtain a cell pellet. After removing the supernatant, cells were resuspended with the appropriate volume of medium to obtain a concentration of between 2 x 10^5 cells/ml and seeded in new tissue-culture dishes/flasks.

Cells were seeded at 2 x 10^6 cells/ml into 35 mm culture wells (2 ml/well) in medium supplemented with 50 ng/ml phorbol 12-myristate 13-acetate (Sigma) for 5 days to differentiate into macrophage.

THP-1 cells were frozen via the standard slow cooling protocol. Briefly, cultures were centrifuged at 1,000 rpm for 5 minutes. The pellet was then resuspended in freezing media and split into cryovials (Nalgene; 1 ml per vial). The vials were placed into a Mr.

Frosty freezing aid (Nalgene) and incubated at -80°C overnight. The next day, the vials were transferred to a liquid nitrogen tank.

2.3 SAA TREATMENT

In SAA treatment studies, cells were cultured to confluence in 6-well plates and stimulated with 5-40 µg/ml of SAA for 0-24 hours. The normal SAA level is considered to be less than 0.1 µM or 1.25 µg/ml. Under inflammatory conditions, the maximal levels could be up to 80 µM or 1 mg/ml [257]. The concentrations of SAA (5ï 40 µg/ml) tested were within the range that represented low-grade inflammation, a level which has been shown to put an individual at risk of CAD by many clinical studies [124, 258]. In the PPARɔ receptor study, cells were pretreated with 1 nM of PPARɔ antagonist, T0070907 for 1 hour and then treated with 20 µg/ml of SAA or 5 µM of PPARɔ agonist, ciglitazone in serum-free medium for 4 and 8 hours. To investigate the effect of possible endotoxin contaminants in recombinant protein sample, SAA (20 µg/ml) was either treated with polymyxin B (50 µg/ml) for 45 minutes at 37°C in PBS or heated at 100°C for 30 minutes.

In the mitogen-activated protein kinases (MAPK) pathway, COX-2 and NF-ʏB pathway study, cells were pretreated with vehicle, 50 µM of ERK1/2 inhibitor, PD98059, 10 µM of p38 inhibitor, SB203580, 10 µM of JNK inhibitor, SP600125, 10 µM of COX-2 inhibitor, NS-398 or 10 µM of NF-ʏB inhibitor, BAY 11-7082 each for 1 hour and then treated with 20 µg/ml SAA in serum-free medium for indicated times. In the receptor blocking study, cells were pretreated with vehicle, 500 ng/ml of FPRL-1 inhibitor, PTX, 5 µM of SR-BI inhibitor, BLT-1, 5 mg/ml of anti-TLR2 or anti-TLR4 for 1 hour and then

treated with 20 µg/ml of SAA for 4 hours. To determine if ERK1/2 phosphorylation was induced by SAA directly or mediated through synthesis of other signaling proteins, 100 µM of the translation inhibitor, cycloheximide (CHX), was added to the cells for 1 hour before SAA treatment.

2.4 MEASUREMENT OF ENDOTOXIN ACTIVITY

The endotoxin activity of SAA was determined using the Limulus amebocyte lysate (LAL) assay kit (Lonza). LAL test is a quantitative test for gram-negative bacterial endotoxin. LAL assay was performed according to the manufacturerôs recommendations. Briefly, the sterile microplate was pre-equilibrated at 37°C for 10 minutes. 50 µl of sample or standard was carefully dispensed into the appropriate microplate well. At time T = 0, 50 µl of LAL was added into each well and mixed by tapping the side of the plate repeatedly. At T = 10 minutes, 100 µl of pre-warmed substrate solution was added and mixed by pipetting up and down. At T = 16 minutes, 100 µl of stop solution (10% sodium dodecylsulfate solution) was added to stop the reaction. Te absorbance was read at 405 nm on a spectrophotometer. The endotoxin concentration was calculated according to the manufacturerôs instructions. We found that 10 µg SAA contained 4.1 endotoxin unites (EU).

2.5 RNA ISOLATION

Total RNA was isolated from fresh cells using RNeasy Mini Kit (Qiagen). The cells were cultured to confluence and treated with 5-40 µg/ml of SAA for 0-24 hours. At the endpoint, cells were washed twice with 1 x PBS and disrupted by addition of Buffer

RLT containing 1% (v/v) ß-mercaptoethanol. The lysate was homogenized by passing 30 times through a 1 ml tip. One volume of 70% ethanol was added to the homogenized lysate and mixed well by pipetting. The sample was applied to an RNeasy mini column and centrifuged for 15 seconds at 13,000 rpm. The flow-through was discarded and the column was washed with Buffer RW1. After washing two more times with Buffer RPE, the column was centrifuged for 2 minutes at 13,000 rpm to dry the RNeasy silica-gel membrane. Finally, 30-50 µl RNase-free water was added directly onto the membrane and centrifuged at 13,000 rpm for 1 minute. The concentration of the eluted total RNA was quantified by NanoDrop N-1000 UV-Vis Spectrophotometer (Thermo Scientific).

2.6 QUANTITATIVE REAL-TIME PCR (qRT-PCR)

Quantitative real-time PCR was used to investigate the gene expression profile. To obtain enough statistical power, each group had at least 3 individual samples. The LightCycler RNA Master SYBR Green I kits (Roche) were used to quantify the starting mRNA of the selected genes. This kit uses a hot-start reverse transcription-PCR protocol to provide very sensitive detection and quantification of defined RNA sequences. The house-keeping gene glyceraldehydes-3-phosphate dehydrogenase (GAPDH) was used as an internal control. Following the manufacturerôs instructions, 90 ng of RNA template, primers, $Mn(OAc)_2$, and LightCycler RNA Master SYBR Green I were mixed well and transferred into LightCycler capillaries. The LightCycler 2.0 system program was set up to conduct reverse transcription, denaturation, amplification, melting curve analysis, and final cooling. The temperature and duration of each procedure was set up as recommended by the manufacturerôs manual.

The sequences of the primers used were as follows:

Table 4 Primer sequences for qRT-PCR analysis

GAPDH	F	5ô- CACTCCACCTTTGACGC -3ô
	R	5ô- GGTCCAGGGGTCTTACTCC -3ô
ABCG1	F	5ô- CAGTCGCTCCTTAGCACCA -3ô
	R	5ô- TCCATGCTCGGACTCTCTG -3ô
ABCA1	F	5ô- GGAGGCAATGGCACTGAGGAA -3ô
	R	5ô- CCTGCCTTG TGGCTGGAGTGT -3ô
LXRŬ	F	5ô- AGCGTCCACTCAGAGCAAG -3ô
	R	5ô- ACAGTCATTCGTGCACATCC -3ô
PPARɔ	F	5ô- TCTGGCCCACCAACTTTGGG -3ô
	R	5ô- CTTCACAAGCATGAACTCCA -3ô
COX-1	F	5ô- GCTATTCCGGCCCCAACT -3ô
	R	5ô- GATGAAGGTGGCATTGACAAACT -3ô
COX-2	F	5ô- ACTGTACGGGGTTTGTGACTGG -3ô
	R	5ô- GAAAGGGCATTAATTAGAATGGGAACG -3ô
SAA1	F	5ô- CTGCAGAAGTGATCAGCG -3ô
	R	5ô- ATTGTGTACCCTCTCCCC -3ô
SAA2	F	5ô- CTGCAGAAGTGATCAGCA -3ô
	R	5ô- ATTATATGCCATATCTCAGC -3ô
SR-BI	F	5ô- ACCGCACCTTCCAGTTCCAG -3ô
	R	5ô- ATCACCGCCGCACCCAAG -3ô

The qRT-PCR conditions were:

Reverse transcription	61°C	20 min	
Denaturation	95°C	1 min	
Denaturation	95°C	5 sec	
Annealing	55°C	10 sec	45 cycles
Extension	72°C	13 sec	

The crossing point of each sample was measured and the relative treatment versus control ratio of each target gene was analyzd with LightCycler Software Version 3.5. A gene-specific mRNA was normalized to GAPDH mRNA. The expression of each mRNA was determined using the $2^{-\varphi CT}$ threshold cycle method [257].

2.7 PROTEIN EXTRACTION

The stimulated and unstimulated cells in 6-well plate were washed with ice-cold 1 x PBS. The cells were lysed with 1 x cell lysis buffer (62.5 mM Tris-HCL, pH 6.8, 2% w/v SDS, 10% glycerol and 50 mM DTT, proteinase inhibitor cocktail). After homogenizing by repeated passing through a 27-gauge needle, detergent insoluble materials were pelleted by centrifugation for 10 minutes at 12,000 rpm at 4°C. The soluble supernatant fraction was transferred to a new tube. Total protein concentrations were determined by BCA protein Assay Kit (Pierce) according to the manufacturerôs instruction with BSA as standard. Protein samples were stored at -80°C.

2.8 MEMBRANE PROTEIN EXTRACTION

Membrane proteins were extracted by plasma membrane protein extraction kit (BioVision). The stimulated and unstimulated cells in 6-well plate were scraped in 1x PBS and harvested by centrifugation at 3000 rpm for 5 minutes. Cells were washed with 1 ml of ice cold 1x PBS before lysis. The cell pellet was homogenized in 1 ml of Homogenize Buffer Mix for 30-50 times on ice. The homogenate was transferred to a 1.5 ml microcentrifuge tube and spinned at 700 g for 10 minutes at 4°C. The resulting pellet was the total cellular membrane protein. The protein concentrations were determined by BCA protein Assay Kit (Pierce). Membrane protein samples were stored at -80°C.

2.9 SDS-PAGE AND WESTERN BLOT

15% SDS-PAGE gels were usually used in this study. The gels were casted as follows:

Table 5. Compositions of SDS-PAGE

Component	**Final concentration**
Separating Gel	
30% Acrylamide: Bis (29:1)	2.25 ml
1.5 M Tris-Cl pH 8.8	1.125 ml
10% SDS	45 µl
10% Ammonium persulphate	45 µl
TEMED	3.6 µl
H_2O	1.035 ml
Stacking Gel	
30% Acrylamide: Bis (29:1)	265 µl
1.0 M Tris-Cl pH 6.8	187.5 µl
10% SDS	15 µl
10% Ammonium persulphate	15 µl
TEMED	1.5 µl
H_2O	1.013 ml

Thirty-microgram of protein samples were loaded and separated via 10-15% SDS-PAGE. After an electrotransfer for 2 hours at 100 V, the nitrocellulose membranes were blocked for 1 hour in blocking buffer (5% non-fat milk, 25 mM Tris, 137 mM NaCl, 3 mM KCl, 0.1% Tween-20, 0.05% sodium azide, pH 7.4,). After blocking, the membranes were washed with TTBS buffer (25 mM Tris, 137 mM NaCl, 3 mM KCl, 0.1% Tween-

20, 0.05% sodium azide, pH 7.6) for three times, 10 minutes each. The membrane was then placed in primary antibodies diluted in 5 ml blocking buffer for 1 hour at room temperature or overnight at 4°C. After washing, the membrane was incubated with diluted secondary antibody for 1 hour at room temperature. The blots were developed with SuperSignal West Pico Chemiluminescent substrate (Pierce) for 5 minute and exposed with Clear Blue X-ray film (Pierce). Anti-ABCA1 antibody (Millipore), anti-ABCG1 antibody (Sigma-Aldrich), anti-LXRŬ antibody (Abcam), anti-PPARↄ antibody (Abcam), anti-I↯B antibody (R&D systems), anti-COX-2 antibody (Cayman Chemical), anti-ERK1/2 antibody (Cell Signaling) and anti-phospho-ERK 1/2 (Thy202/Tyr204) (Cell Signaling) antibody were used at a concentration of 1:1000. Anti-ɓ-actin antibody (Sigma-Aldrich) was used at a concentration of 1:5000. Anti-rabbit secondary antibody (Cell Signaling) and anti-mouse secondary antibody (Thermo Scientific) coupled to horseradish peroxidase were used at a concentration of 1:10000.

2.10 NUCLEAR PROTEIN EXTRACTION

Nuclear protein was isolated using the Nuclear Extract Kit. Briefly, HepG2 cells (1×10^6 cells) were incubated with 20 µg/ml of SAA for different times as indicated. Cells were washed twice with 5 ml of ice-cold PBS/Phosphatase Inhibitor Solution (1 x PBS, 20 mM NaF, 1 mM ɓ-glycerophosphate, 1 mM Na_3OV_4) and centrifuged at 300 x g for 5 minutes at 4°C to harvest the cells. Cell pellet was resuspended in 300 µl of ice-cold Hypotonic Buffer (20 mM Hepes, pH 7.5, 5 mM NaF, 10 µM Na_2MoO_4, 0.1 mM EDTA) and incubated on ice for 15 minutes to allow cells to swell. Then 30 µl of 10% Nonidet P-40 was added into the cells and followed by 30 seconds centrifugation at 4°C in a

microcentrifuge (Beckman). The pellet was resuspended in 30 µl of ice-cold extraction buffer (10 mM Hepes, pH 7.9, 0.1 mM EDTA, 1.5 mM $MgCl_2$, 420 mM NaCl, 0.5 mM DTT, 0.5 mM PMSF, 1 µg/ml Pepstatin A, 1 µg/ml Leupeptin, 10 µg/ml Aprotinin, 20 mM NaF, 1 mM ß-glycerophosphate, 10 mM Na_3OV_4, 25% glycerol) and vortexed for 15 seconds at highest setting. The tubes were rocked gently on ice for 30 minutes on a shaking platform (Stuart Scientific). Finally, the samples were centrifuged at 14,000 x g for 10 minutes at 4°C. The supernatant (nuclear fraction) was transferred into a pre-chilled microfuge tube and stored at -80°C in aliquots. One small aliquot of nuclear extract was used to quantitate the protein concentration.

2.11 CHOLESTEROL EFFLUX ASSAY

Cells were seeded on six-well plates at a density of 5×10^5 cells/well. After incubation for 24 hours, the cells were labeled with 1 µCi/ml [^{3}H]cholesterol (PerkinElmer) for 24 hours in medium containing 10% FBS. The cells were washed five times with PBS containing 1 mg/ml BSA and equilibrated in serum-free medium containing 0.2% fatty acid-free BSA for 16 hours. HepG2 cells labeled with [^{3}H] cholesterol were preincubated with SAA (20 µg/ml) or H_2O as a control for 4 hours. Following incubation, the cells were washed extensively with PBS to remove all radioactivity in the preincubation medium. Thereafter, cells were incubated for 1-24 hours at 37 °C in media with or without lipoproteins or lipid free apolipoproteins (HDL, 40 µg/ml; apoA-I, 10 µg/ml). Following incubation, the medium was collected, and cells were washed three times with PBS containing 1 mg/ml fatty acid-free BSA. Radioactivity in the medium was measured directly in a liquid scintillation counter. Cells were lysed

with 0.1 N NaOH and 0.1% SDS for 30 minutes at room temperature and counted for radioactivity. Efflux was calculated as the percentage of counts in the medium to the counts in the medium and cells together.

2.12 PPARɔ ACTIVITY ASSAY

PPARɔ transcription factor activity was assayed using an enzyme-linked immunosorbent assay-based kit to detect and confirm activation of the PPARɔ transcription factor (Active Motif, Carlsbad, CA, USA). HepG2 cells were seeded on the six-well plate in the serum-free medium for 24 hours and treated with SAA (20 µg/ml) or one of the following controls: LPS (4 ng/ml and 100 ng/ml), heat-treated LPS and SAA (100 °C, 30 minutes), LPS and SAA treated with polymyxin B (50 µg/ml, 1 hour), and apoA-I (20 µg/ml) for 4 hours. The cells were then rinsed, and nuclear protein was extracted as described in 2.10. Nuclear extracts were added to a 96-well plate containing immobilized oligonucleotides bearing peroxisome proliferators-response elements (5ô-AACTAGGTC AAAGGTCA-3ô). After 1 hour, the wells were incubated with diluted primary PPARɔ antibody to detect the accessible epitope on PPARɔ protein upon DNA binding. The horseradish peroxidase-conjugated secondary antibody was added and incubated for 1 hour at room temperature. The reaction was stopped with stopping solution and the absorbance was read at 450 nm on a spectrophotometer (Spectra Plus, TECAN).

2.13 ELECTROPHORETIC MOBILITY SHIFT ASSAY (EMSA)

HepG2 cells were seeded on the six-well plate in the serum-free medium for 24 hours and treated with SAA (20 µg/ml) for 4 hours. Nuclear extracts were prepared with a Nuclear Extraction Kit (Active Motif, Carlsbad, CA, USA). The double-stranded oligonucleotide probe containing the PPRE motif (5ô-CAAAACTAGGTCAAAGGTCA-3ô) was labeled with biotin using the Biotin 3ô-End DNA Labeling Kit (Pierce, Rockford, IL, USA). Labeling reaction mixture consisting of 25 µl of ultrapure water, 10 µl of 5x TdT reaction buffer, 5 pmol of probe, 5 µl of 5 µM Biotin-11-dUTP and 5 µl of 2 U/µl TdT (terminal deoxynucleotidyl transferase) was added in a 0.2 ml PCR tube and the reaction was incubated at 37°C for 30 minutes. 2.5 µl of 0.2 M EDTA was added into the tube to stop the reaction. 50 µl of chloroform:isoamyl alcohol (24:1) was added into each reaction to extract the TdT. The aqueous phase was kept for EMSA assay. The probes were annealed by mixing equal amounts of labeled complementary oligos, denatured at 90°C for 1 minute, and slowly cooled and incubated at 48°C (melting temperature) for 30 minutes.

PPARɔ binding activity was determined using the light shift chemiluminesencent EMSA kit (Pierce). The nucleoprotein binding reaction was performed via combination of 5 µg of nuclear extract and labeled probe for 30 minutes in all reactions at room temperature in the presence or absence of a 200-fold excess of unlabeled specific PPRE probe or unlabeled mutated PPRE probe (5ô-CAAAACTAGCACAAAGCACA-3ô). For the supershift experiment, extracts were preincubated with 2 µg of monoclonal anti-PPARɔ (Active Motif) for 30 minutes before the labeled probe was added. Protein/DNA mixtures were separated on 6% non-denaturing polyacrylamide gels in 0.5x TBE (45 mM

Tris-HCl, 45 mM Boric acid, 1 mM EDTA, pH 8.3) at 100 V. Proteins and bound probes were transferred to a positively charged nylon membrane (Pierce) in 0.5x TBE at 380 mA for 1 hour. The transferred DNA was cross-linked to the membrane with UV stratalinker 1800 (Stratagene). The biotin-labeled DNA was detected with a Chemiluminescent Nucleic Acid Detection Module (Pierce), developed and exposed with Clear Blue X-ray film (Pierce).

For NF-ʢB EMSA assay, the double-stranded consensus oligonucleotides used in this study was: 5ô-AGTTGAGGGGACTTTCCCAGGGC-3ô. The unlabeled mutated probe was: 5ô-AGTTGAGGCGACTTTCCCAGGC-3ô.

2.14 TRANSFECTION AND LUCIFERASE ASSAY

The PPRE-luc reporter and *Renilla* luciferase construct were purchased from SABiosciences. The PPRE-luc construct encodes the firefly luciferase reporter gene under the control of a minimal (m) CMV promoter and tandem repeats of the PPAR transcriptional response element. This construct monitors both increases and decreases in the transcriptional activity of PPAR. The constitutively expressing *Renilla* construct encodes the *Renilla* luciferase reporter gene under the control of a CMV immmediatly early enhancer/promoter and acts as an internal control for normalizing transfection efficiencies and monitoring cell viability. PPARɔ cDNAs were cloned into mammalian expression vector pcDNA3.1 between KpnI and XhoI restriction sites. To measure the PPARɔ activity, HepG2 cells (1.25×10^5 cells/well) were transfected with PPRE-luc or *Renilla* luciferase construct and pcDNA3.1- PPARɔ using Lipofectamine 2000 reagent (Invitrogen) according to the manufacturerôs protocol. After transfection for 48 hours, the

cells were stimulated by SAA (20 µg/ml) or H_2O for 4 hours, lysed and subjected to luciferase assays using a Dual-Luciferase Reporter Gene Assay system (Promega) according to the manufacturerôs instructions. Serum-free medium was used for the treatment of HepG2 cells with SAA (20 µg/ml).

For luciferase activity assays, a Dual-Luciferase Reporter Gene Assay system (Promega) was used. Briefly, the medium was removed, cells were rinsed with 1x PBS and lysed by incubation for 15 minutes at room temperature with 1x Passive Lysis Buffer. Aliquots of 20 µl of cell lysate were transferred to white opaque 96-well plate (Nunc) prior to addition of 100 µl of Luciferase Assay Buffer II. Firefly luciferase activity was determined by an automatic luminometer *(*Wallac 1420 VICTOR^2 multilabel counter, PerkinElmer life sciences). Renilla luciferase activity was measured by the same machine after dispensing 100 µl of Stop & Glo Reagent. Triplicate wells were prepared for each condition and each experiment was repeated at least three times.

2.15 EIA FOR 15d-PGJ$_2$

The 96-well based EIA kit of 15d-PGJ$_2$ was purchased from Cayman Chemical. Cells cultured in six-well plates were pretreated with one of the following experimental controls: 50 µM PD98059, 10 µM COX-2 inhibitor, NS-398 or vehicle for 1 hour. The cells were then treated with 20 µg/ml of SAA for 2 hours. The cells were then homogenized in assay buffer by repeated passing through a 27-gauge needle. An aliquot of the cell lysate was used for protein determination. Briefly, the kit uses a polyclonal antibody against 15d-PGJ$_2$ to bind, in a competitive manner, the prostaglandin in the sample or an alkaline phosphatase molecule that has 15d-PGJ$_2$ covalently attached to it.

After a simultaneous incubation, the excess reagents were washed away and p-nitrophenyl phosphate substrate was added. After a short incubation time, the enzyme reaction was stopped and the yellow color generated was evaluated on a microplate reader at 405 nm. The concentration of intracellular 15d-PGJ_2 was determined by the EIA kit according to the manufacturerôs instructions.

2.16 NF-ŞB (p50) TRANSCRIPTION FACTOR ASSAY

The nuclear NF-ŞB level was measured by NF-ŞB (p50) Transcription Factor Assay Kit. This assay combines the principal of the electrophoretic mobility shift assay (EMSA) and ELISA. Briefly, 10 µg nuclear extract was incubated for 1 hour in the wells pre-coated with a specific double stranded DNA (dsDNA) sequence containing the NF-ŞB response elements. After washing, the sample wells were incubated with specific primary antibody against NF-ŞB (human p50) for 1 hour. The sample wells were washed again and HRP-conjugated secondary antibody was added and incubated for another 1 hour at room temperature. After a thorough washing, the samples wells were incubated with 100 µl of developing solution for 15-45 minutes. When the positive control sample turned into dark blue color, 100 µl of stop solution was added into each well. The absorbance was read at OD 450 nm in a spectrophotometric plate reader (Spectra Plus, TECAN).

2.17 SAA-HDL ASSOCIATION

To study the effect of lipid-associated SAA, high density lipoprotein (HDL)-associated SAA was prepared in medium via addition of various concentrations of HDL

to SAA (20 µg/ml) before incubation at room temperature for 15 minutes with shaking. The medium was then incubated at 37 °C for 15 minutes before treatment.

2.18 siRNA-MEDIATED GENE SILENCING

Scrambled control RNA oligonucleotides and siRNA to SAA1, SAA2, ABCA1, ABCG1 and SR-BI obtained from Dharmacon were used to suppress their expression in HepG2 cells. The transfection of siRNA was performed using Lipofectamine 2000 (Invitrogen) according to the manufacturerôs instructions. Briefly, HepG2 cells grown in 6-well plates were transfected with 100 pmol of siRNA using Lipofectamine 2000 in Opti-MEM medium (Invitrogen). After 4 hours incubation, the medium was changed to complete DMEM medium. The cells were incubated for a further 44 hours, washed and stimulated with 20 µg/ml of SAA for 4 hours. The cells were harvested for RNA extraction, nuclear extraction, quantitative real-time PCR, cholesterol efflux assay and PPARɔ transcriptional activity assay.

The sequences of the primers used were as follows:

Table 6. siRNA sequences for gene silencing.

Name	Cat. No.	siRNA sequence
ABCA1	J-004128-06	5ô-GAAGAAAACUGGUGUCUAU-3ô
	J-004128-07	5ô-GGAGAUGGUUAUACAAUAG-3ô
	J-004128-08	5ô-GCACUAGGAUGGCAAUCAU-3ô
	J-004128-09	5ô-AAACAUUGCUGCAUAGUCU-3ô
ABCG1	J-008615-05	5ô-UCAUUGGCCUGCUGUACUU-3ô
	J-008615-06	5ô-GCGCAUCACCUCGCACAUU-3ô
	J-008615-07	5ô-GGAAAUGGUCAAGGAGAUA-3ô
	J-008615-08	5ô-AUACAAGACCCUCCUGAAA-3ô
SAA1	J-019361-05	5ô-UUACAUCGGCUCAGACAAA-3ô
	J-019361-06	5ô-CAGCGAUGCCAGAGAGAAU-3ô
	J-019361-07	5ô-CUGGCCUGCCUGAGGGGUA-3ô
	J-019361-08	5ô-CCCAAUCACUUCCGACCUG-3ô
SAA2	J-016279-09	5ô-CCGAUCAGGCUGCCAAUAA-3ô
	J-016279-10	5ô-CCAGAGACUCACAGGCCAU-3ô
	J-016279-11	5ô-UCAAAGUUAGUGAGGUCUA-3ô
	J-016279-12	5ô-GUCCAGAGAAGCUGAGAUA-3ô
SR-BI	J-010592-05	5ô-GGACAAGUUCGGAUUAUUU-3ô
	J-010592-06	5ô-GAACGUGCCUUCAUGAACC-3ô
	J-010592-07	5ô-GGGAGACUCUUCACACAUU-3ô
	J-010592-08	5ô-GAACUGCUCUGUGAAACUG-3ô
ON-TARGETplus		5ô-UGGUUUACAUGUCGACUAA-3ô

NON-targeting Pool	D-001810-10-20	5ô-UGGUUUACAUGUUGUGUGA-3ô
		5ô-UGGUUUACAUGUUUUCUGA-3ô
		5ô-UGGUUUACAUGUUUUCCUA-3ô

2.19 BACTERIAL WORK

2.19.1 Media

Luria Broth (LB) containing10 g of tryptone, 5 g of NaCl and 5 g of yeast extract in 1 liter sterile water was used for all bacteria culture in this project. LB agar plate was used for initial bacteria growth. 100 µg/ml of ampicillin was used for selection of bacteria carrying transformed vectors whenever necessary.

2.19.2 Competent cell preparation

DH5Ŭ *supE*44 *AlacU*169 (p80 *lacZ* AM15) *hsdR17 recA1 endA1 gyrA96 thi-1 relA1 E.coli* cells (NEB) were streaked onto LB agar plates and cultured overnight at 37°C. A single colony was then picked and inoculated into 50 ml LB media and incubated at 300 rpm, 37°C until the OD_{600} value reached 0.6. The cultures were harvested via centrifugation at 4000 g for 5 minutes at 4°C. The resultant pellet was resuspended in 30 ml of cold 0.1 M $MgCl_2$ (Sigma) and centrifuged again at 4000 g for 5 minutes at 4°C. With the supernatant discarded, the pellet was resuspended in 20 ml of 0.1 M $CaCl_2$ (Sigma) and kept on ice for 30 minutes. The cells were collected via centrifugation at 4000 g for 5 minutes at 4°C, resuspended in 2 ml of cold 0.1 M $CaCl_2$/15% glycerol (Sigma) and aliquoted to 100 µl/tube to be stored at -80°C. These bacteria were then ready for transformation.

2.19.3 Isolation of plasmid DNA from E.coli

2.19.3.1 Small scale preparation of plasmid DNA

Small scale extraction of plasmid DNA was performed following a standard miniprep protocol. Briefly, a 1.5 ml overnight culture of *E.coli* was transferred to a 1.7 ml eppendorf tube and the medium was removed by spinning the cells at maximum speed (13,300 rpm) for 1 minute in a microfuge (Sorvall Legend micro 17 centrifuge, Thermo Scientific). The supernatant was discarded and the pellet was resuspended in 100 µl of ice-cold solution I (25 mM Tris, pH 8.0, 10 mM EDTA, pH 8.0, 50 mM glucose) by vigorous vortex. 200 µl of freshly prepared solution II (0.2 M NaOH, 0.1% SDS) was then added and the tube was immediately inverted 5 times to mix. Following 2 minutes of incubation on ice, 150 µl of cold solution III (3.0 M potassium acetate, 0.5 M acetic acid, pH 4.8) was added and the tube was then vortexed briefly to mix again. After 5 minutes incubation on ice, the tube was centrifuged at 13,300 rpm for 5 minutes and the supernatant was transferred to a new tube. 0.9 ml of 100% ethanol was then added to precipitate the DNA and the mixture was vortexed shortly. After 5 minutes of incubation at room temperature, the tube was centrifuged at the same speed for 5 minutes. The supernantant was removed carefully and the pellet was rinsed with 1 ml of 70% ethanol. The tube was centrifuged again and the supernatant was discarded. The DNA pellet was air-dried and dissolved in 25 µl of TE buffer with 20 µg/ml of RNase (Promega). The samples were stored at -20°C for further analysis.

2.19.3.2 Large scale preparation of plasmid DNA

Large scale extraction of plasmid DNA was carried out using the QIAGEN midi-

preparation kit (Hilden, Germany). An overnight 3 ml of *E.coli* culture was refreshed in 100 ml of LB containing respective selection antibiotic, ampicillin (Amp). The cells were grown at 37°C with vigorous shaking at 200 rpm for 8 hours. The cells were harvested by centrifugation at 6,500 rpm in Beckman JA-14 rotor for 15 minutes at 4°C. The medium was discarded and 4 ml of buffer P1 was added to lyse the cells. Another 4 ml of buffer P2 was added and mixed gently by inverting it several times. After 5 minutes incubation at room temperature, 3 ml of chilled buffer P3 was added and the tube was inverted several times again. Following 15 minutes incubation on ice, the tube was then centrifuged at 13,000 rpm for 30 minutes at 4°C. The supernatant was removed promptly and subjected to another round of centrifugation. The supernatant was transferred to another tube promptly. At the same time, a QIAGEN-tip 100 was equilibrated with 4 ml of buffer QBT and the column was emptied by gravity flow. The supernatant obtained earlier was added into the column and was emptied by gravity flow. The QIAGEN-tip 100 was washed twice with 10 ml of buffer QC. The DNA was eluted with buffer QF. The DNA collected was precipitated with 3.5 ml of isopropanol. After 15 minutes incubation at room temperature, the tube was centrifuged at 13,000 rpm for 30 minutes at 4°C. The supernatant was discarded and the resulting pellet was washed with 1.5 ml of 70% ethanol and centrifuged again at 13,000 rpm for 20 minutes at 4°C. The pellet was air-dried and dissolved in 100 µl TE buffer, pH 8.0 containing RNase. The resulting plasmid was stored at -20°C.

2.20 CLONING

2.20.1 Cloning of SAA1 in the pcDNAÊ 3.1(+) vector

2.20.1.1 Reverse transcriptase-PCR and purification

Total RNA from the cells was extracted using RNeasy MiniKit (QIAGEN) according to the manufacturerôs protocol, and concentrations were determined spectrophotometrically at ∂260. 100 ng of RNA was used as the template for RT-PCR using a One-step RT-PCR Kit (Promega). The primers used were SAA1F: 5ô-CAGGTACCATGAAGCTTCTC-3ô and SAA1R: 5ô- GGCAACTCGAGTCAGTATTTC TC-3ô. 4.3 µl of ddH_2O, 4 µl of 5x AMV buffer, 0.4 µl of 10 mM dNTPs mixture, 1 µl of both primers (10 µM), 2.5 µl of 25 mM $MgSO_4$ and 4 µl of template RNA (100 ng) were mixed together in a 200 µl PCR tube. 0.4 µl of AMV reverse transcriptase (2 units) and 0.4 µl of *Tfl* polymerase (2 units) were added to the mixture finally to make up a 50 µl reaction. The reaction conditions were as follows:

Reverse transcription	45ºC	45 min	
Initial denaturation	94ºC	2 min	
Denaturation	94ºC	30 sec	35 cycles
Annealing	55ºC	45 sec	
Extension	68ºC	45 sec	
Final extension	68ºC	7 min	

After subjecting to gel electrophoresis to ensure the correct size, SAA1 RT-PCR products were precipitated on ice using 100% ethanol for 30 minutes. It was then spun down at 14,000 rpm for 15 minutes. The PCR product pellet was washed with 70% ethanol and dissolved in 50 µl of TE buffer, pH 8.0.

2.20.1.2 Digestion

Restriction enzyme digestion was performed using restriction enzymes from New England Biolabs (NEB). The RT-PCR products and the vector pcDNAÊ 3.1(+) were digested with *XhoI* and *KpnI* at 37°C for three hours. The digestion reaction mixture consisting of 0.5 µl (10-20 units) of each enzyme, 3 µl of 10x buffer, 0.3 µl of 100x BSA, 1-2 µg of RT-PCR products or pcDNAÊ 3.1(+) and nuclease-free water was incubated at 37°C for three hours.

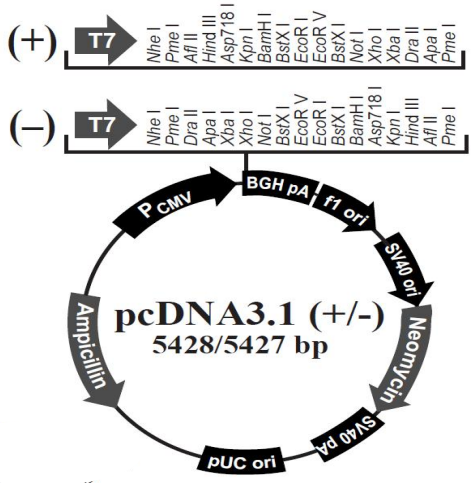

Figure 8. Map of pcDNAÊ 3.1(+). This figure summarizes the feature of pcDNAÊ 3.1(+) vector.

2.20.1.3 Gel purification

The digested products were purified using kit from QIAGEN. The digested products were first separated on 1% agarose gel and the DNA bands whose size corresponding to the digested plasmid and RT-PCR products were cut from the gel. The agarose slices were weighted to the nearest 10 mg and buffer QG was added (3 volumes of buffer QG to 1 volume of gel). The agarose gel slices were then incubated at 65°C for 10 minutes until the gel slices were completely dissolved in buffer QG. After incubation, the tubes were centrifuged briefly to collect the sample at the bottom of the tube and 1 gel volume of isopropanol was added to the sample. A QIAquick column was placed in a collection tube and the respective samples were loaded into each column. The tubes were incubated for 1 minute at room temperature and the samples were centrifuged at 14,000 rpm for 1 minute after incubation. The flow-through was discarded and the column was washed with 750 µl of buffer PE. The tubes were centrifuged at 14,000 rpm for 1 minute and the collection tubes were replaced with new 1.5 ml eppendorf tubes. 50 µl of EB buffer (10 mM Tris-Cl, pH 8.5) was added directly to the top of the glass fiber matrix in the column. After incubating the samples for 1 minute at room temperature, the tubes were centrifuged at 14,000 rpm for 1 minute to elute DNA sample.

2.20.1.4 Ligation

The vector pcDNAÊ 3.1(+) was ligated with SAA1 using T4 DNA ligase (NEB) based on the molar ratio of 3:1 (insert:vector) in a 20µl of reaction mixture. Ligation was performed at room temperature for 2 hours.

2.20.1.5 Transformation

20 µl of DNA ligation mixture was added to 100 µl of competent DH5Ŭbacteria and incubated on ice for 30 minutes. Heat shock was applied at 42°C for 2 minutes, and the bacteria were placed on ice again for 2 minutes. Recovery was performed by adding 900 µl of LB and the sample was incubated at 37°C with vigorous shaking for 1 hour. The cell pellet was collected via centrifugation, and resuspended in 100 µl of LB media and plated out onto LB amp+ plates. The plates were then incubated overnight at 37°C and colonies were picked, inoculated and expanded in LB media with 100 µg/ml of ampicillin. Plasmid DNA was prepared from transformed *E.coli* cell pellets as described in 2.19.3.

2.20.1.6 Selection and DNA sequencing

Plasmids obtained by small-scale preparation were first digested for 2 hours at 37°C with *XhoI* and *KpnI* to check for the plasmid with insert. The plasmid was then served as the template for DNA sequencing. BigDye^{TM} Terminator Cycle Sequencing Ready Reaction kit (Applied Biosystem from Perkin-Elmer Corp., Foster, CA, USA) was used. Sequencing reaction mixture consisting of 8 µl of Terminator Ready Reaction mix, (~1 µg) of DNA template, 1 µl of 50 µM appropriate primer (forward & reverse primer respectively) and 10 µl of deionized water was added in a 0.2 ml PCR tube and a thermal cycling was carried out according to the following program: 25 cycles of denaturation at 96 °C for 30 seconds, annealing of primer at 50°C for 15 seconds and extension at 60°C for 4 minutes. To precipitate the extended DNA, the extension reaction was incubated with 2.0 µl of 3 M sodium acetate and 50 µl of 95% ethanol at room temperature for 20 minutes. It was then centrifuged at 14,000 rpm for 30 minutes. The supernatant was then

carefully aspirated and the pellet was rinsed with 250 µl of 70% ethanol followed by centrifugation at 14,000 rpm for 5 minutes. The air-dried sample was dissolved in 12 µl of Hi-Di Formamide and analyzed in ABI PRISM®3100 Genetic Analyzer (Applied Biosystems Inc, USA).

2.20.2 Other subclonings

2.20.2.1 Generation of pcDNA3.1-SAA1-NLS

The cloning procedures were almost the same as described above. The plasmid pcDNA3.1-SAA1-NLS was constructed by inserting a 318 bp *XhoI* to *KpnI* fragment carrying the SAA1cDNA sequence without the first 18-amino acid signal peptide into pcDNA3.1 vector.

2.20.2.2 Generation of pcDNA3.1-SAA1-G8D

A 369 bp *XhoI* to *KpnI* fragment carrying the SAA1 cDNA sequence with a single nucleotide G→A substitution at codon 8 was inserted into pcDNA3.1 vector, which resulted in a single amino acid substitution, altering codon 8 from a glycine (GGC) to an aspartic acid (GAC).

2.20.2.3 Generation of pcDNA3.1-SAA1Δ1-11

A 336 bp *XhoI* to *KpnI* fragment carrying the truncated SAA1 cDNA sequence with a deletion of codons from 1 to 11 was inserted into pcDNA3.1 vector, which resulted in a deletion of the wild-type sequence $^{+1}$RSFFSFLGEAF^{+11}.

2.20.2.4 Generation of pcDNA3.1-PPARɔ

A 1.4 kb *XhoI* to *KpnI* fragment carrying the human PPARɔ cDNA sequence was inserted into pcDNA3.1 vector.

2.21 PLASMID DNA TRANSFECTION

Cells were seeded at 8 x 10^5 cells/well into 6-well plate (2 ml/well) and transfected using lipofectamine 2000 (Invitrogen) according to the manufacturerôs instructions. Briefly, 10 µl of lipofectamine 2000 and 4 µl of DNA were diluted in 250 µl of Opti-MEM medium (Invitrogen) separately. After 5 minutes incubation at room temperature, the diluted DNA was combined with the diluted lipofectamine 2000 and incubated for 20 minutes at room temperature. 500 µl of complexes was added into each well and mixed gently by rocking the plate back and forth. After 4 hours incubation under standard incubator conditions, the medium was replaced with 2 ml of fresh medium supplemented with 10% fetal bovine serum (FBS) and the cells were further incubated for an additional 68 hours under the same conditions, resulting in a total transfection time of 72 hours. The cells were harvested and processed for Western blot analysis and ELISA assay.

2.22 DETECTION OF SAA SECRETION

After culturing transfected cell for 3 days, medium was collected and cells were incubated with lysis buffer [62.5 mM Tris-HCl buffer pH 6.8, 2% sodium dodecyl sulphate (SDS), 10% glycerol, 50 mM dithiothreitol (DTT)] for 30 minutes. Then cell lysates and medium were assayed for human SAA protein using SAA enzyme-linked

immunosorbent assay (ELISA) kit (Biosource).The assay was performed according to the manufacturerôs instruction and absorbance of samples were read at 450 nm using spectrophotometer (Spectra Plus, TECAN). SAA concentration was determined using standard curve obtained from protein standards provided by the kit.

2.23 STATISTICAL ANALYSIS

Measurements were expressed as mean ± standard deviation (SD) from at least three samples. For comparison of two samples, data were analyzed using a 2-tailed Studentôs t-test and statistically significant differences were reported when $P<0.05$. For multiple comparisons, data were analyzed by ANOVA. Statistically significance of relevant comparisons was assessed by Bonferroni post hoc analysis and reported when $P<0.05$.

CHAPTER III

RESULTS

3.1 SAA ACTIVATES PPARɔ THROUGH EXTRACELLULAR-REGULATED KINASE 1/2 AND COX-2 EXPRESSION

3.1.1 SAA induces PPARɔ and expression of its target genes in HepG2 cells

The expression levels of PPARɔ and its target genes LXRŬ, ABCG1 and ABCA1 in HepG2 were examined in relation to varying concentrations and times of exposure to SAA stimulation. The transcript levels for these four genes were all induced after stimulation for 4 hours by SAA in a concentration-dependent manner (Fig. 9a). The effect of SAA on the mRNA levels of PPARɔ and LXRŬ was very transient. We could only detect a mild increase for both after stimulation for 4 hours. The increases in mRNA levels for ABCG1 and ABCA1 were more pronounced than those for PPARɔ and LXRŬ. For ABCG1, the effect of SAA stimulation remained for up to 24 hours (Fig. 9b), the maximum time point in this study. Western blot analysis confirmed the induction of ABCG1, ABCA1 and LXRŬ protein levels by stimulation with 20 µg/ml of SAA over time (Fig. 9c).

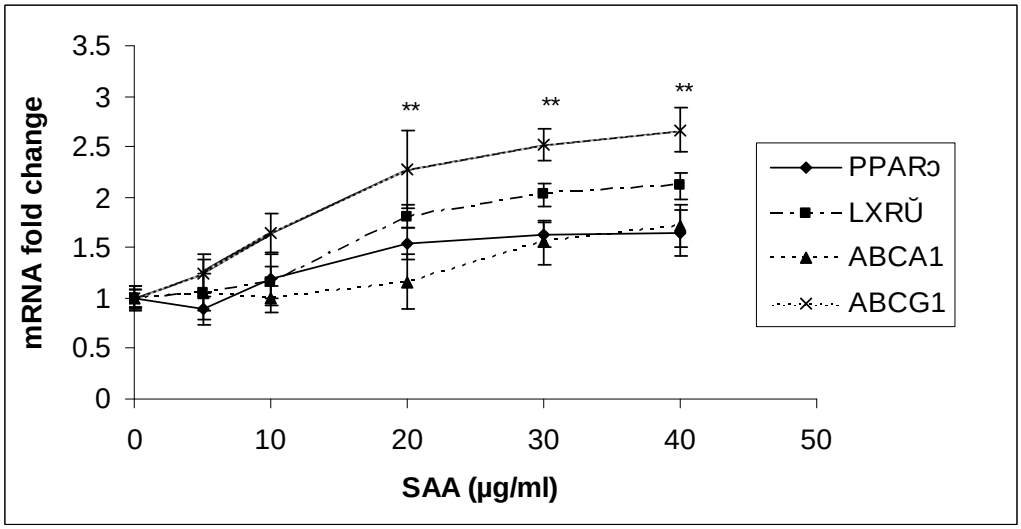

(a)

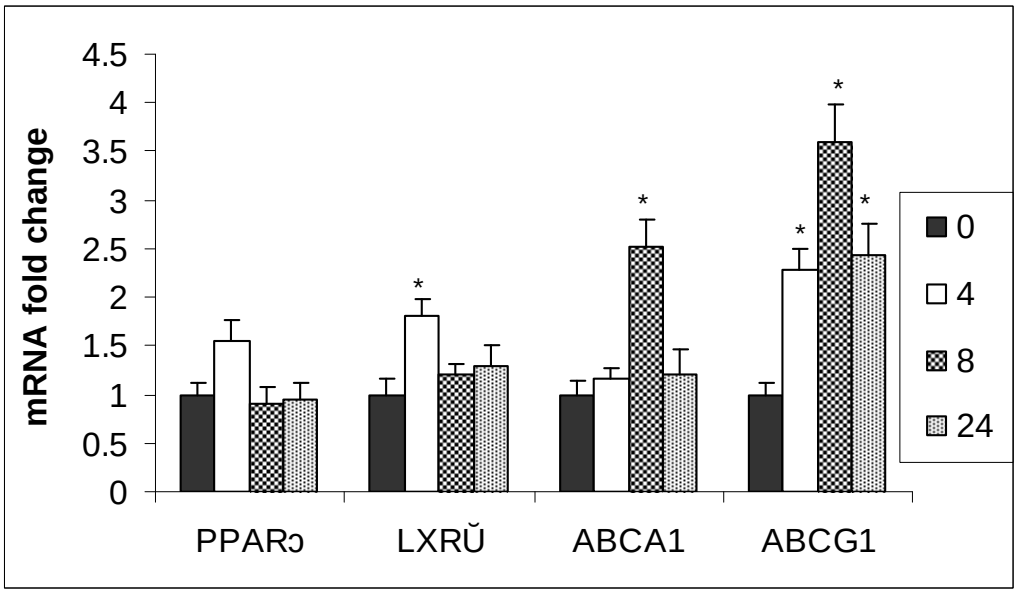

(b)

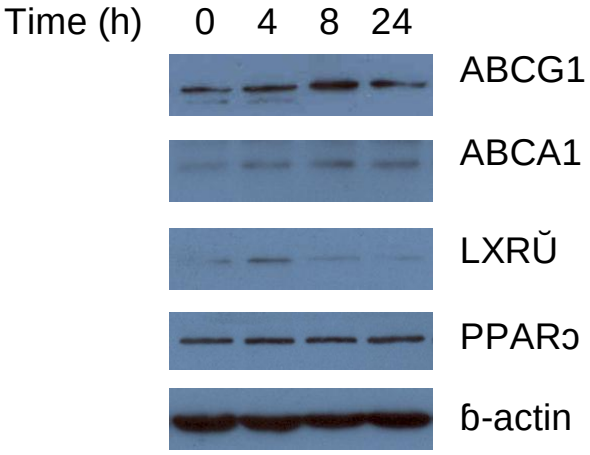

(c)

Figure 9. SAA induces PPARɔ, LXRŬ, ABCA1 and ABCG1 gene expression in HepG2 cells. HepG2 cells were treated with 5-40 µg/ml of SAA for 4 hours (a) and 20 µg/ml of SAA for indicated times (b). Total RNA was extracted and real-time quantitative RT-PCR was performed to determine mRNA expression levels of each gene. The mRNA levels of each gene were standardized for glyceraldehyde-3-phosphate dehydrogenase (GAPDH) levels. The results from at least 3 separately performed experiments are expressed relative to the controls and presented as the mean fold change ± SD. (c) HepG2 cells were incubated with 20 µg/ml of SAA for the indicated times. Protein samples were immunoblotted with anti-ABCG1, anti-ABCA1, anti-LXRŬ, anti-

PPARↄ and anti-ϐ-actin antibodies. ***P*<0.05 vs 0 µg/ml SAA treatment for all the genes. **P*<0.05 vs 0 group. n=3 to 4.

3.1.2 SAA facilitates cholesterol efflux in HepG2 cells

The ability of SAA to facilitate cholesterol efflux was examined using purified lipid-free SAA. The results shown in Figure 9 indicated that when HepG2 cells labeled with [^{3}H]cholesterol were preincubated with SAA (20 µg/ml), no significant changes in the amount of efflux of cholesterol into the medium without HDL or apoA-I acceptor were observed. However, the amount of cholesterol efflux was significantly increased in the presence of HDL (Fig. 10a). This increase was more drastic when apoA-I (10 µg/ml) was used as the main cholesterol efflux acceptor (Fig. 10b).

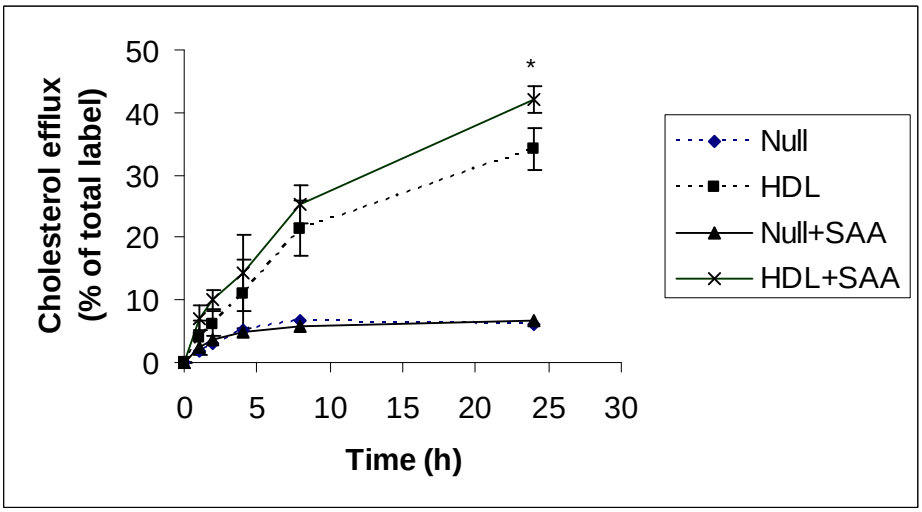

(a)

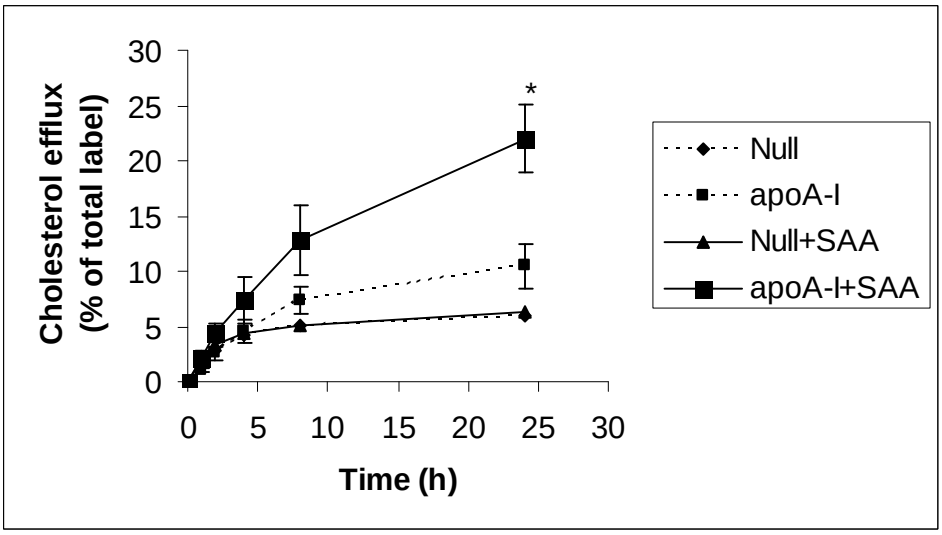

(b)

Figure 10. SAA facilitates cholesterol efflux in HepG2 cells. HepG2 cells were labeled with 1 µCi/ml [^{3}H] cholesterol for 24 h, equilibrated in medium in the absence of cholesterol for 16 h. The cells were then preincubated with 20 µg/ml of SAA or distilled water for 4 h. After this incubation, the cells were washed with 1x PBS for four times. The cells were then incubated with medium consisted of DMEM/BSA alone (null) or the same medium containing 40 µg/ml of HDL (HDL) (a) or 10 µg/ml of apoA-I (apoA-I) (b) at 37 °C for different periods for the determination of cellular efflux. Medium was collected at the indicated time points and assayed for [^{3}H] cholesterol. Cells were lysed with 0.1% SDS and 0.1 M NaOH lysis buffer, and radioactivity was determined by scintillation counter. The average values are represented (± SD) as the percentage of the radioactivity in medium relative to the total radioactivity in cells and medium. * P<0.05 vs HDL or apoA-I. n=4 to 5.

To clarify the roles of ABCA1 and ABCG1 on SAA-induced cholesterol efflux, we next examined the effect of acute suppression of ABCA1 or/and ABCG1 on cholesterol efflux using synthetic interfering RNA (siRNA) targeting human ABCA1 and ABCG1, respectively. As shown in Figure 11a, siRNAs specific to ABCA1 and ABCG1 efficiently reduced ABCA1 protein levels by ~ 50%. Knockdown of ABCA1 or ABCG1 expression reduced SAA-induced cholesterol efflux to HDL and apoA-I in HepG2 cells (Fig. 11b and 11c). The cholesterol efflux to HDL and apoA-I were more severely impaired in ABCA1 and ABCG1 double-knockdown HepG2 cells. Together, these data

indicated essential roles of ABCA1 and ABCG1 in cholesterol efflux to either apoA-I or HDL.

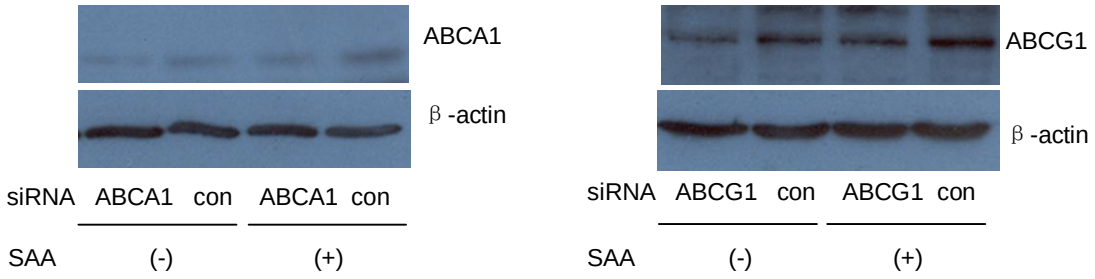

(a)

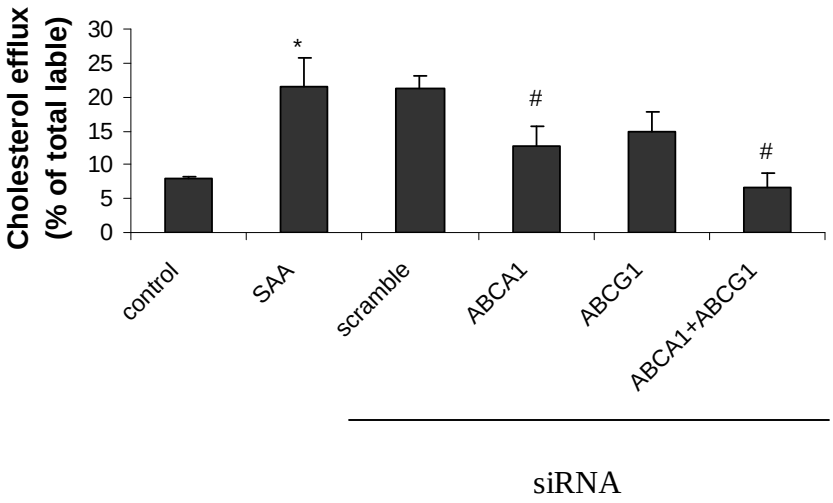

(b)

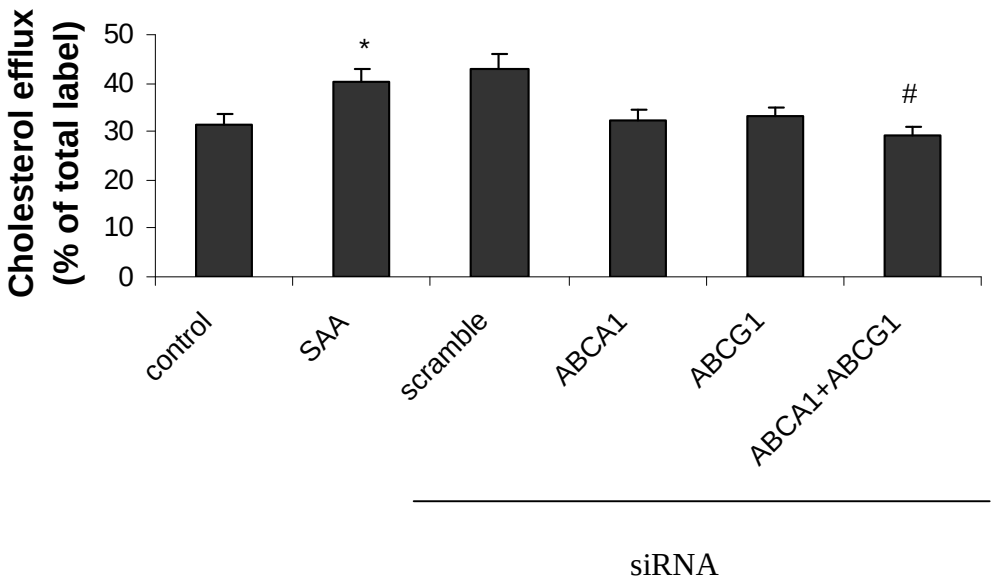

(c)

Figure 11. SAA-facilitated cholesterol efflux in HepG2 cells was mediated by ABCA1 and ABCG1. (a) HepG2 cells were transfected with control (scrambled siRNA), ABCA1 siRNA or ABCG1 siRNA for two days, and then incubated with SAA (20 μg/ml) for 4 h. Protein samples were immunoblotted with anti-ABCG1, anti-ABCA1 and anti-ϐ-actin antibodies. (b) HepG2 cells were transfected with scrambled siRNA, ABCA1 siRNA or ABCG1 siRNA for 24 h. HepG2 cells were labeled with 1 μCi/ml [^{3}H] cholesterol for another 24 h, equilibrated in medium in the absence of cholesterol for 16 h. The cells were then preincubated with 20 μg/ml of SAA or distilled water for 4 h. After this incubation, the cells were washed with 1x PBS for four times. The cells were then incubated with medium consisted of DMEM/BSA alone (control) or the same medium containing 10 μg/ml of apoA-I (apoA-I) (b) or 40 μg/ml of HDL (HDL) (c) at 37 °C for 24 h. Cholesterol efflux was measured as described before. The results from at least 4 separately performed experiments are presented as the mean ± SD. * P<0.05 vs control group. # P<0.05 vs SAA group. n=4 to 5.

3.1.3 SAA enhances PPARↄ activity in HepG2

As both ABCA1 and ABCG1 are downstream target genes of PPARↄ, we performed electrophoretic mobility shift assay (EMSA) to investigate the effect of SAA on PPARↄ binding activity. As shown in Figure 12a, SAA increased PPRE DNA binding activity in HepG2 cells. The sequence specificity of SAA-induced PPRE binding was demonstrated by inhibition of binding with an excess of unlabeled PPRE probe, while the

binding was not affected by the same molar excess of oligonucleotide with a mutated PPRE motif. The identity of the PPAR-oligonecleotide complex was verified by a supershift assay. To further examine the effect of SAA on PPARↄ activity, HepG2 cells were co-transfected with a luciferase reporter construct containing PPRE (PPRE-luc) and a PPARↄ expression vector. With the dual-luciferase assay system, the PPAR Reporter (luc) can easily and rapidly monitor PPARↄ transcriptional activity in cells. As shown in Figure 12b, SAA increased luciferase activity in a concentration-dependent manner.

We also examined the PPARↄ activity in HepG2 cells using an enzyme-linked immunosorbent assay-based PPARↄ transcription factor activity assay kit. As shown in Figure 12c, 5 µM PPARↄ agonist, ciglitazone, increased the PPARↄ transcriptional activity almost by eight-fold compared to the control. SAA (20 µg/ml) also increased PPARↄ transcriptional activity by more than three-fold, although the effect was milder than that of ciglitazone.

The effect of PPARↄ antagonist T0070907 on SAA-induced PPARↄ activation was examined via the pretreatment of HepG2 cells with of T0070907 (1 nM), for one hour. The treated cells were then stimulated with SAA (20 µg/ml) and ciglitazone (5 µM). The enhanced PPARↄ transcription activity stimulated by SAA and ciglitazone was significantly inhibited by T0070907 (Fig. 12c).

We next investigated whether the PPARↄ activation was a direct effect of SAA or resulted from contaminating lipopolysaccharide (LPS) in the SAA preparation. The LPS content in the recombinant SAA was 0.1 ng/µg of protein or less, translating into 4 ng/ml LPS or less in 40 µg/ml of SAA. LPS at this concentration and at a higher concentration of 100 ng/ml that we had tested was unable to induce PPARↄ activation (Fig. 12d). Given

that most proteins are heat-labile while LPS is heat-resistant, we examined the ability of heat-treated SAA (20 µg/ml) and LPS (100 ng/ml) to induce PPARↄ activation. As shown in Figure 10d, SAA could no longer induce PPARↄ activation after being heated at 100 °C for 30 minutes. LPS had no effect on transcription activation with or without heat treatment. In parallel experiments, polymyxin B (PMB), an amphiphilic cyclic polycationic peptide that specifically binds to LPS and neutralizes its effect, had a minimal effect on the potency of SAA-induced PPARↄ activation. These results indicate that the trace amount of LPS in the SAA preparation did not contribute to the PPARↄ activation. In another control experiment, apoA-I was used in the PPARↄ activation assay. Like SAA, apoA-I is another major apolipoprotein of HDL, and they share similar structure (amphipathic helices) and function (lipid transport). As shown in Figure 11d, apoA-I has no effect on PPARↄ transcriptional activity. The gene expression levels of ABCG1 and ABCA1 after SAA stimulation for eight hours, as well as PPARↄ and LXRŬ after SAA stimulation for four hours, were also inhibited by the PPARↄ antagonist, T0070907 (Fig. 12e).

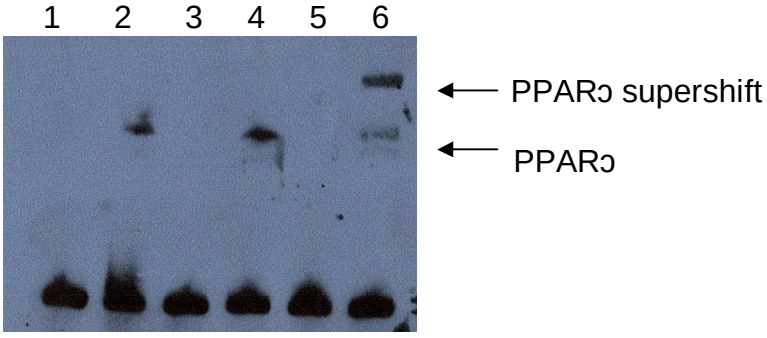

(a)

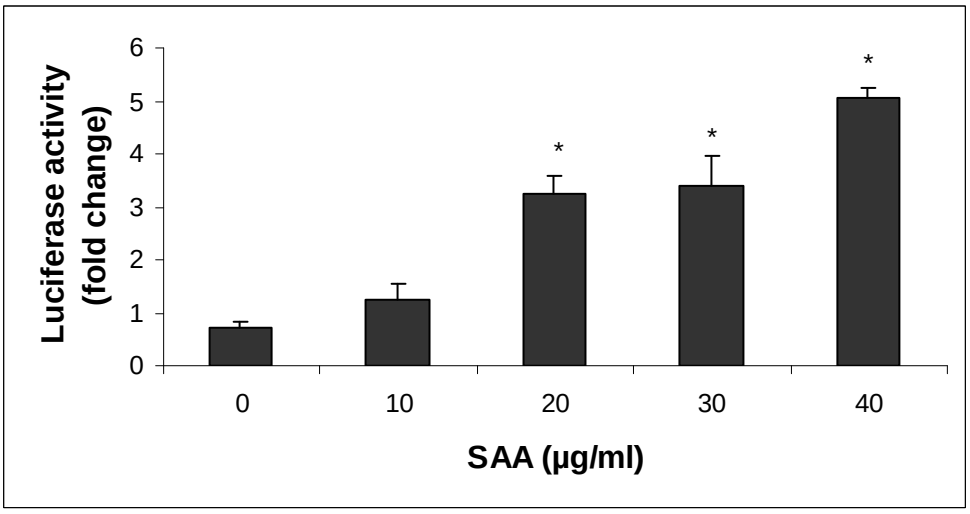
Luciferase activity
(fold change)
6
5
4
3
2
1
0
*
*
*
0
10
20
30
40
SAA (μg/ml)

(b)

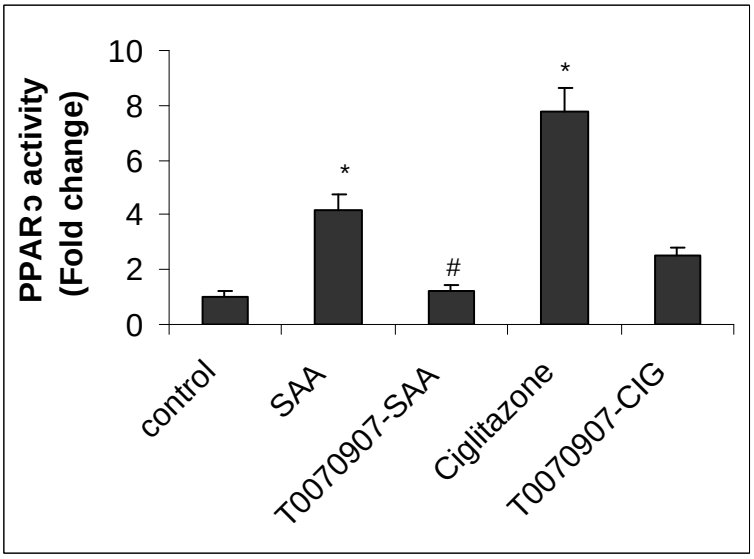
PPARɔ activity
(Fold change)
10
8
6
4
2
0
*
*
#
control
SAA
T0070907-SAA
Ciglitazone
T0070907-CIG

(c)

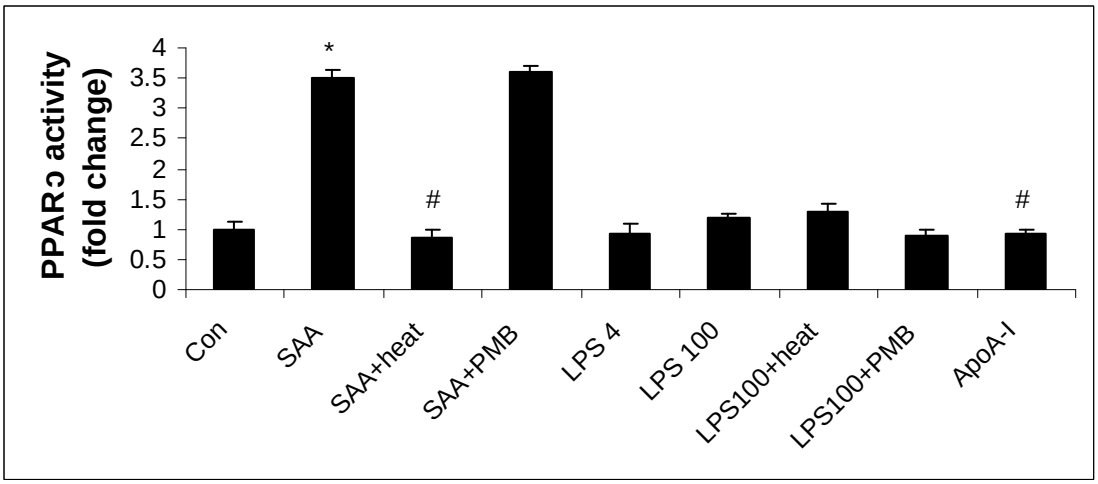

(d)

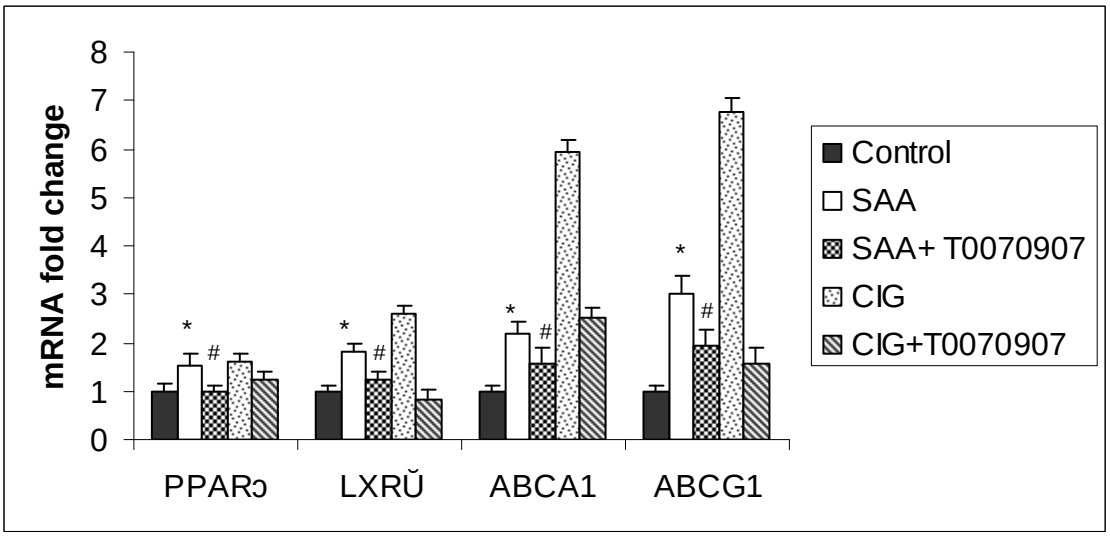

(e)

Figure 12. SAA enhances PPARɔ activation and SAA-induced PPARɔ target genes expressions are inhibited by PPARɔ antagonist. (a) HepG2 cells were stimulated with 20 μg/ml of SAA for 4 hours and nuclear extracts were prepared. EMSA assay was performed using biotin-labeled PPRE probe. Unlabeled PPRE sequence of its mutant were added as specific or non-specific competitors as indicated. Lane 1, control; 2, SAA treatment; 3, SAA + unlabeled probe; 4, SAA + unlabeled mutant probe; 5, free probe; 6, SAA + anti-PPARɔ. (b) HepG2 cells were transfected with PPARɔ expression vector plus PPRE-luc reporter constructs. PPRE-luc reporter activity was measured with a Dual-Luciferase Reporter Gene Assay system after incubation of transfected cell cultures with different doses of SAA for 4 hours. (c) HepG2 cells were pretreated with 1 nM of T0070907 or vehicle for 1 hour and then treated with 20 μg/ml of SAA or 5 μM of ciglitazone for 4 hours. PPARɔ transcriptional activity was determined by a PPARɔ

transcription factor activity assay kit. (d) HepG2 cells were incubated with LPS (4 ng/ml and 100 ng/ml), SAA (20 µg/ml), heat-treated LPS and SAA (100°C for 30 minutes), polymyxin B (50 µg/ml, 1 hour)-treated SAA and LPS and apoA-I (20 µg/ml) for 4 hours and followed by the PPARɔ transcriptional activity assay. (e) Real-time quantitative RT-PCR was performed to determine mRNA expression levels of each gene, standardizing with GAPDH levels. The mRNA levels for PPARɔ and LXRŬ were determined 4 hours after SAA (20 µg/ml) stimulation while the mRNA levels for ABCA1 and ABCG1 were measured 8 hours after treatment. The results from at least 3 separately performed experiments are expressed relative to the controls and presented as the mean fold change ± SD. * P<0.05 vs 0 or control group. #P<0.05 vs SAA group. n=3 to 5.

3.1.4 SAA-induced PPARɔ activation is suppressed by HDL

Although SAA is largely associated with HDL in circulation, it has been speculated that it is available in lipid-free/lipid-poor forms at the site of atherosclerotic lesion formation. Therefore, functional differences between lipid-associated and lipid-free SAA are of great interest. The effects of HDL on SAA-induced PPARɔ activation was examined by incubating a constant concentration of SAA with varying concentrations of HDL. The addition of increasing concentrations of HDL caused a dose-dependent suppression of SAA-induced PPARɔ activation while HDL alone had no effect on PPARɔ activation (Fig. 13).

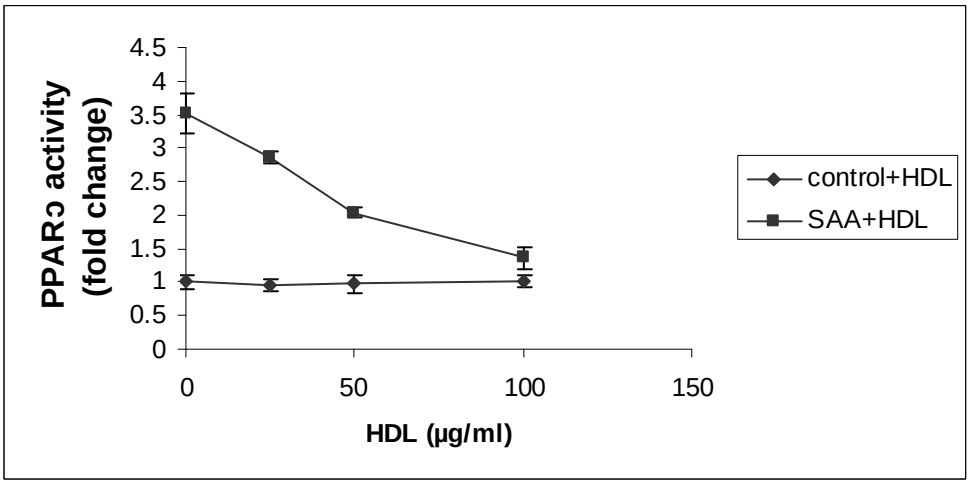

Figure 13. SAA-induced PPARↄ activity is suppressed in the presence of HDL. HepG2 cells were incubated with media containing 20 µg/ml of SAA and increasing concentrations of HDL (25-100 µg/ml) (SAA+HDL) or media containing HDL only (control+HDL) for 4 hours. PPARↄ transcription activity was determined by a PPARↄ transcription factor activity assay kit as previously described. The results from at least 3 separately performed experiments are expressed relative to the controls and presented as the mean fold change ± SD. n= 3 to 5.

3.1.5 *De novo* protein synthesis is required for the SAA-induced PPARↄ activation

Cycloheximide (CHX) is a protein biosynthesis inhibitor. In this study, we examined whether *de novo* protein synthesis is required for the SAA-induced PPARↄ activation. In a time-course experiment, SAA was shown to increase PPARↄ activity between 2 and16 hours. The SAA effect on PPARↄ subsided after 8 hours. As shown in Fig. 14a, the increased PPARↄ activity was generally suppressed by CHX, indicating endogenous expressed SAA or intermediate molecule(s) involved in SAA-induced PPARↄ activation. However, CHX could not completely abolish the PPARↄ activation induced by SAA.

Acute-phase SAA is synthesized mainly in liver. As such, it is necessary to establish whether the observed PPARↄ activation could be due to the endogenously produced SAA protein. With siRNA gene silencing of SAA1 and SAA2, quantitative RT-PCR demonstrated 50-60% of mRNA knockdown (Fig. 14b). As shown in Fig. 14c, SAA treatment increased PPARↄ activation, which was reduced by the knockdown of SAA1, suggesting that endogenously expressed SAA1 might also play a role in SAA-induced PPARↄ activation. PPARↄ activity was not affected by SAA2 knockdown.

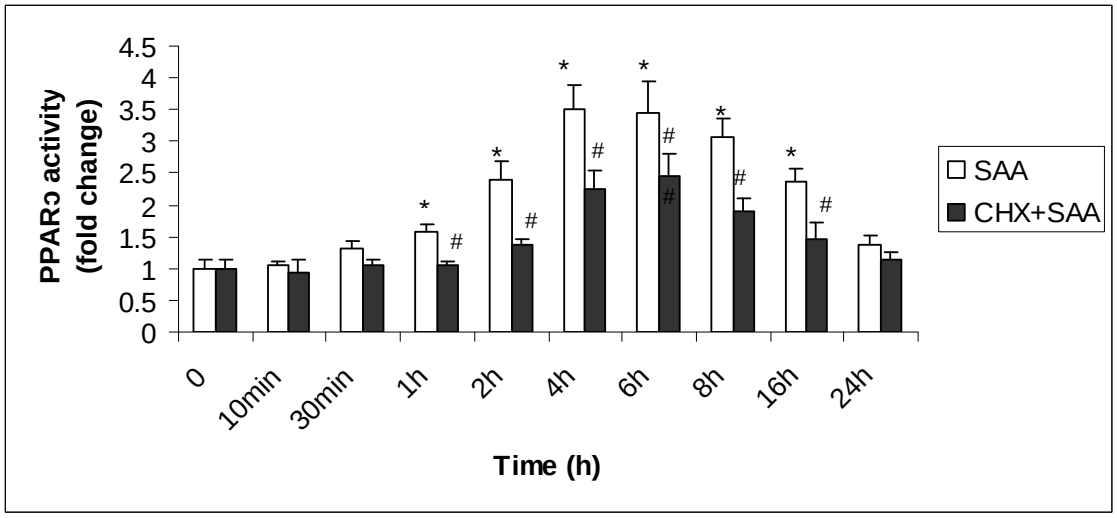
PPARɔ activity
(fold change)
4.5
4
3.5
3
2.5
2
1.5
1
0.5
0
0
10min
30min
1h
2h
4h
6h
8h
16h
24h
Time (h)
SAA
CHX+SAA

(a)

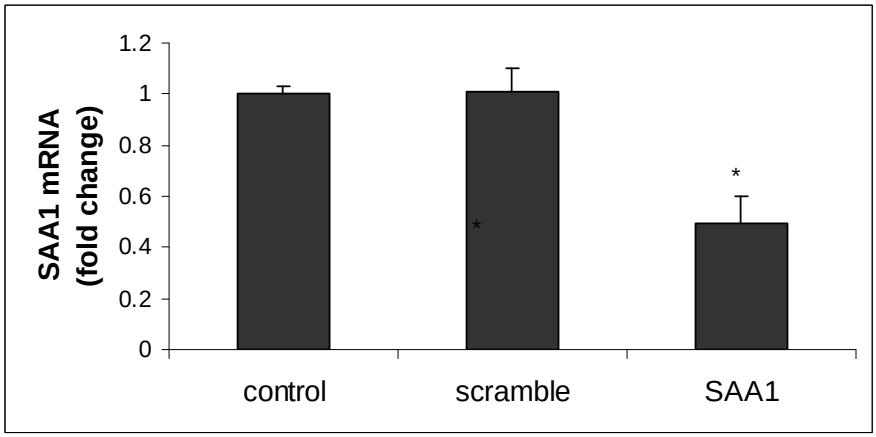
SAA1 mRNA
(fold change)
1.2
1
0.8
0.6
0.4
0.2
0
control
scramble
SAA1

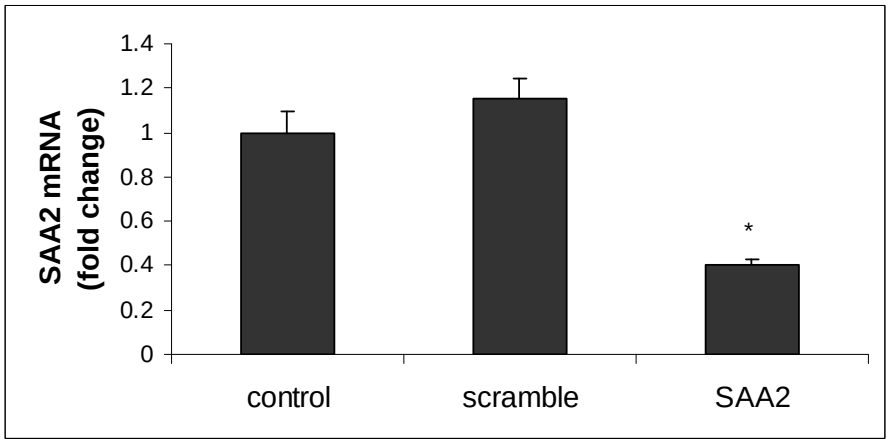
SAA2 mRNA
(fold change)
1.4
1.2
1
0.8
0.6
0.4
0.2
0
control
scramble
SAA2

(b)

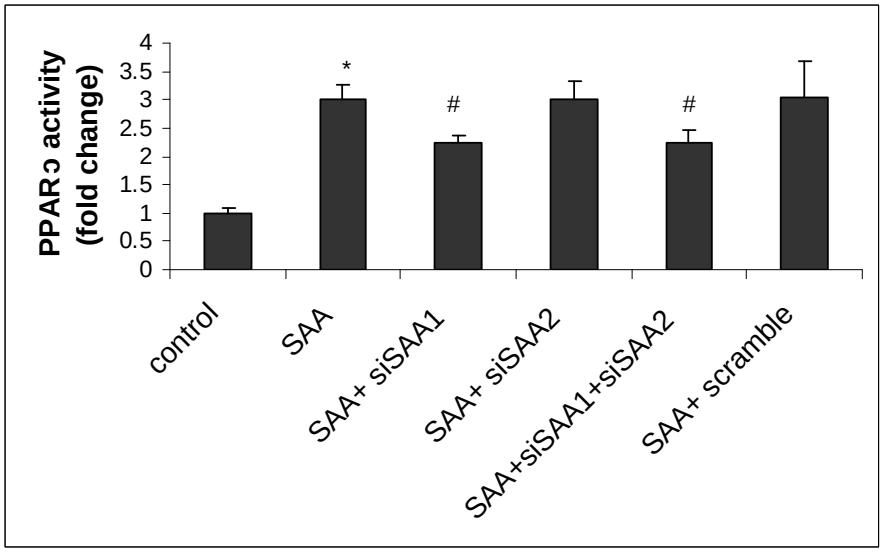

(c)

Figure 14. *De novo* protein synthesis is required for the SAA-induced PPARɔ activation. (a) Cells were incubated with 100 µM cycloheximide (CHX) for 1 hour before SAA (20 µg/ml) treatment for indicated times. PPARɔ transcription activity was determined as described before. (b) HepG2 cells were treated with 100 pmol of siRNA to SAA1 or SAA2 or scrambled siRNA (control). RNA was extracted and the mRNA levels for SAA1 and SAA2 were measured by real-time RT-PCR. (c) PPARɔ transcription activity was determined as described before.The results from at least 3 separately performed experiments are expressed relative to the controls and presented as the mean ± SD. *P<0.05 vs 0 or control group. #P<0.05 vs SAA group. n=3 to 5.

3.1.6 SAA-induced PPARɔ activation and cholesterol efflux in HepG2 are partially mediated by SR-BI

We also assessed the contribution of scavenger receptor class B type I (SR-BI) in SAA-induced PPARɔ activation and cholesterol efflux by using siRNA against SR-BI. Examination of SR-BI level by quantitative RT-PCR demonstrated 60% mRNA knockdown (data not shown). As shown in Figure 15, siRNA-mediated SR-BI gene silencing partially inhibited PPARɔ activation and cholesterol efflux induced by SAA treatment. However, siRNA could not completely block the SAA effects, which indicated

the involvement of other receptors in SAA-induced PPARɔ activation and cholesterol efflux.

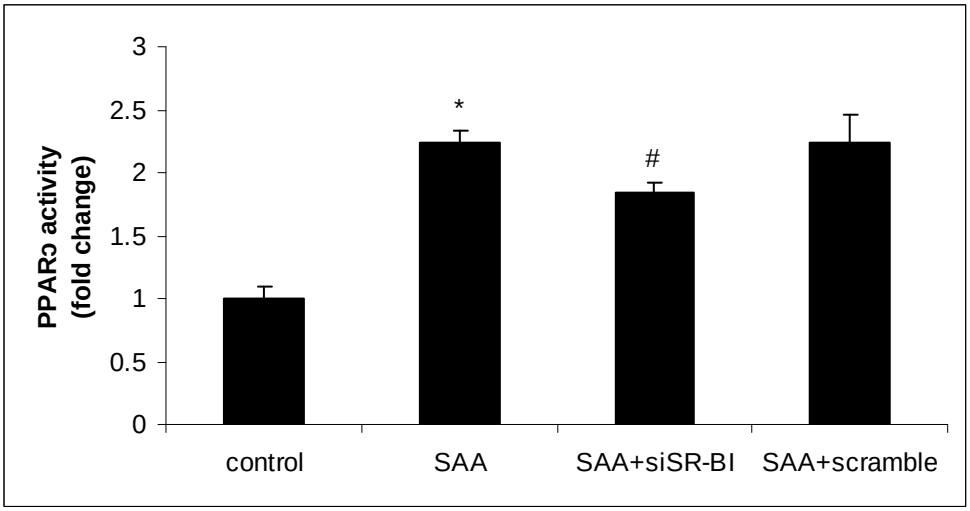

(a)

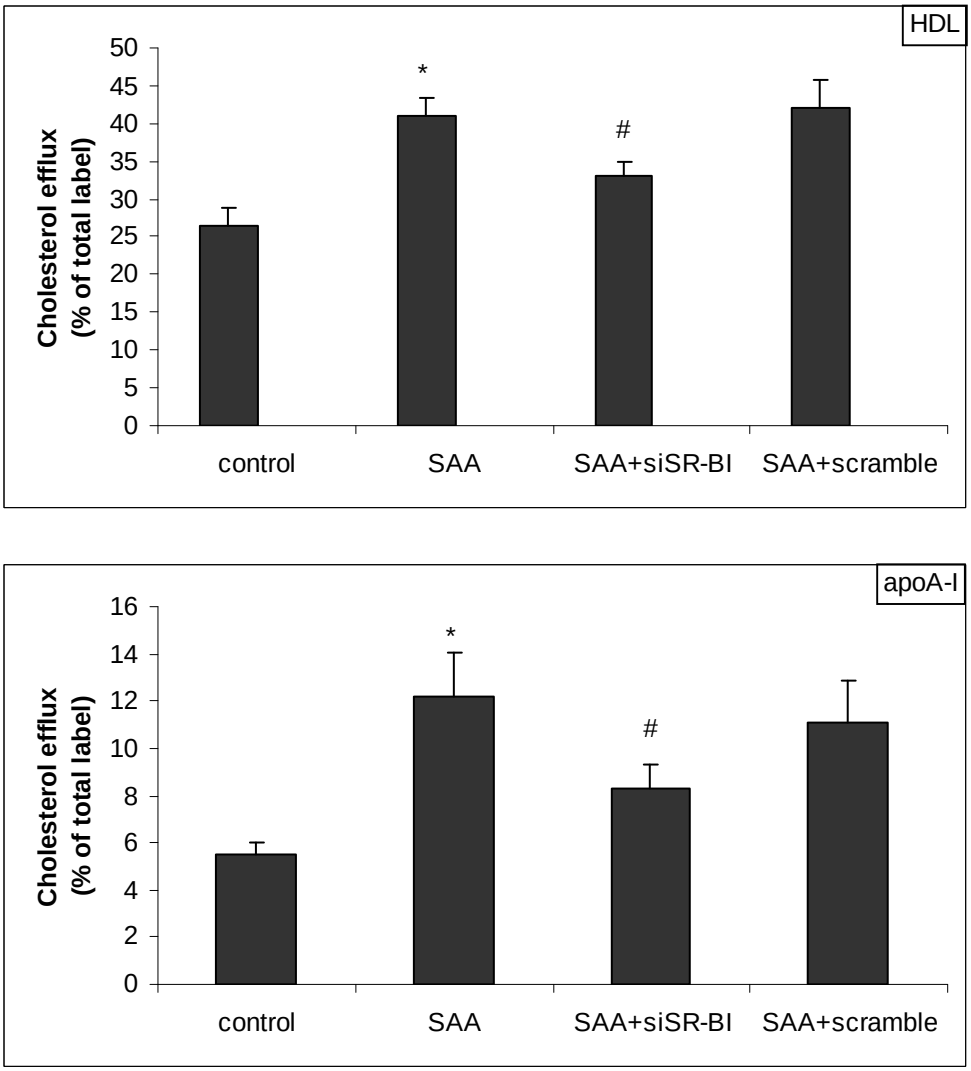

(b)

Figure 15. SAA-induced PPARɔ activation and cholesterol efflux in HepG2 is partially mediated by SR-BI. HepG2 cells were treated with 100 pmol of siRNA to SR-BI or scrambled siRNA for 48 hours before SAA (20 μg/ml) treatment for 4 hours. (a) PPARɔ transcription activity and (b) cholesterol efflux were determined as described before. * $P<0.05$ vs Control. #$P<0.05$ vs SAA group. n=3.

3.1.7 SAA elevates the intracellular 15d-PGJ_2 level

As PPARɔ can be activated by a number of intracellular fatty acids such as 15d-PGJ_2 [136, 139, 257], we examined the effect of SAA on the intracellular 15d-PGJ_2 level

in HepG2 cells using an enzyme immunoassay. As shown in Figure 16, SAA increased intracellular 15d-PGJ_2 level by more than 3-fold.

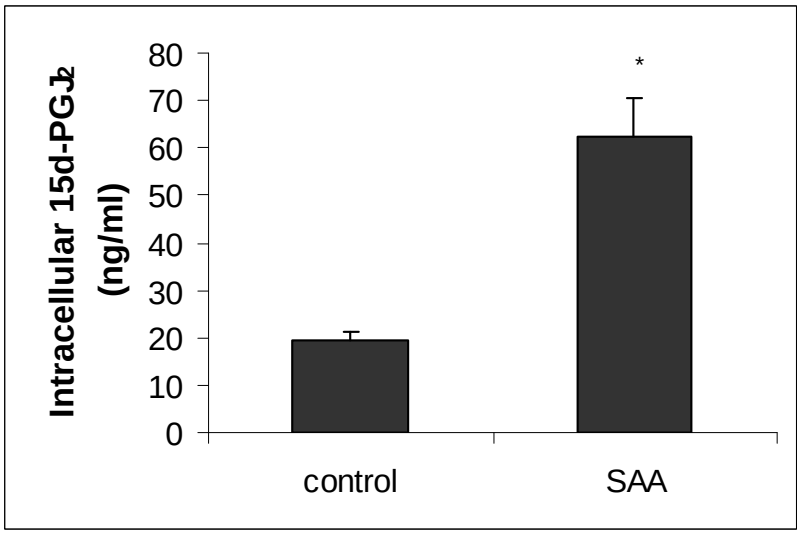

Figure 16. SAA induces intracellular 15d-PGJ_2 in HepG2. HepG2 cells were incubated with 20 μg/ml of SAA for 4 hours, and then the cells were lysed with lysis buffer. The concentrations of 15d-PGJ_2 were determined by EIA. The results from 3 separately performed experiments are presented as the mean ± SD. * P<0.05 vs control group. n=3.

3.1.8 SAA induces COX-2 expression

As the 15d-PGJ_2 level could be induced by COX expression [258, 259], we next examined whether COX expression could be induced by SAA stimulation. SAA treatment had no effect on the expression of COX-1 mRNA (Fig. 17a). On the other hand, after treatment of HepG2 cells with 20 μg/ml SAA for 4 hours, both the mRNA level and the protein level of COX-2 were increased and remained so for up to 24 hours as revealed by real-time RT-PCR and Western blot analysis, respectively (Fig. 17b and 17c).

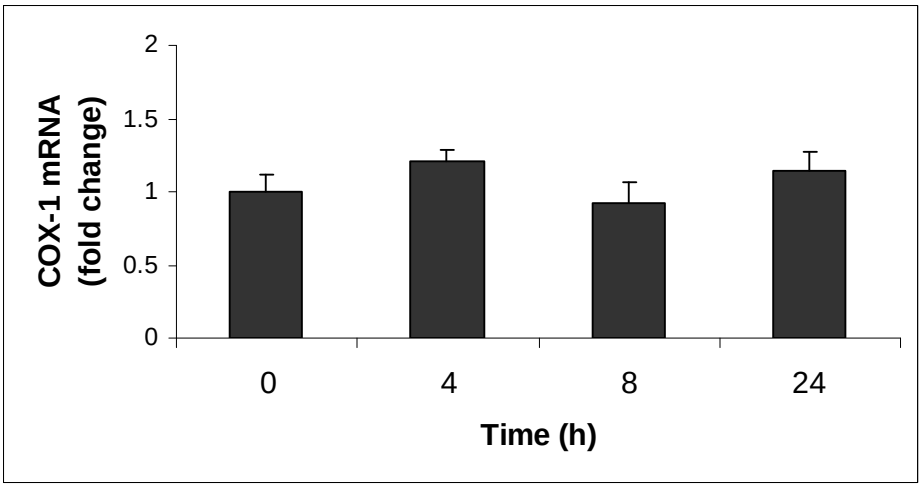
COX-1 mRNA
(fold change)
2
1.5
1
0.5
0
0
4
8
24
Time (h)

(a)

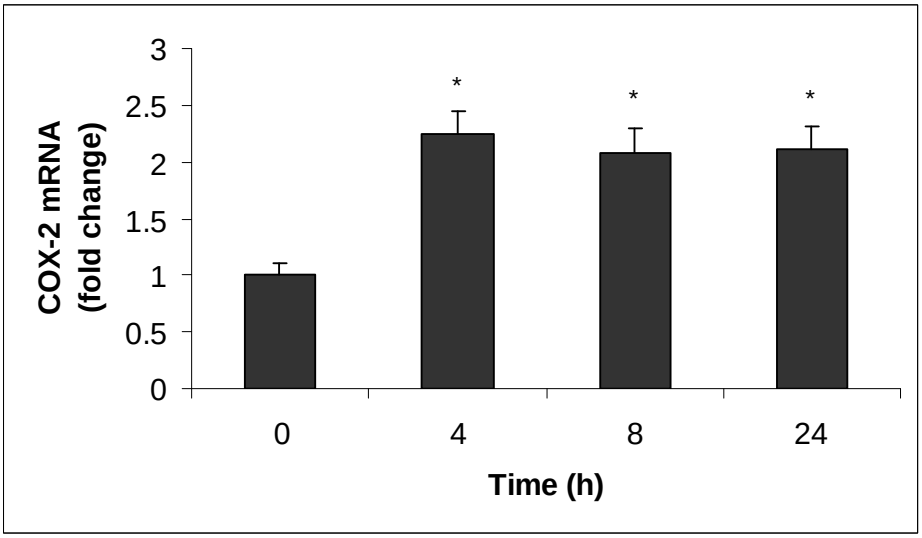
COX-2 mRNA
(fold change)
3
2.5
2
1.5
1
0.5
0
*
*
*
0
4
8
24
Time (h)

(b)

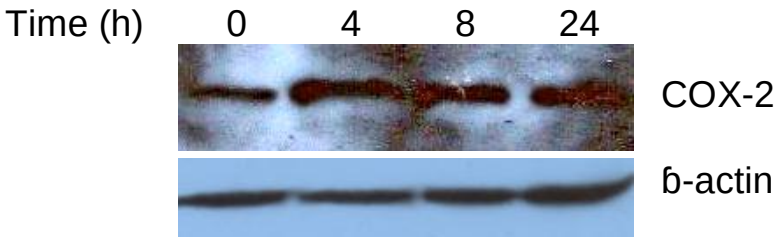
Time (h)
0
4
8
24
COX-2
b-actin

(c)

Figure 17. SAA induces COX-2 gene expression in HepG2 cells. HepG2 cells were treated with 20 µg/ml of SAA for indicated times. Total RNA was extracted and real-time quantitative RT-PCR was performed to determine mRNA expression levels of COX-1 (a) and COX-2 (b). The mRNA levels of COX-1 and COX-2 were standardized for glyceraldehyde-3-phosphate dehydrogenase (GAPDH) levels. The results from 3 separately performed experiments are expressed relative to the controls and presented as the mean ± SD. (c) HepG2 cells were incubated with 20 µg/ml of SAA for the indicated times. Protein samples were immunoblotted with anti-COX-2 and anti-ϐ-actin antibodies. * $P<0.05$ vs 0 group. n=3.

3.1.9 SAA-induced PPARↃ activation is mediated by ERK1/2-dependent COX-2 expression, and protein translation is required

Recent reports showed that lipid-free SAA can activate MAPK [120, 215, 217], which are important signaling molecules that regulate COX-2 expression [260-262]. Therefore, we speculated on the involvement of MAPK signals in SAA-induced COX-2 in HepG2 cells. Our Western blot data have shown that SAA could induce ERK1/2 phosphorylation. To evaluate if this is the direct effect of SAA or if it occurs through the synthesis of signaling proteins, the HepG2 cells were incubated with 100 µM cycloheximide (CHX). ERK1/2 phosphorylation could be observed for the first 30 minutes despite cycloheximide pretreatment and was only suppressed subsequently while ERK1/2 protein levels were unchanged by cycloheximide. For cells not pretreated with CHX, ERK1/2 phosphorylation could be sustained for up to 6 hours, the maximum duration of this experiment (Fig. 18a). These data indicated that the initial 30 minutes of phosphorylation might be the direct effect of exogenous SAA that did not require any synthesis of endogenous signaling proteins, whereas the later effects were perhaps dependent on endogenous protein that may take more time to synthesize. However, phosphorylation of p38 and JNK could not be detected in HepG2 cells after SAA treatment. We then examined the effect of ERK1/2 specific inhibitor PD98059 on SAA-

induced COX-2 mRNA expression. As shown in Figure 18b, SAA-induced COX-2 mRNA expression was blocked by PD98059, which indicated the involvement of ERK1/2 in SAA-induced COX-2 expression. In addition, both NS-398 and PD98059 had an inhibitory effect on SAA-induced ABCA1 and ABCG1 mRNA expression (Fig. 18c). The SAA-induced intracellular 15d-PGJ_2 level was also partially suppressed by these two inhibitors (Fig. 18d). Furthermore, SAA-enhanced PPARↄ activation was also inhibited by NS-398 and PD98059 (Fig. 18e). SAA-facilitated cholesterol efflux was inhibited by the same COX-2 and ERK1/2 inhibitors (Fig. 18f and 18g). These results suggested that PPARↄ activation is medicated by ERK1/2-dependent COX-2 expression.

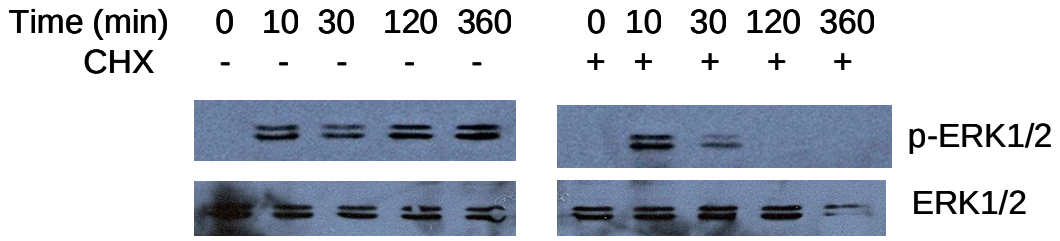

(a)

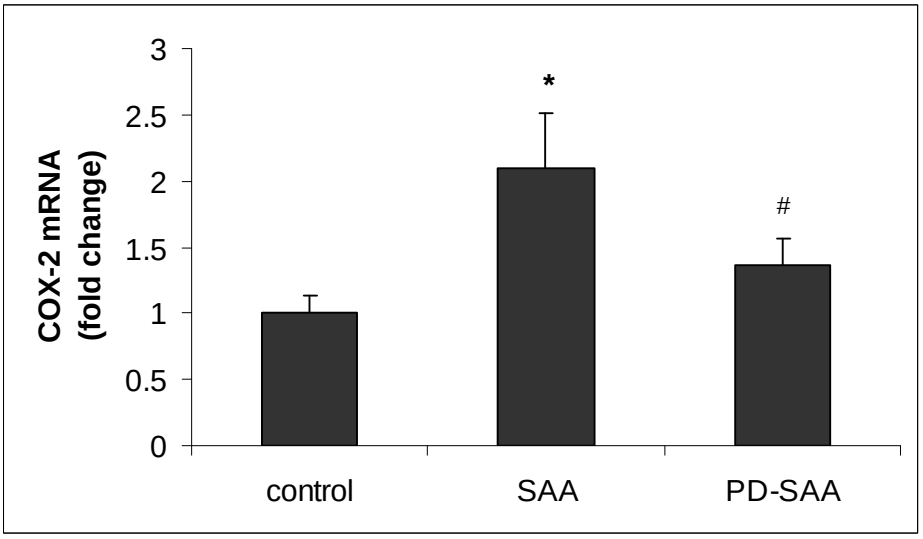

(b)

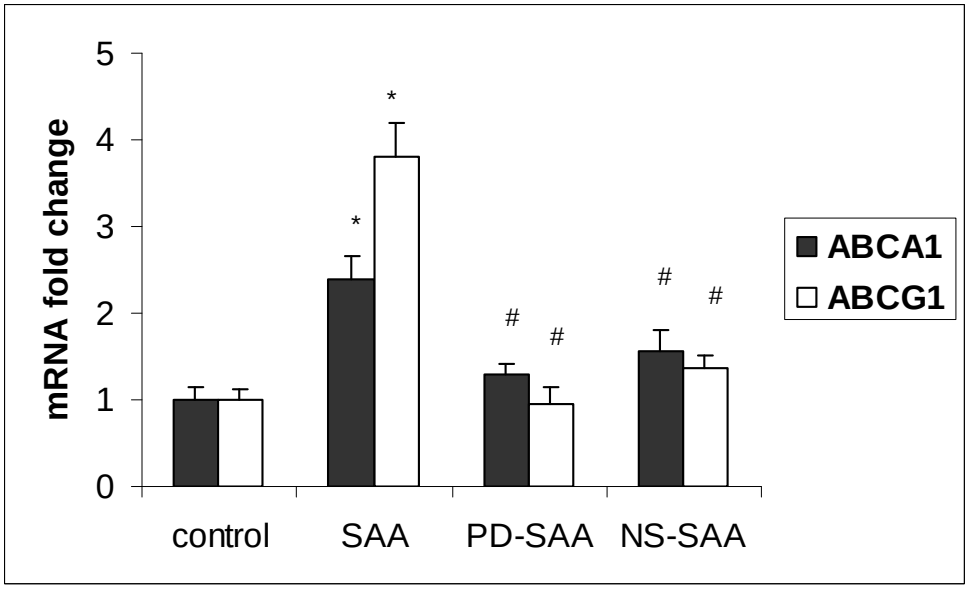
mRNA fold change
5
4
3
2
1
0
control
SAA
PD-SAA
NS-SAA
ABCA1
ABCG1
*
*
#
#
#
#

(c)

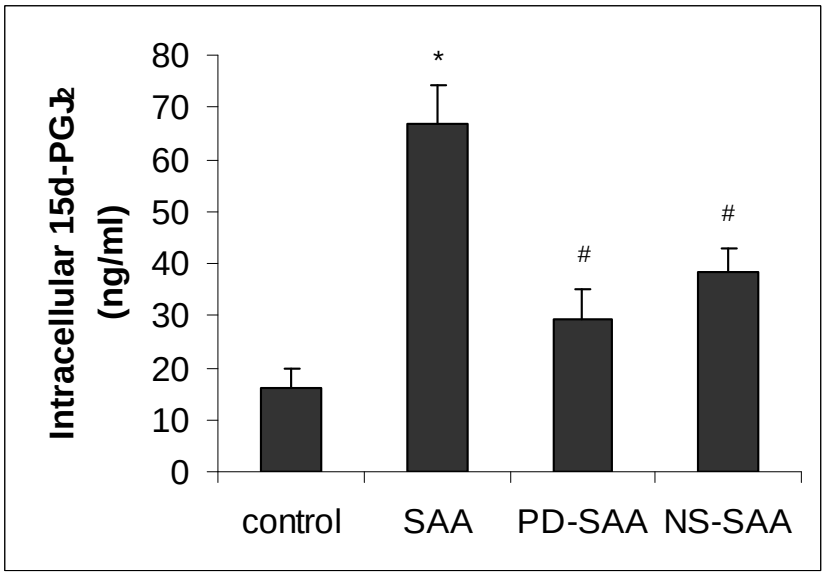
Intracellular 15d-PGJ2 (ng/ml)
80
70
60
50
40
30
20
10
0
control
SAA
PD-SAA
NS-SAA
*
#
#

(d)

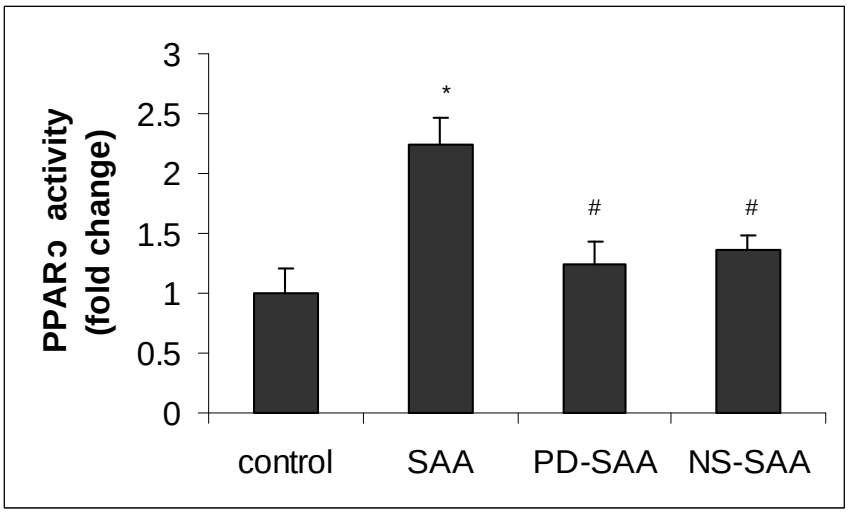
PPARɔ activity
(fold change)
3
2.5
2
1.5
1
0.5
0
*
#
#
control
SAA
PD-SAA
NS-SAA

(e)

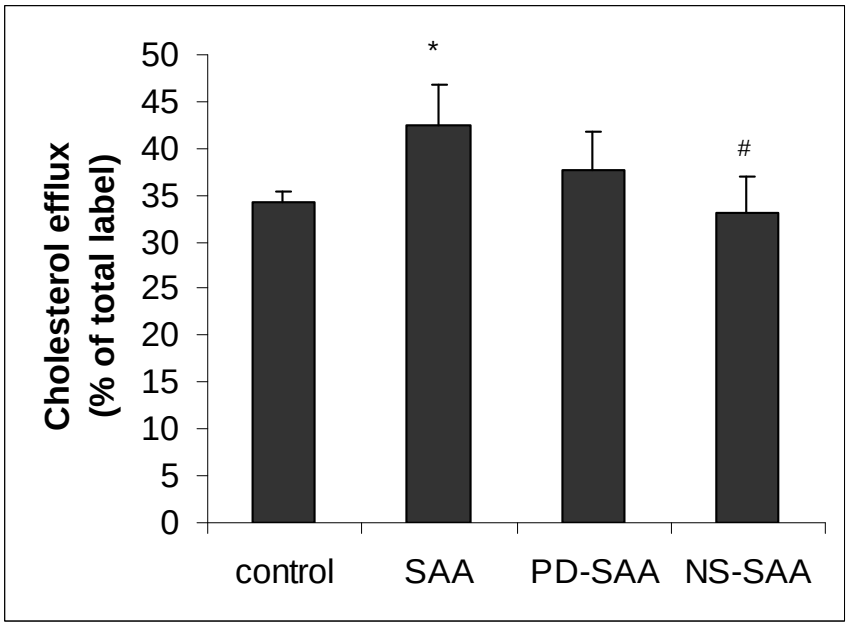
Cholesterol efflux
(% of total label)
50
45
40
35
30
25
20
15
10
5
0
*
#
control
SAA
PD-SAA
NS-SAA

(f)

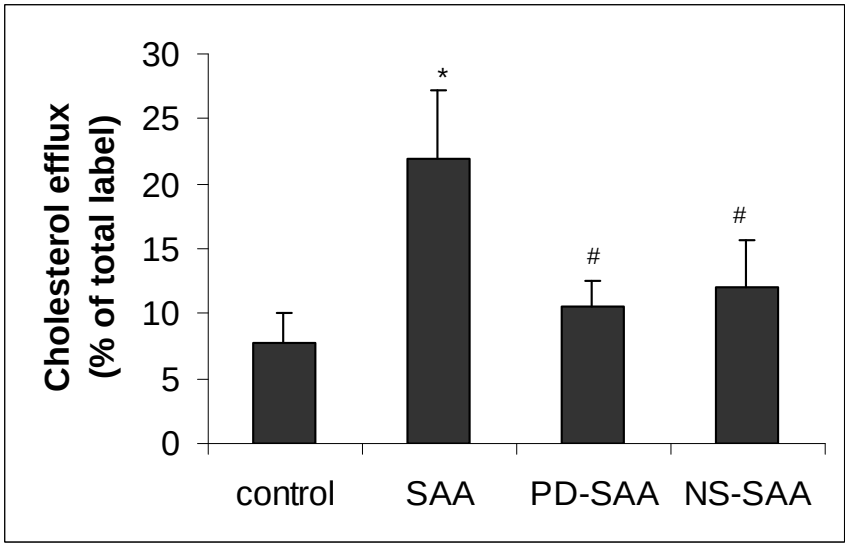

(g)

Figure 18. SAA-induced PPAR activation is mediated by ERK1/2-dependent COX-2 expression. (a) Cells were incubated with or without 100 µM cycloheximide (CHX) for 1 hour before SAA (20 µg/ml) treatment for indicated time periods. Protein samples were immunoblotted with anti-phospho ERK1/2 (p-ERK), and anti-ERK1/2 antibodies. HepG2 cells were pretreated with 10 µM NS-398 (NS) or 50 µM PD98059 (PD) or vehicle for 1 hour and then treated with 20 µg/ml of SAA for 4 hours (For ABCA1 and ABCG1 mRNA quantitation, cells were treated with 20 µg/ml of SAA for 8 hours). mRNA expression levels of COX-2 (b) ABCA1 and ABCG1 (c) were quantified as described before. (d)The concentrations of 15d-PGJ_2 were determined by EIA assay. (e) PPARɔ transcriptional activities were measured as described before. (f) HDL (40 µg/ml) or (g) apoA-I (10 µg/ml) was used as the cholesterol efflux acceptor for the cholesterol efflux assay. Cholesterol efflux was also determined as before. The results from at least 3 separately performed experiments are presented as the mean ± SD.* $P<0.05$ vs control group. #$P<0.05$ vs SAA group. n=3 to 4.

3.1.10 SAA has the same PPARɔ activation effects in HCAEC and THP-1 cell lines

After establishing that SAA could induce PPARɔ activation, we further examined the effect of SAA on PPARɔ in two other cell lines, HCAEC and THP-1, to determine whether this effect is cell line specific. As shown in Figure 19, SAA could increase the PPARɔ activity in both cell lines and PPARɔ activation effect was even drastic in THP-1 cell line.

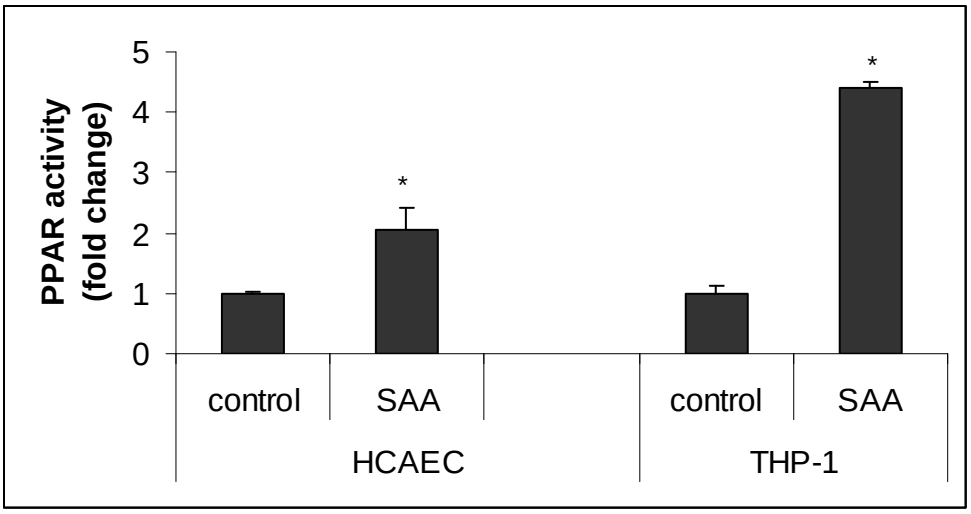

Figure 19. SAA enhances PPARↃ activity in HCAEC and THP-1 cell lines. THP-1 cells were seeded on 6-well plate at a density of 2 x 10^6/well and differentiation was induced with 50 ng/ml phorbol 12-myristate 13-acetate (PMA) for 5 days. HCAEC (2 x 10^6/well) and THP-1 cells were treated with 20 µg/ml of SAA for 4 hours and nuclear protein was extracted. PPARↃ transcription activity was determined by a PPARↃ transcription factor activity assay kit. The results from 3 separately performed experiments are expressed relative to the controls and presented as the mean fold change ± SD. * P<0.05 vs control group. n=3.

3.2 SAA ACTIVATES PPARↃ THROUGH NF-ϞB ACTIVATION

3.2.1 SAA stimulates NF-ϞB activity

To investigate the effect of SAA on NF-ϞB activity in hepatocytes, we used an enzyme-linked immunosorbent assay-based NF-ϞB (p50) transcription factor activity assay kit. HepG2 cells were stimulated with 20 µg/ml of SAA for various lengths of time. As shown in Figure 20a, SAA stimulated NF-ϞB (p50) transcriptional activity by almost two-fold 30 to 60 minutes after stimulation. NF-ϞB (p50) transcriptional activity returned to basal level 120 minutes after stimulation by SAA, which indicates that SAA has a transient effect on NF-ϞB activation.

As lipopolysaccharide (LPS) had also been reported to be able to activate NF-ϞB, we next investigated whether the NF-ϞB activation was a direct effect of SAA or resulted

from contaminating LPS in the SAA preparation. The LPS content in the recombinant SAA is less than or equal to 0.1 ng/µg protein, translating into less than or equal to 2 ng/ml LPS for 20 µg/ml SAA. LPS at this concentration or at a concentration of 20 ng/ml was unable to induce significant NF-ϰB activation (Fig. 20b). Given that most proteins are heat-labile while LPS is heat-resistant, we examined the ability of heat-treated SAA (20 µg/ml) and LPS (20 ng/ml) to induce NF-ϰB activation. As shown in Figure 19b, NF-ϰB activity was not affected by heating LPS at 100°C for 30 minutes. In contrast, SAA could no longer induce NF-ϰB activation after the same heat treatment. In parallel experiments, polymyxin B (PMB), an amphiphilic cyclic polycationic peptide that specifically binds to LPS and neutralizes its effect, had a minimal effect on the potency of SAA-induced NF-ϰB activation. These results indicate that the trace amount of LPS in the SAA preparation cannot account for the NF-ϰB activation.

NF-ϰB activation has been reported to be associated with IϰB phosphorylation and subsequent degradation [263, 264], thus, the effect of SAA on IϰB degradation was also examined. Stimulation of HepG2 with 20 µg/ml of SAA for 30-45 minutes elicited a degradation of IϰB, thus supporting our observation of NF-ϰB activation by SAA stimulation (Fig. 20c). An electrophoretic mobility shift assay showed that SAA stimulated binding activity to a consensus NF-ϰB site in 30 minutes, which was effectively competed with the unlabeled NF-ϰB probe (Fig. 20d). The binding was not affected by the same molar excess of oligonucleotide with mutated sequence. The identity of the NF-ϰB oligonecleotide complex was verified by supershift assay (Fig. 20d).

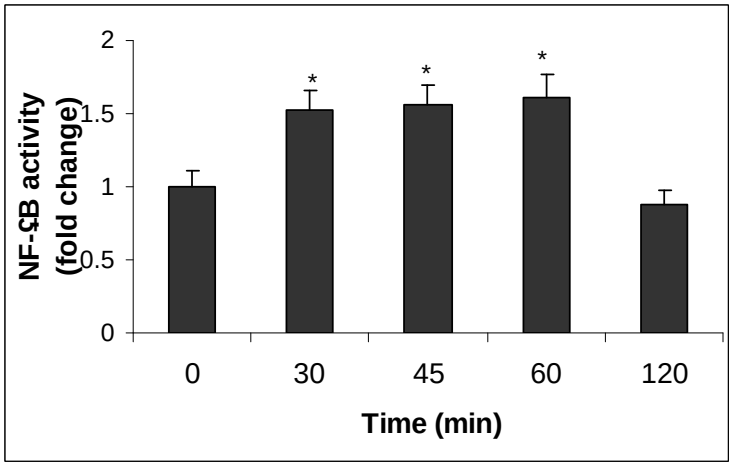
NF-ȹB activity
(fold change)
2
1.5
1
0.5
0
*
*
*
0
30
45
60
120
Time (min)

(a)

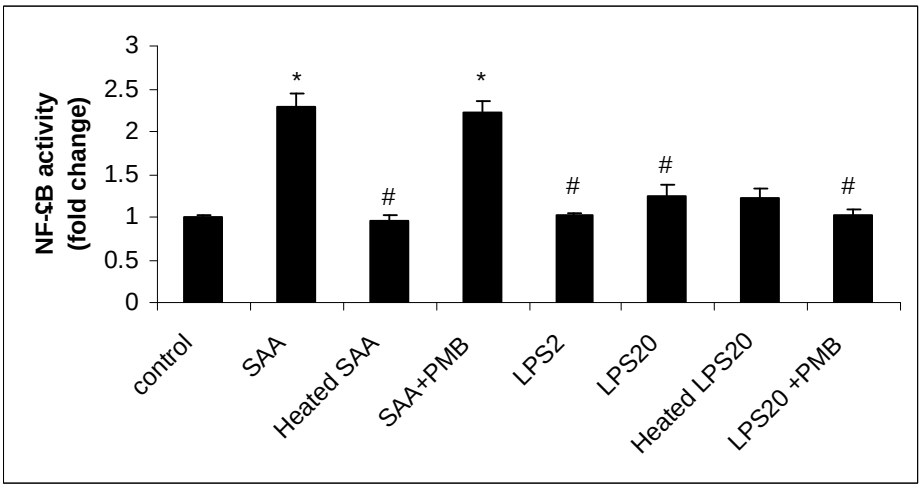
NF-ȹB activity
(fold change)
3
2.5
2
1.5
1
0.5
0
*
*
#
#
#
#
control
SAA
Heated SAA
SAA+PMB
LPS2
LPS20
Heated LPS20
LPS20 +PMB

(b)

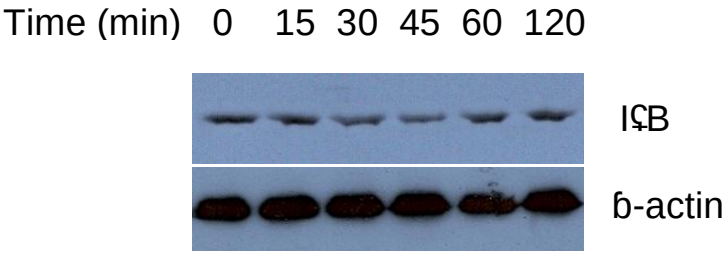
Time (min) 0 15 30 45 60 120
IȹB
ɓ-actin

(c)

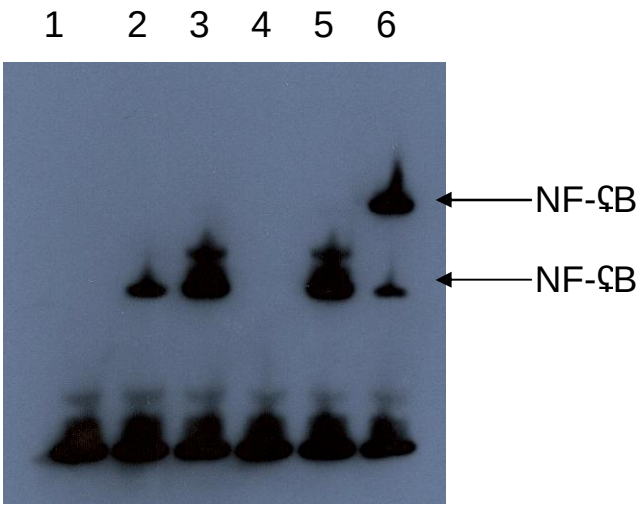

(d)

Figure 20. SAA stimulates NF-kB activation. HepG2 cells were stimulated with SAA (20 μg/ml) for indicated times. (a) NF-ʢB activity was examined using an ELISA kit. (b) HepG2 cells were incubated with SAA (20 μg/ml), LPS (2 ng/ml and 20 ng/ml), heat-treated LPS and SAA (100°C for 30 minutes), polymyxin B (50 μg/ml, 1 hour)-treated LPS and SAA, and apoA-I (20 μg/ml) for 4 hours and followed by the NF-kB transcriptional activity assay. (c) Protein samples were Immunoblotted with anti-I ʢB antibodies. (d) 30 min after SAA stimulation, EMSA was performed to determine the binding activity of NF-kB. The concentration of the unlabeled probes used for competition was 200-fold in excess. Lane 1, free probe; 2, control; 3, SAA treatment; 4, SAA + unlabeled probe; 5, SAA+unlabeled mutant probe; 6, SAA + anti-NF-ʢB. The results from at least 3 separately performed experiments are expressed relative to the controls and presented as the mean ± SD. * $P<0.05$ vs 0 or control group. #$P<0.05$ vs SAA group. n=3 to 5.

3.2.2 SAA-induced COX-2 expression and PPARↄ activation are through NF-ʢB pathway

Our previous data [265] showed that SAA could activate PPARↄ transcriptional activity through COX-2 expression. The promoter region of COX-2 contains two putative NF-ʢB binding sites [266]. NF-ʢB had been shown to be a positive regulator of COX-2 expression [267, 268]. Our previous data also showed that COX-2 was involved in the SAA-induced PPARↄ activation through the ERK1/2 pathway. To assess the role of NF-ʢB in COX-2 expression and PPARↄ activation, we examined the effect of specific

pathway inhibitors on COX-2 expression and PPARɔ activation. Our data confirmed that SAA stimulation increased the COX-2 expression (Fig. 21a) and that COX-2 inhibitor, NS398, could partially suppress SAA-induced PPARɔ activation (Fig. 21b). Preincubation with NF-ɮB inhibitor, BAY 11-7082, was shown to significantly inhibit SAA-stimulated COX-2 expression and SAA-induced PPARɔ activation (Fig. 21a and 21b), indicating that both SAA-stimulated COX-2 expression and SAA-induced PPARɔ activation is through NF-ɮB pathway. In our previous study, we found that SAA could increase intracellular 15d-PGJ_2, a potent PPARɔ ligand, through COX-2 overexpression. In this study, the increased intracellular 15d-PGJ_2 stimulated by SAA was reduced by BAY 11-7082 (Fig. 21c), suggesting the role of NF-ɮB in PPARɔ activation.

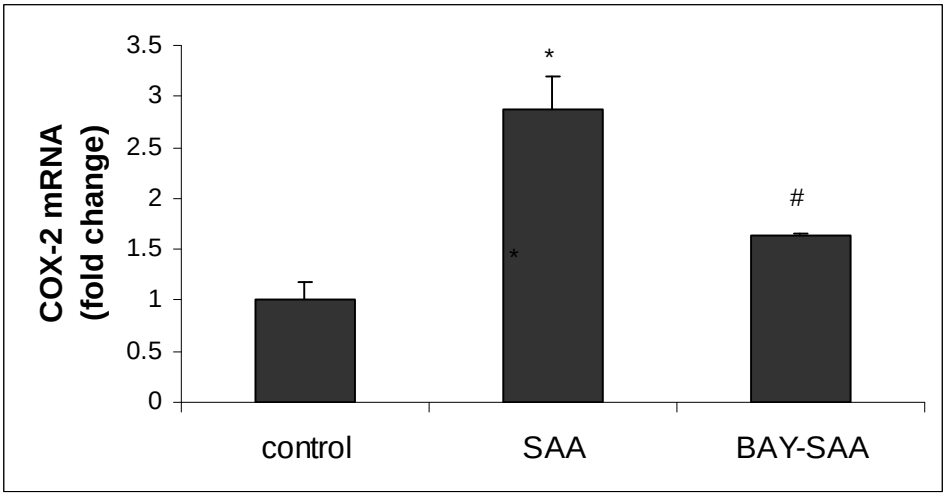

(a)

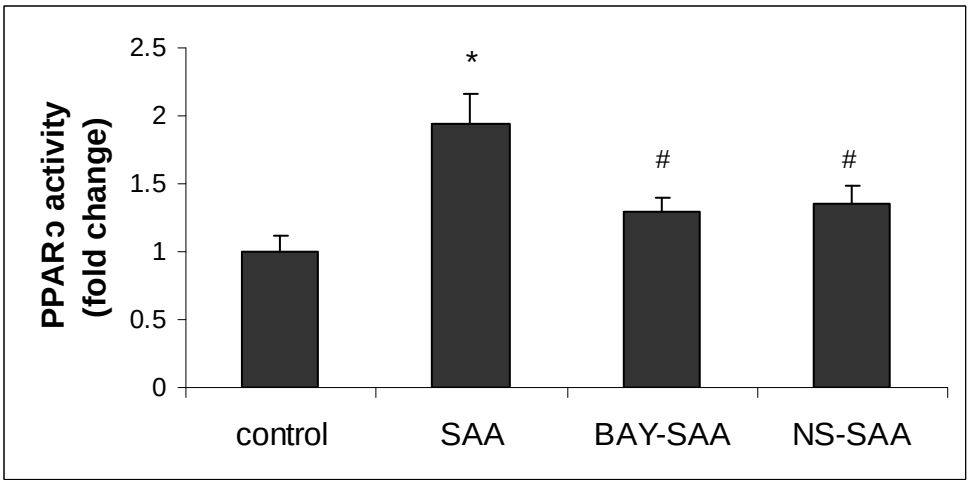

(b)

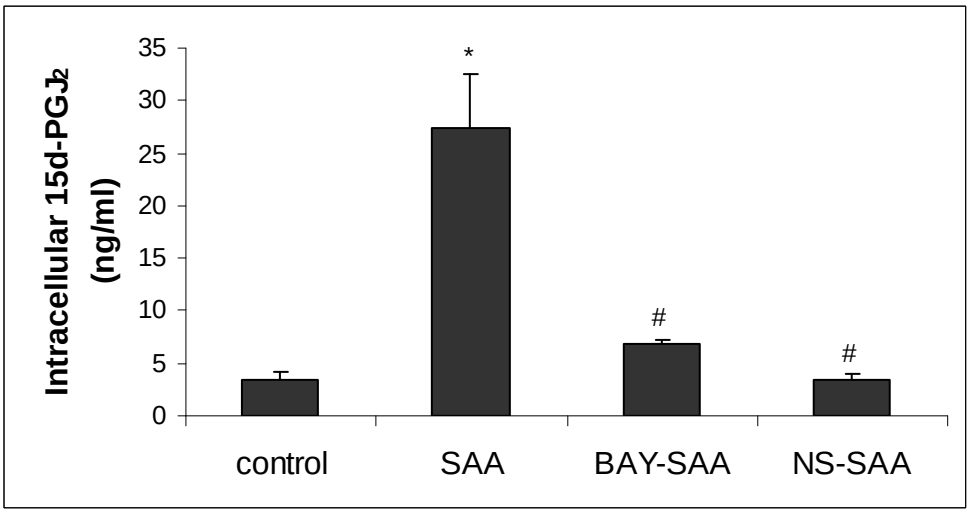

(c)

Figure 21. SAA-induced COX-2 expression and PPARɔ activation is through NF-ʂB pathway. HepG2 cells were pre-incubated with 10 μM of BAY11-7082, 10 μM NS-398 or vehicle before SAA stimulation (20 μg/ml) for 4 hours. (a) Total RNA was extracted and real-time quantitative RT-PCR was performed to determine mRNA expression levels of COX-2. The mRNA levels of COX-2 were standardized for glyceraldehyde-3-phosphate dehydrogenase (GAPDH) levels. (b) PPARɔ transcription activity was determined by a PPARɔ transcription factor activity assay kit. (c) 15d-PGJ_2 level was measured by an EIA kit. The results from at least 3 separately performed experiments are expressed relative to the controls and presented as the mean ± SD. **P*<0.05 vs control group. #*P*<0.05 vs SAA group. n=3 to 5.

3.2.3 SAA-induced PPARɔ activation is completely blocked by the combination of ERK1/2 and NF-ʏB inhibitors

As mentioned in section 3.1.9 that ERK1/2 inhibitor, PD98059, could partially suppress the SAA-induced PPARɔ activation. Here, we investigated the effect of the combination of both ERK1/2 (PD98059) and NF-ʏB (BAY 11-7082) inhibitors on PPARɔ activation. While the SAA-induced PPARɔ activation was only partially blocked by either ERK1/2 or NF-ʏB inhibitor, the combination of both inhibitors completely inhibit the PPARɔ activation (Fig. 22).

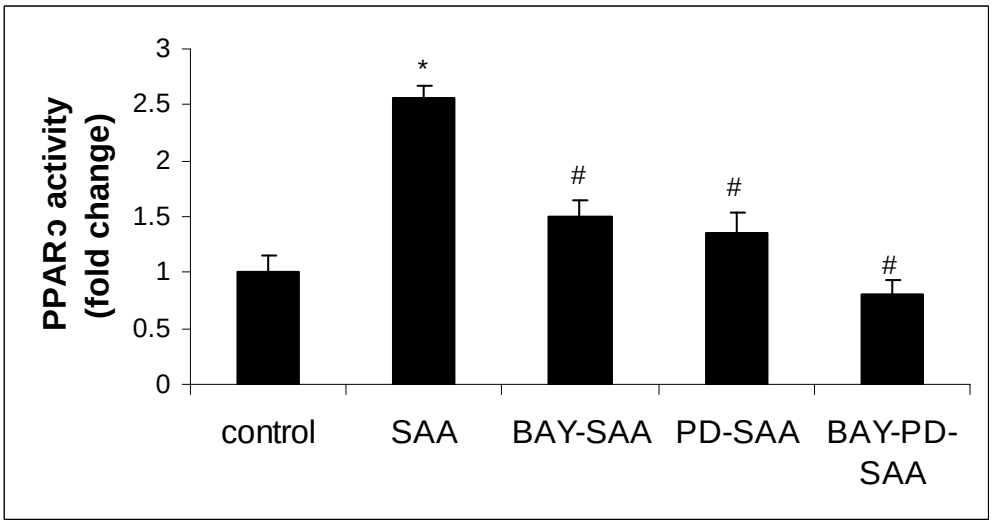

Figure 22. SAA-induced PPARɔ activation is completely blocked by the combination of ERK1/2 and NF-ʏB inhibitors. Cells were pre-incubated with 10 µM of BAY11-7082, 50 µM PD98059, 10 µM of BAY11-7082 + 50 µM PD98059 or vehicle before SAA stimulation (20 µg/ml) for 4 hours. PPARɔ transcription activity was determined by a PPARɔ transcription factor activity assay kit. The results from at least 3 separately performed experiments are expressed relative to the controls and presented as the mean ± SD. * P<0.05 vs Control group. #P<0.05 vs SAA group. n=3 to 5.

3.2.4 SAA-induced NF-ʏB activation is suppressed by HDL

Although SAA is largely associated with HDL in circulation, it has been speculated that it is available in lipid-free/lipid-poor forms at the site of atherosclerotic

lesion formation. Therefore, functional differences between lipid-associated and lipid-free SAA are of great interest. Studies were performed to determine if HDL-associated SAA induces NF-ʁB activation or if the association with HDL affects these effects by incubating a constant concentration of SAA with varying concentrations of HDL. The addition of increasing concentrations of HDL caused a dose-dependent suppression in SAA-induced NF-ʁB activation while HDL alone had no effect on NF-ʁB activation (Fig. 23). HDL (25 µg/ml) cultured with SAA reduced the SAA-induced response by 14%, and suppression reached 33% and 96% with 50 and 100 µg/ml HDL, respectively. Inhibition with 50-100 µg/ml HDL was statistically signigicant (P<0.05).

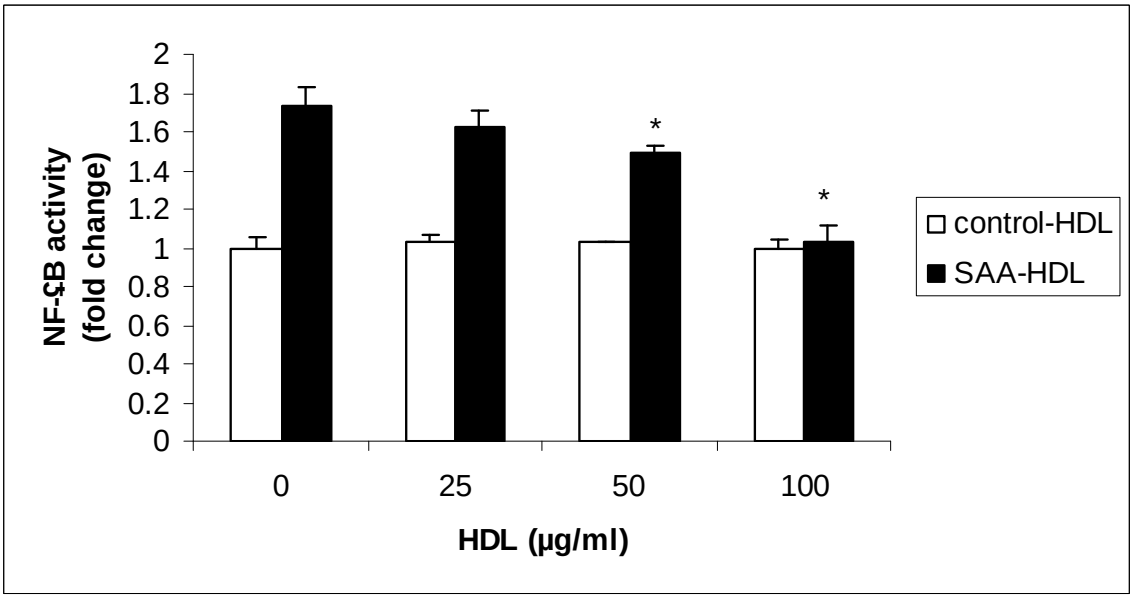

Figure 23. SAA-induced NF-ʁB activity is inhibited by HDL association. HepG2 cells were incubated with media containing 20 µg/ml of SAA and increasing concentrations of HDL (25-100 µg/ml) (SAA-HDL) or media containing HDL only (control-HDL) for 4 hours. NF-ʁB activity was determined as described before. The results from at least 3 separately performed experiments are expressed relative to the controls and presented as the mean ± SD. * P<0.05 vs 0 group. n=3 to 5.

3.3 SAA-INDUCED EFFECTS ARE MEDIATED BY DIFFERENT RECEPTORS

3.3.1 FPRL-1 and TLR4 are involved in SAA-induced PPARɔ and NF-ʏB activation

As the effects of SAA have been postulated to be initiated by its binding to specific membrane receptors, we further examined the involvement of FPRL-1, SR-BI, TLR-2 and TLR-4 in SAA-induced effects. PTX is a known inhibitor for FPRL-1. BLT-1 is a low-molecular weight compound that has known to be an inhibitor of SR-BI selective uptake and cholesterol efflux. Specific antibodies against TLR2 and TLR4 were also used to examine the involvement of these two receptors in the SAA-induced effects. In this study, we found that pretreatment of HepG2 cells with PTX, a known effective FPRL-1 inhibitor, and anti-TLR4 antibody caused a marked reduction in COX-2 expression (Fig. 24a). However, BLT-1 and anti-TLR2, which effectively blocks SR-BI and TLR2 respectively, had no significant effect on SAA-induced COX-2 expression (Fig. 24a). Preincubation of HepG2 cells with PTX, anti-TLR2 and anti-TLR4 demonstrated a partial inhibitory effect to SAA-induced NF-ʏB activation (Fig. 24b). Pretreatment of HepG2 cells with PTX, anti-TLR2 and anti-TLR4 also showed a similar inhibitory effect to SAA-induced PPARɔ activation, although to a less extent (Fig. 24c). Our data indicated that FPRL-1 and TLR4 are likely to be the receptors through which SAA mediates its effects to initiate COX-2 expression, NF-ʏB and PPARɔ activation. TLR2 apprears to be involved in SAA-induced NF-ʏB and PPARɔ activation.

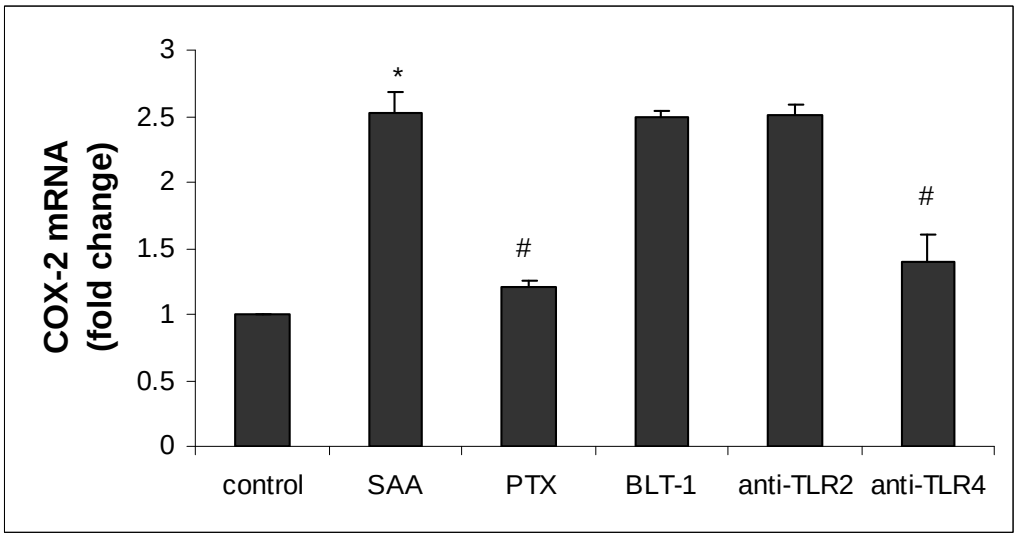
COX-2 mRNA
(fold change)
3
2.5
2
1.5
1
0.5
0
*
#
#
control
SAA
PTX
BLT-1
anti-TLR2
anti-TLR4

(a)

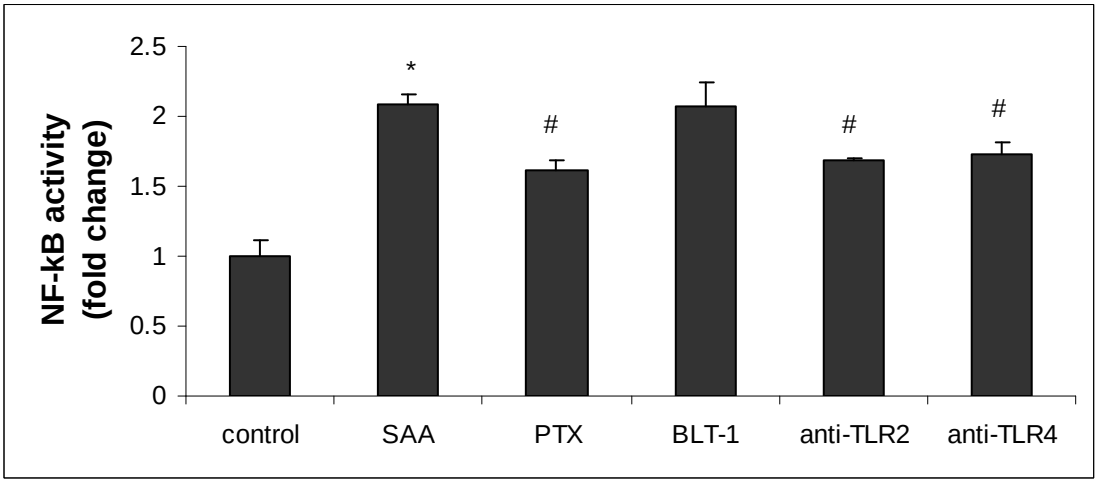
NF-kB activity
(fold change)
2.5
2
1.5
1
0.5
0
*
#
#
#
control
SAA
PTX
BLT-1
anti-TLR2
anti-TLR4

(b)

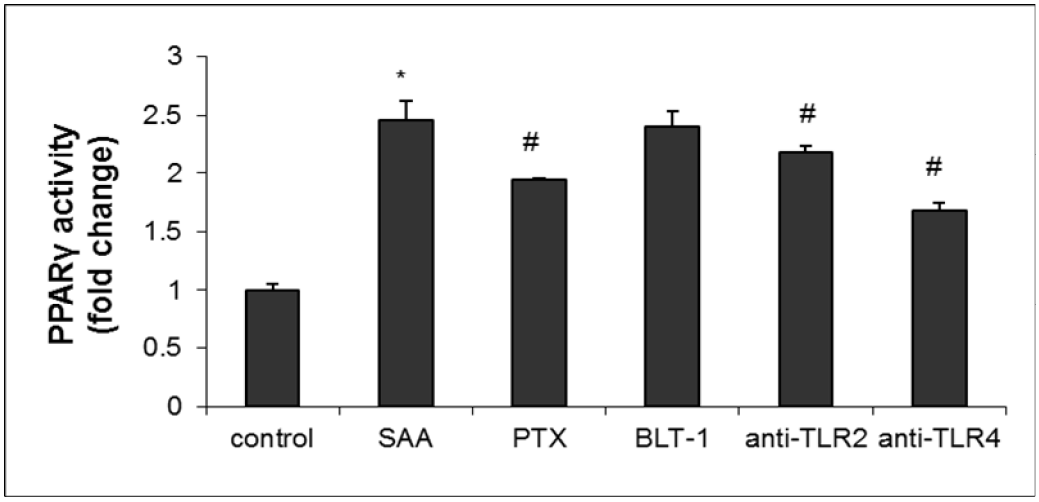

(c)

Figure 24. FPRL-1 and TLR4 are involved in SAA-mediated effects. HepG2 cells were pretreated with 500 ng/ml of pertussis toxin (PTX), 5 μM of BLT-1, 5 μg/ml of anti-TLR2, and 5 μg/ml of anti-TLR4 for 1 hour and then treated with 20 μg/ml of SAA for 4 hours. (a) Total RNA was extracted and real-time quantitative RT-PCR was performed to determine mRNA expression levels of COX-2. The mRNA levels of COX-2 were standardized for glyceraldehyde-3-phosphate dehydrogenase (GAPDH) levels. (b) NF-ʕB activity was examined as desribed before. (c) PPARↄ transcription activity was determined by a PPARↄ transcription factor activity assay kit as described before. The results from 3 separately performed experiments are expressed relative to the controls and presented as the mean ± SD. * P<0.05 vs Con group. # P<0.05 vs SAA group. n=3.

3.3.2 SAA-enhanced cholesterol efflux is partially through SR-BI

We next assessed the contribution of these receptors in SAA-enhanced cholesterol efflux. As shown in Figure 25, treatment with BLT-1 could partially inhibit the cholesterol efflux to HDL (Fig. 25a) and apoA-I (Fig. 25b), suggesting the involvement of SR-BI. However, the efflux levels in both cases were not completely blocked by BLT-1. Therefore, our data supports the partial involvement of SR-BI in SAA-enhanced cholesterol efflux. The SAA-enhanced cholesterol efflux to HDL and apoA-I was also slightly suppressed by PTX, anti-TLR2 and anti-TLR4, but the reduction was not statistically significant.

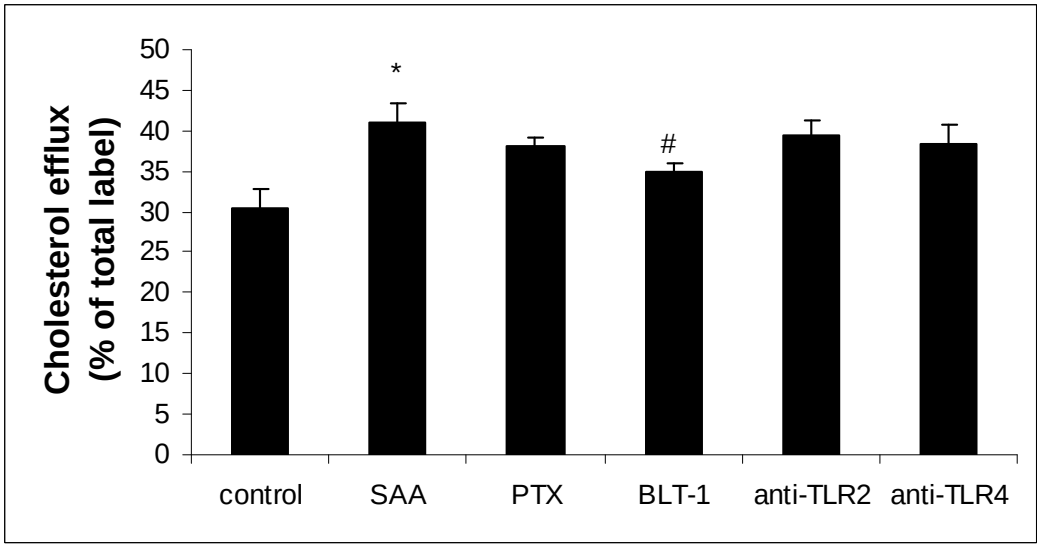

(a)

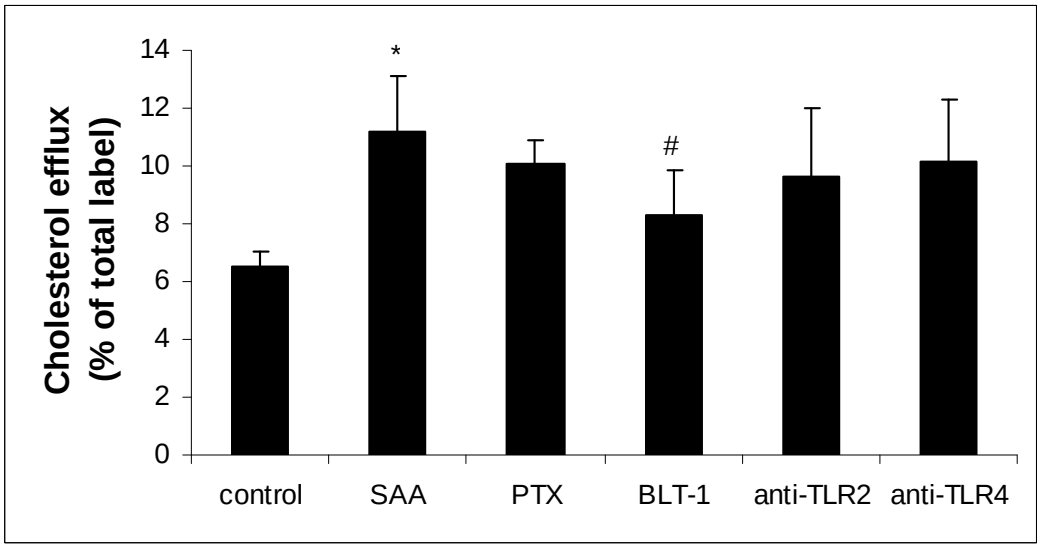

(b)

Figure 25. SAA-enhanced cholesterol efflux is partially through SR-BI. Radiolabeled HepG2 cells were pretreated with 500 ng/ml of pertussis toxin (PTX), 5 μM of BLT-1, 5 μg/ml of anti-TLR2, and 5 μg/ml of anti-TLR4 for 1 hour and then treated with 20 μg/ml of SAA for 4 hours. Cholesterol efflux was measured as described before after an efflux period of 24 hours with (a) HDL (40 μg/ml) or (b) apoA-I (10 μg/ml). The average values are represented (± SD) as the percentage of the radioactivity in medium relative to the total radioactivity in cells and medium. The results from at least 3 separately performed experiments are expressed relative to the controls and presented as the mean ± SD.* $P<0.05$ vs control group. # $P<0.05$ vs SAA group. n=3 to 5.

3.3.3 NF-ϰB and PPARɔ activation via FPRL-1 is SAA-selective

The finding that FPRL-1 stimulation by SAA induced NF-ϰB and PPARɔ activation led us to examine whether other FPRL-1 agonists also elicit the similar effects. Thus, we investigated the effects of several FPRL-1 agonists such as MMK-1 [269], WKYMVM [270], HFYLPM [271] and F-peptide (EGSDTITLPCRIKQFINMWQE) [272] on NF-ϰB and PPARɔ activation. As shown in Figure 26, none of these FPRL-1 agonists, except SAA, stimulated NF-ϰB and PPARɔ activation, suggesting that NF-ϰB and PPARɔ activation via FPRL-1 is SAA-selective. We also examined the effect of an FPRL-1 antagonist, WRW4 (Trp-Arg-Trp-Trp-Trp-Trp) [273]. The pretreatment of WRW4 dramatically inhibited SAA-induced NF-ϰB and PPARɔ activation (Fig. 26).

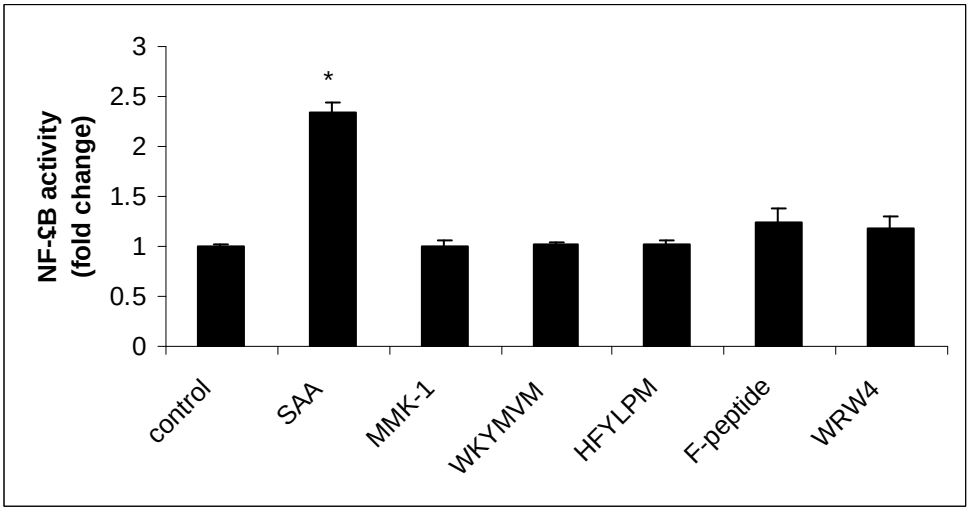

(a)

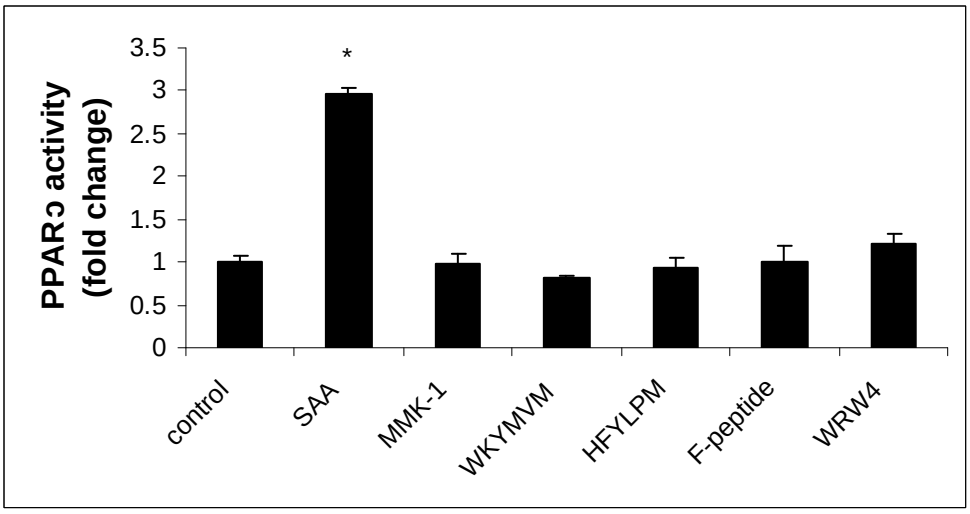

(b)

Figure 26. NF-ʕB and PPARɔ activation via FPRL-1 is SAA-selective. HepG2 cells were stimulated with several FPRL-1 agonists (1 μM WKYMVM, 30 μM F-peptide, 1 μM MMK-1, 5 μM HFYLPM), and 20 μg/ml SAA or pretreated with 10 μM WRW4 and then treated with 20 μg/ml SAA for 4 hours. (a) NF-ʕB and (b) PPAR activities were measured as described before. The results from at least 3 separately performed experiments are expressed relative to the controls and presented as the mean ± SD.* $P<0.05$ vs control group. n=3 to 5.

3.4 THE N-TERMINAL IS ESSENTIAL FOR SAA PROTEIN EXPRESSION, SECRETION AND CHOLESTEROL EFFLUX

3.4.1 mutSAA protein expression and secretion are impaired in HEK293 cells

The transfection host Human Embryonic Kidney (HEK) 293 cells secrete very low level of SAA, therefore, we chose this cell line to examine the effect of endogenously expressed protein and to identify the functional domain and essential amino acid of SAA in cholesterol efflux. Quantitative real-time PCR data showed that mRNA of SAA in cells transfected with wild-type and mutant SAA plasmids increased significantly compared with cells incubated with transfection reagent and cells

transfected with control plasmid (Fig. 27). No large discrepancy was observed in the mRNA of SAA among all the transfected cells despite of different SAA constructs.

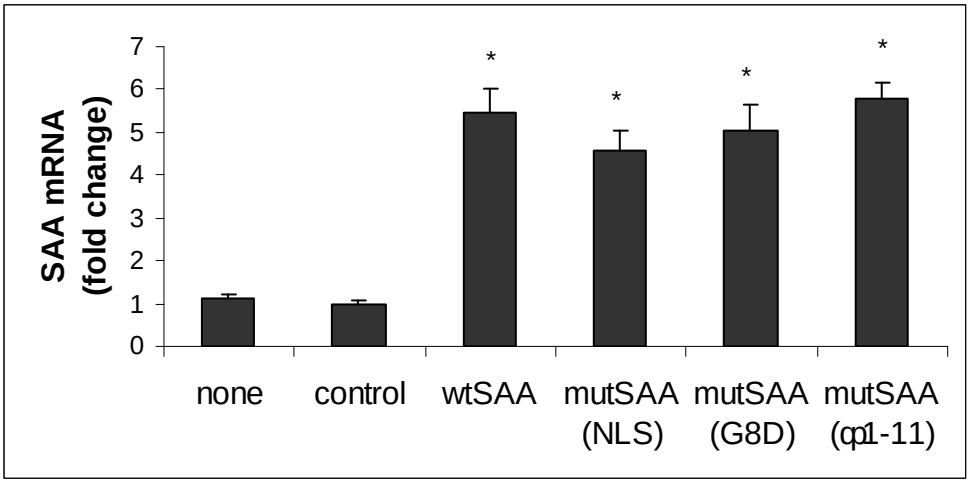

Figure 27. The SAA mRNA levels are similar after transfection with different constructs. HEK293 cells were transfected with SAA or mutSAA constructs using lipofectamine 2000 for 3 days under standard conditions. mRNA expression levels of SAA were quantified as described before. Control, cells were transfected with empty plasmid pcDNA3.1 without SAA sequence; mutSAA (NLS), SAA construct without the leading sequence peptide from -18 - -1; mutSAA (G8D), SAA construct with an amino acid substitution of Glycine to Aspartic acid at the 8th residue; mutSAA (ϕ1ð 11), SAA construct with the deletion of first 11 amino acids; none, cells were incubated with transfection reagent only. Experimental results are expressed as means ± S.D. The results from least 3 separately performed experiments are expressed relative to the controls and presented as the mean ± SD.* $P<0.05$ vs control group. n=3.

The SAA protein expression in HEK293 cells was determined by measuring SAA concentration in the medium of transfected HEK293 cells using ELISA three days after transfection. Table 6 shows the expression of SAA protein levels in the medium as well as in the cell lysates. Cells transfected with wild-type SAA construct yielded high protein expression and approximately 90% of wild-type SAA was secreted to the medium. In contrast, the total yield of mutant SAA proteins decreased dramatically. In addition, the

majority of mutant proteins were found to be present in the cell lysate. Only 32-48% of mutant SAA protein was secreted to the medium, which suggested an essential role of the leading peptide (-18 ð -1 segment) and the first 11 amino acids, especially the 8th residue in the expression and secretion of SAA protein.

Plasmid used for the transfection	SAA concentration in the medium (ng/ml)	SAA concentration in cell lysate (ng/ml)
wild-type SAA	1196.52 ± 152.92	143.12 ± 2.19
mutSAA (NLS)	50.70 ± 2.58	54.64 ± 8.57
mutSAA (G8D)	200.39 ± 35.38	429.12 ± 17.59
mutSAA (φ1ð 11)	220.21 ± 22.77	236.67 ± 12.67
Control	0	0
None	0	0

Table 7. ELISA measurement of SAA in transfected HEK293 cells. HEK293 cells were transfected with SAA or mutSAA constructs using lipofectamine 2000 for 3 days under standard conditions. Cells were lysed in 1 ml of lysis buffer containing 1% Triton X-100, 150 mM of NaCl, 50 mM of EDTA and 1x protease inhibitors mixtures.SAA concentrations in the medium and cell lysate were determined by ELISA in duplicate experiments. None, cells were incubated with transfection reagent only; control, cells were transfected with empty plasmid pcDNA3.1 without SAA sequence; mutSAA (NLS), SAA construct without the leading sequence peptide from -18 - -1; mutSAA (G8D), SAA construct with an amino acid substitution of Glycine to Aspartic acid at the 8th residue; mutSAA (φ1ð 11), SAA construct with the deletion of first 11 amino acids. The results from 4 separately performed experiments are expressed relative to the controls and presented as the mean ± SD.

3.4.2 Cholesterol efflux is impaired in HEK293 cells transfected with mutSAA constructs

Transfected cells were labeled with [^{3}H]cholesterol one day after transfection. The results showed the cholesterol efflux to HDL increased significantly in cells expressing wild-type SAA compared to the cholesterol efflux level in cells transfected with empty vector and in cells incubated with transfection reagent (Fig. 28). The cholesterol efflux to HDL was impaired severely in cells expressing mutant SAA proteins (NLS, G8D and ¤1-11).

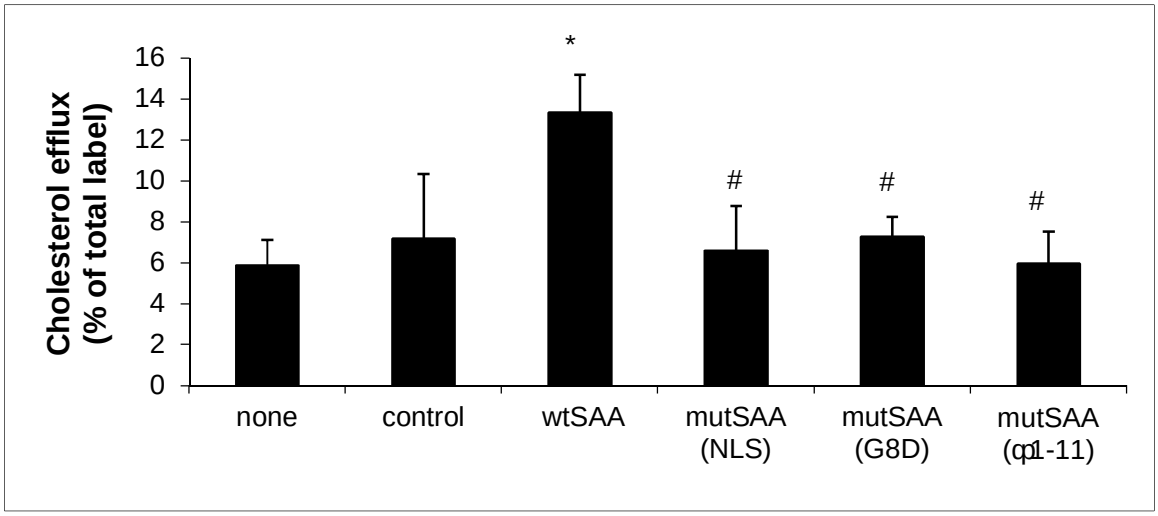

Figure 28. Cholesterol efflux is impaired in HEK293 cells transfected with mutSAA constructs. Transfected HEK293 cells were labeled with [^{3}H] cholesterol for 24 hours at 37°C, equilibrated in medium in the absence of cholesterol for 16 hours. After the equilibration, the cells were washed with 1x PBS for four times. The cells were then incubated with medium containing 40 µg/ml of HDL at 37 °C for 24 hours. Medium was collected and assayed for [^{3}H] cholesterol. Cells were lysed with 0.1% SDS and 0.1 M NaOH lysis buffer, and radioactivity was determined by scintillation counter. The average values are represented (± SD) as the percentage of the radioactivity in medium relative to the total radioactivity in cells and medium. Control, cells were transfected with empty plasmid pcDNA3.1 without SAA sequence; wtSAA, cells were transfected with pcDNA3.1-wild-type SAA; mutSAA (NLS), cells were transfected with SAA construct without the leading sequence peptide from -18 - -1; mutSAA (G8D), cells were transfected with SAA construct with an amino acid substitution of Glycine to Aspartic acid at the 8th residue; mutSAA (¤1ð 11), cells were transfected with SAA construct

with the deletion of first 11 amino acids; none, cells were incubated with transfection reagent only. The results from at least 3 separately performed experiments are expressed relative to the controls and presented as the mean ± SD.* $P<0.05$ vs control group. # $P<0.05$ vs SAA group. n=4 to 5.

3.4.3 PPARɔ activity is impaired in HEK293 cells transfected with mutSAA constructs

The cells were subjected to PPARɔ activity assay 72 hours after transfection. The results showed the PPARɔ activity increased significantly in cells expressing wild-type SAA compared to that in cells transfected with empty vector and in cells incubated with transfection reagent only (Fig. 29). The PPARɔ activity was impaired severely in cells expressing mutant SAA proteins (NLS, G8D and ɋ1-11).

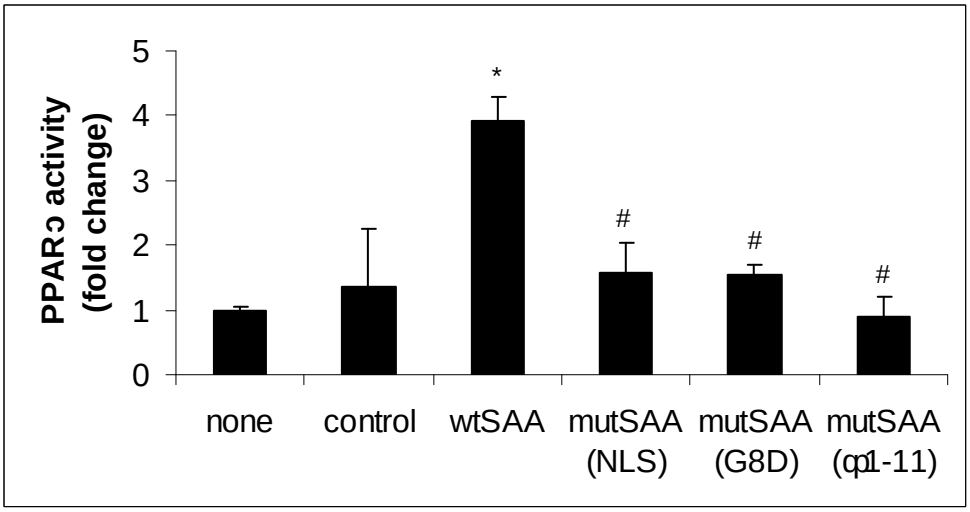

Figure 29. PPARɔ activity is impaired in HEK293 cells transfected with mutSAA constructs. HEK293 cells were transfected with SAA or mutSAA constructs using lipofectamine 2000 for 3 days under standard conditions. Cells were lysed, nuclear proteins were extracted and PPARɔ activity assay were performed as described previously. None, cells were incubated with transfection reagent only; control, cells were transfected with empty plasmid pcDNA3.1 without SAA sequence; mutSAA (NLS), SAA construct without the leading sequence peptide from -18 - -1; mutSAA (G8D), SAA construct with an amino acid substitution of Glycine to Aspartic acid at the 8th residue; mutSAA (ɋ1ð 11), SAA construct with the deletion of first 11 amino acids. The results from 4 separately performed experiments are expressed relative to the controls and presented as the mean ± SD.

CHAPTER IV

DISCUSSION

SAA is one of the major acute phase plasma proteins involved in multiple physiological and pathological processes. As the liver is the major site of SAA synthesis, we chose the human hepatocellular carcinoma cell line (HepG2) to conduct the experiments. The normal SAA level is considered to be less than 0.1 µM or 1.25 µg/ml. Under inflammatory conditions, the maximal levels could be up to 80 µM or 1 mg/ml. The concentrations of SAA (5ï 40 µg/ml) tested were within the range that represented low-grade inflammation [257]. Our data have shown that SAA could activate PPARɔ through the ERK1/2 and NF-ʏB pathways, leading to upregulation of PPARɔ target gene expression, such as ABCA1 and ABCG1 (Fig. 30). We also demonstrated that SAA-induced PPARɔ activation is dependent on COX-2. The finding that preincubation of HepG2 with SAA increased cholesterol efflux suggests that SAA may serve to promote the efflux of cholesterol from the liver. SAA-induced PPARɔ activation has not been reported previously in studies involving SAA. Furthermore, the receptors involved in SAA-induced effects were also investigated. The effect of SAA on PPARɔ activity is mediated, at least in part, by FPRL-1, TLR4 and SR-BI receptors. Finally, we found that the N-terminal of SAA is essential for SAA protein expression, secretion and PPARɔ activation.

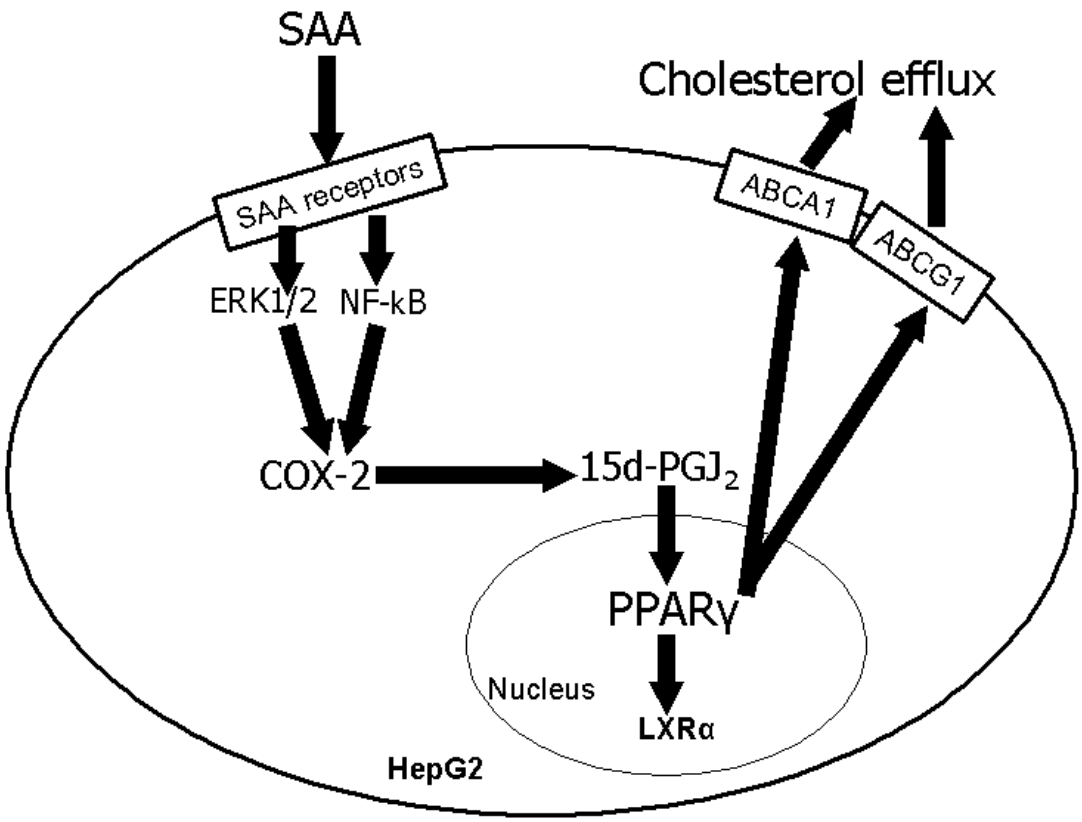

Figure 30. Schematic diagram of the proposed mechanism of cholesterol efflux through SAA-induced PPARɔ activation of its target genes.

4.1 SAA INDUCES PPARɔ ACTIVATION

In this study, we found PPARɔ transcriptional activity was increased by three-fold because of SAA stimulation in HepG2 cells. However, there was no significant corresponding change in the PPARɔ mRNA levels. The data demonstrated that the PPARɔ inhibitor T0070907 had a significant inhibitory effect on PPARɔ transcription, which is consistent with a previous publication [274]. T0070907 covalently binds to Cys313 of PPARɔ, inducing conformational changes that block the recruitment of transcriptional cofactors to the PPARɔ-RXR heterodimer. However, further experiments should be carried out to elucidate this observation. We employed three approaches to

evaluate the relationship between SAA and PPARɔ: ELISA, EMSA and PPRE-luc reporter system. Our data showed that SAA strengthened PPRE binding and enhanced PPARɔ transcriptional activity. The expression levels of PPARɔ target genes such as ABCA1 and ABCG1 were also increased by SAA treatment.

The finding that SAA induces PPARɔ activation could have relevance to the role of SAA in atherogenesis. Some recent studies have suggested that SAA may be atheroprotective [126]. Although some other studies have suggested a proatherogenic role of SAA signaling, this role may depend on the cell type involved as well as the specific receptors and signaling pathways downstream of SAA stimulation. There seems to be abundant evidence for a proatherogenic role of SAA signaling in endothelial cells and monocytes [116, 217]. In contrast, our data suggest that SAA signaling in hepatocytes may have antiatherogenic consequences through PPARɔ activation.

As SAA-induced PPARɔ activation is the key finding of our study, we would like to know whether this effect also applies to other cell lines. Both endothelial cells and monocytes play important roles in atherosclerosis development, we repeated the PPARɔ activity assay in a endothelial cell line, human coronary artery endothelial cells (HCAEC), and a monocyte cell line, human acute monocytic leukemia cell line, THP-1. Both of them showed an enhancement in PPARɔ activity after SAA stimulation, though the response of THP-1 to SAA treatment was more drastic, indicating that the discovery was not a cell-specific effect.

A recent study reported that porcine recombinant SAA protein reduced the level of PPARɔ expression by 60% and its target gene (aP2, LPL and ACC1) mRNA levels were also decreased in porcine differentiated adipocytes [275]. The discrepancy between

their observations and our findings could be due to tissue specific regulation of these genes as well as distinct cofactors involved in the transcriptional machinery. Most importantly, PPARɔ activity was not measured in their study.

In another study, it was reported that adipocyte hypertrophy induced SAA3 mRNA expression in murine preadipocytes (3T3-L1) [276]. The researchers found PPARɔ DNA binding activity to be decreased in hypertrophic adipocytes but without any change in PPARɔ mRNA levels. However, their study was based on a murine cell line and the reported increase in SAA was SAA3 and not SAA1, the acute-phase protein we studied. Although the relative map positions and transcriptional orientations provide strong evidence that human SAA1 and mouse SAA1 are evolutionary homologs, as are human SAA2 and mouse SAA2, comparison of the amino acid sequence alignments of SAA isoforms in mice and human demonstrated that mouse SAA3 is most similar to the human isoform SAA1. It was speculated that mouse SAA3 might be functionally similar to human SAA1 based on the sequence similarity. However, the hypothesis has not been confirmed. In addition, human SAA1 is predominantly expressed in liver while mouse SAA3 is primarily expressed extrahepatically and most abundant in adipose tissue and colon. In their study, the decrease in PPARɔ activity and increase in SAA3 were parallel observations and the authors did not establish any link between murine SAA3 and PPARɔ DNA binding activity. We had established in our paper that SAA1 is able to activate PPARɔ. SAA was an observed effect in their study after induction of adipocyte hypertrophy (the cause), whereas SAA1 was tested as the cause for other effects in our study. Furthermore, their effects were detected 6-7 days after hypertrophy induction whereas we examined PPARɔ activity 4 hours after SAA treatment.

The protein biosynthesis inhibitor, CHX, was shown to have an inhibitory effect on SAA-induced PPARↄ activation, suggesting that another signaling molecule or endogenous SAA could play a role in this process. In order to determine whether the unknown molecule is a cytokine or endogenously produced SAA, the PPARↄ activity assay was repeated with siRNA against SAA1 and SAA2. Knockdown of SAA1 could partially reduce the PPARↄ activation induced by exogenous SAA while siSAA2 did not show such effects. The possibility of one or several other signaling molecules being involved in this process could not be excluded, and more experiments need to be conducted.

4.2 SAA INDUCES THE EXPRESSION OF ABCA1 AND ABCG1, AND ENHANCES CHOLESTEROL EFFLUX

In this study, we showed that SAA could induce ABCA1 and ABCG1 expression in HepG2 cells. Both ABCA1 and ABCG1 play important roles in cholesterol efflux. Thus, functional expression of both ABC transporters is critical for preventing atherogenesis. It has been reported that SAA induces ABCA1 and ABCG1 in macrophages [126]. Both of them are members of the ATP-binding cassette transporter family. Our results have shown that SAA-induced ABCA1 and ABCG1 expression is mediated by PPARↄ activation. Furthurmore, siRNA to ABCA1 and ABCG1 decreased the SAA-induced cholesterol efflux. These data suggested that the activation of PPARↄ might lead to an anti-atherogenic effect through cholesterol efflux.

Accumulating evidence has shown that SAA could facilitate cholesterol efflux [98, 99, 103, 110]. The data in these studies showed that SAA may enhance cholesterol

efflux by functioning as an acceptor and by increasing the availability of cellular free cholesterol. We demonstrated through this study that SAA could increase the efflux of cholesterol to both HDL and apoA-I. However, the increase in cholesterol efflux was more drastic when apoA-I was used as the cholesterol efflux acceptor compared to HDL. The possible reason for this observation could be the different acceptor specificity for ABCA1 and ABCG1. ABCA1 is a key regulator of the export of cholesterol to lipid-free apolipoproteins, forming nascent HDL, but it is unlikely to be involved in the export of cholesterol to mature HDL [238]. ABCG1 facilitates the export of cholesterol to HDL but not to lipid-free apoA-I [277]. When HDL was used as the efflux acceptor, only the overexpressed ABCG1 could facilitate cholesterol efflux. ABCA1 would not be effective as HDL is not the appropriate acceptor for ABCA-1-dependent cholesterol efflux, although it was upregulated through SAA stimulation. On the other hand, when apoA-I was used as an acceptor, ABCA1 could facilitate the efflux of cholesterol to apoA-I to form nascent HDL, which in turn could serve as an acceptor for ABCG1-mediated cholesterol efflux. Therefore, with the use of apoA-I as the acceptor, both ABCA1 and ABCG1 could contribute to the cholesterol efflux while only ABCG1 could contribute to the efflux when HDL is used. A recent study suggested that ABCA1 and ABCG1 operate in synergy to mediate the efflux of cholesterol to apoA-I [278]. Previous studies have shown that SAA could enhance cholesterol efflux either through being a cholesterol acceptor [103] or by improving the availability of intracellular cholesterol through activation of neutral cholesterol ester hydrolase (nCEH) and deactivation of acyl-CoA cholesteryl acyl transferase (ACAT) [98, 99]. ACAT esterifies cholesterol for storage, and nCEH de-esterifies cholesterol for transport. By inhibiting ACAT and enhancing

nCEH activities, SAA shifts the equilibrium from stored cholesterol ester to transportable free cholesterol, thereby promoting cholesterol efflux. Here, we propose that an additional mechanism in which SAA could induce cholesterol efflux indirectly through upregulation of the efflux mediators ABCA1 and ABCG1 might be in place. This is a novel mechanism and our experimental evidence has suggested addition action points of SAA in cholesterol efflux. This study showed an important link between inflammatory signals and lipid efflux pathways in hepatocytes. It is highly possible that the induction of ABCA1 and ABCG1 by SAA facilitates the resolution of inflammatory lesions and represents a beneficial role of the hepatocytes in the context of atherosclerosis.

4.3 THE EFFECT OF SAA IS NOT DUE TO BACTERIAL CONTAMINATION IN RECOMBINANT SAA PROTEIN

The SAA we used is a recombinant protein produced in *Escherichia coli*. In previous studies, bacterial contamination of recombinant proteins has complicated data interpretation when evaluating SAA-induced effects. We have taken precautions in the determining whether SAA or the contaminating bacterial product, such as LPS, is responsible for the PPARɔ and NF-ʏB activation. Although the endotoxin content of SAA preparation is negligible (0.1 ng/µg), we examined the possible contribution of LPS on the SAA-induced PPARɔ and NF-ʏB activation using polymyxin B, a potent inhibitor of LPS. Polymyxin B (PMB) is an amphophilic cyclic polycationic peptide that forms a complex with LPS and prevents LPS-induced proinflammatory cytokine production.

We concluded that the SAA-induced PPARɔ activation was not due to trace amounts of endotoxin contaminating the recombinant protein (Ò 4 ng/ml of LPS in

culture with 40 µl/ml of SAA) because of the following: 1) LPS at much higher concentration (100 ng/ml for PPARↄ activity assay and 20 ng/ml for NF-ʢB activity assay) did not significantly induce PPARↄ or NF-ʢB activation after 4 hours stimulation; 2) heat denaturation destroyed the ability of SAA to induce PPARↄ and NF-ʢB activation, whereas heat-treated LPS retained its ability to slightly induce PPARↄ and NF-ʢB activation; 3) SAA-induced PPARↄ and NF-ʢB activation was not affected by polymyxin B treatment, which specifically binds to LPS and neutralizes its effect.

4.4 LIPID-FREE SAA AND HDL-CONJUGATED SAA HAVE DIFFERENT EFFECTS

In our study, we used a lipid-poor recombinant synthetic human SAA as well as a HDL-associated SAA. SAA is known to exist in plasma mainly as a HDL apolipoprotein [90]. This raises the question of the physiological relevance of the lipid-poor SAA. Although most of the SAA in plasma is associated with lipoproteins, it is possible that sufficient SAA may exist in a lipid-free form to exert its physiological function. Evidence of the relevance of the lipid-poor SAA comes from the analysis of serum SAA distribution during an acute phase reaction induced by LPS injection in mice [279]. In this study, 15% of SAA was present in the lipid-poor form. Considering the high levels of SAA synthesized during the acute phase response, the physiological functions of the lipid-poor SAA demonstrated in various studies could be easily contributed to this portion [57, 215, 217]. During the acute phase reaction, the serum concentration of SAA may reach 80-1000 µg/ml [53], exhausting the capacity of HDL to bind all of the SAA and allowing some of the SAA to be in a lipid-poor form . In addition, there is evidence

that suggests that newly synthesized SAA is secreted in a lipid-free form from hepatocytes [280]. It is possible that local production of SAA may contribute to its accumulation and that the SAA is potentially available to the cells in a free, non-lipoprotein-bound form to activate PPARↃ and enhance cholesterol efflux.

The acute phase response is associated with a decline in plasma HDL cholesterol and apoprotein A-I [281]. The mechanism responsible for decreased plasma HDL is not clearly understood. It was assumed that SAA enrichment of HDL probably is responsible for decreased plasma apoA-I and HDL levels because SAA could displace apoA-I from HDL and SAA-enriched HDL particles are rapidly cleared from the circulation [282]. However, this proposal appears unlikely since the drop in plasma HDL during the acute phase response occurs rapidly and before SAA accumulation [281]. The prior hypothesis of reverse cholesterol transport (RCT) proposes that the majority of plasma HDL originates from peripheral tissue and is subsequently transferred to the liver [283]. Recent studies have challenged this model based on the finding of reconstitution of ABCA1-deficient mice with bone marrow from wild-type mice does not result in restoration of plasma HDL cholesterol levels, suggesting that monocytes and macrophages may not be a significant source of plasma HDL [250]. Furthermore, overexpression of ABCA1 in liver raised plasma HDL concentration [284] and plasma HDL concentration in liver-specific Abca1-knockout mice was 80% lower than those of wild-type mice [249]. These findings suggest that liver is the major source of HDL.

Our study provided new insight into the observed decrease of HDL and increase of SAA during the acute phase. We showed that SAA stimulation to HepG2 cells increased the cholesterol efflux to both HDL and apoA-I, which is in accordance with the

previous conclusion and liver might be an important organ to contribute to HDL generation, especially in the acute phase response. To compensate for the plasma HDL decrease during acute phase, the increased plasma SAA concentration might result in HDL generation by promoting intracellular cholesterol efflux from hepatocytes. As SAA is synthesized mainly in the liver, hepatocytes may be exposed to an even higher concentration of SAA and contribute to the HDL generation through PPARↄ activation.

We also examined the effect of HDL-associated SAA on PPARↄ activation. The data show that HDL did not alter basal PPARↄ activity, but the association with HDL inhibits the SAA-induced PPARↄ activation. This is consistent with several previous studies which demonstrated that HDL inhibited the chemotactic activity of SAA [52] and decreased tissue factor and $sPLA_2$ induction [116, 234]. It is possible that HDL either competes for receptor binding sites, thereby reducing SAA triggering, or the HDL-SAA complex is a less effective activator.

Interestingly, although both SAA and apoA-I are mainly associated with HDL in blood and apoA-I can be replaced by SAA as the major apolipoprotein in HDL during the acute-phase response, apoA-I itself did not induce PPARↄ, indicating a unique function for SAA.

4.5 SAA INDUCES COX-2 EXPRESSION AND SUBSEQUENTLY INCREASES THE INTRACELLULAR 15d-PGJ_2 LEVEL

It is well known that 15d-PGJ_2, one of the ultimate dehydration products of PGD_2, is a strong PPARↄ activator [136]. Because COXs have the ability to produce

prostaglandins, we speculated that SAA may induce endogenous prostaglandin production via COXs expression.

Cyclooxygenase (COX) is the key and rate-limiting enzyme in the conversion of arachidonic acid (AA) to prostaglandins (PGs), which are lipid metabolites that are involved in several physiological and pathological processes, including inflammation [285]. Two distinct COX isoforms have been characterized, COX-1 and COX-2, that differ in terms of regulatory mechanisms, tissue distribution and preferential coupling to upstream and downstream enzymes [286-288]. COX-1, which is constitutively expressed in most tissues, has been classically considered as the isoform primarily responsible for homeostatic PG synthesis [289]. By contrast, COX-2 is mainly induced in response to inflammatory stimuli, which led to the concept that selective inhibition of COX-2 can reduce inflammation without affecting the physiological functions of COX-1-derived PGs.

COX-2 catalyzes the conversion of arachidonic acid to PGG_2 and further to PGH_2. PGH_2 is subsequently modified into PGD_2. The bioactive 15-deoxy-φ12,14-prostaglandin J_2 (15d-PGJ_2), which is physiologically formed by dehydration and isomerization of the PGD_2 [290]. Recent study suggested that intracellular 15-deoxy-$\varphi^{12,14}$-prostaglandin J_2 (15d-PGJ_2) level could be increased by COX-2 overexpression [258, 259]. It has been reported that SAA induces COX-2 expression in monocytes and epithelial cells [214, 233]. However, the mechanisms of SAA-induced COX-2 expression are not clearly understood.

Our results demonstrated that SAA did not induce COX-1 expression but induced COX-2 expression, suggesting that SAA-induced COX-2 expression was selective. Some

groups also reported that 15d-PGJ_2 level could be induced by COX-2 expression [258]. In accordance with these results, we found that SAA stimulation increased the intracellular 15d-PGJ_2 level and this induction was probably due to the COX-2 overexpression. We also showed that COX-2 inhibitor, NS398, exerted an inhibitory effect on the SAA-induced 15d-PGJ_2, suggesting the involvement of COX-2. The enhanced PPARↄ activity by SAA was also partially but significantly inhibited by NS398. These results suggest that COX-2-mediated increase in intracellular 15d-PGJ_2 level is one of the mechanisms by which SAA induces PPARↄ activation.

The role of COX-2 in atherosclerosis is a controversial issue in the past several years. It has been reported that selective COX-2 inhibition suppresses atherosclerotic lesion formation in LDL receptor-deficient mice [291], indicating that COX-2 act as an inducer of atherosclerosis. Conversly, several recent studies have showed that treatment with COX-2 inhibitors in humans does not decrease, but rather increases cardiovascular events [292-294]. According to our findings, it is possible that several eicosanoids produced by COX-2 may play a protective role in controlling atherosclerotic progression, through the activation of PPARↄ.

4.6 SAA-INDUCED COX-2 EXPRESSION COULD BE MEDIATED THROUGH ERK1/2 AND NF-ⱡB

SAA-induced COX-2 expression had been shown in monocytes and endothelial cells [233], but the underlying mechanism is not clearly elucidated. MAPKs are important signaling molecules that regulate COX-2 expression [260]. Previous study showed that PPARↄ activation could be mediated by overexpression of COX-2 [295].

Therefore, several pathways which could induce the overexpresion of COX-2 may also activate PPARↃ.

Firstly, our data revealed that SAA induced COX-2 expression in HepG2 cells and that this was mediated by ERK1/2 activation. In addition, SAA-induced PPARↃ activation was inhibited by inhibitors of COX-2 and ERK1/2, suggesting that SAA-induced PPARↃ activation is mediated by ERK1/2-dependent COX-2 expression. However, the pattern of SAA-induced ERK1/2 phosphorylation we found in this study was slightly different from the some other ERK1/2 activation pattern. In some of the studies, the ERK1/2 activation could be detected within 10 minutes after SAA stimulation and it usually subsides after 15 minutes [120, 215]. We showed that SAA increased the level of phosphorylation of ERK1/2 at 10 minutes, and this effect remained up to 6 hours. These data are in line with the results that lipid-free SAA can activate MAPKs, especially ERK1/2, from several other studies [120, 215, 217]. We also evaluated whether ERK1/2 phosphorylation is the direct effect of SAA or through the synthesis of signaling proteins by using the translation inhibitor cycloheximide (CHX). ERK1/2 phosphorylation could be observed for the first 30 minutes despite cycloheximide pretreatment and was only suppressed subsequently while ERK1/2 protein levels were unchanged by cycloheximide. These data indicated that the initial 30 minutes of ERK1/2 phosphorylation might be the direct effect of SAA that did not require any synthesis of signaling proteins whereas the later effects were perhaps dependent on cytokines which may take a longer time to synthesize. With the use of PD98059, an ERK1/2 inhibitor, PPARↃ activation, COX-2 induction, an increased intracellular 15d-PGJ_2 level, and enhanced cholesterol efflux caused by SAA treatment were suppressed.

Secondly, our data also showed that the COX-2 overexpression stimulated by SAA could also through the NF-ϰB pathway. We showed that treatment of human HepG2 cells with SAA resulted in the enhanced degradation of IϰB and increased NF-ϰB transcriptional activity. The results from electrophoretic mobility shift assay confirmed that the DNA binding activity of NF-ϰB was increased by SAA stimulation. Our data also demonstrated that SAA-induced PPARↄ activation was partially inhibited by the NF-ϰB pathway inhibitor, Bay 11-7082, confirming its involvement in PPARↄ activation. Inhibition studies also showed that the same inhibitor partially suppressed the SAA-induced COX-2 expression and 15d-PGJ_2 elevation, the two essential steps in SAA-induced PPARↄ activation. Taken together, these results support that NF-ϰB plays an important role in SAA-induced COX-2-dependent PPARↄ activation. Furthermore, we found that SAA-induced PPARↄ activation was completely abolished when the ERK1/2 and NF-ϰB pathways were blocked at the same time, suggesting these two pathways are essential in SAA-enhanced PPARↄ activity.

4.7 THE RECEPTORS INVOLVED IN SAA-INDUCED EFFECTS

The underlying mechanisms of SAA effects have raised interests on this molecule in recent years. Several potential receptors for SAA have been postulated, including scavenger receptor B-I (SR-BI) [109] and its human orthologue CLA-1 [215], receptor for advanced glycation end products (RAGE) [116], formyl peptide receptor-like 1 (FPRL1) [57], hepaticexpressed Tanis receptor [122], and toll-like receptors [120]. Whether these receptors are essential or dispensable for SAA-induced ERK1/2 mediated PPARↄ activation remains to be determined.

The toll-like receptors (TLRs) are key players of the innate immune system, functioning as pattern recognition receptors that recognize a wide range of microbial pathogens. In addition to microbial products, several endogenous TLR ligands have been identified [296]. For example, high-mobility group box 1 is a ubiquitous, host-derived protein that interacts with multiple TLRs and plays a role in inflammation [297]. The presence of of endogenous TLR ligands supports the notion that TLRs play an essencial role in the detection of danger signals [298, 299]. The acute-phase proteins, such as SAA, could be danger-signaling molecules [299] which, when recognized by the host, may initiate immune response [298]. Seong and Matzinger have hypothesized that endogenous TLR ligands are characterized by the exposure of hydrophobic portions that would act as a universal damage-associated molecular pattern to initiate repair, remodeling, and immunity [299]. As SAA contains hydrophobic amino acid-rich regions that associate with lipoprotein and other ligands [300], it is very likely that it serves as a TLR ligand. SAA is also known to be a ligand for human FPRL-1 [301], which is coupled to the GŭI proteins for transmembrane signaling. FPRL-1 is involved in SAA-induced chemotaxis, proinflammatory cytokine production and secretion, and matrix metalloproteinase-9 production [113, 115, 301].

However, no data have been reported on the possible involvement of these receptors in SAA-induced NF-ʕB and PPARɔ activation as well as cholesterol efflux. In this study, we explored the roles of FPRL-1, SR-BI, TLR2 and TLR4 in SAA stimulated effects. Our results provided evidence that FPRL-1, TLR2 and TLR4 may function as receptors for lipid-poor SAA and subsequently activate NF-ʕB and PPARɔ. With the use of inhibitors for FPRL-1 (PTX) as well as SR-BI (BLT-1) and antibodies against TLR2

and TLR4, both NF-ϞB and PPARↃ activity caused by SAA were significantly suppressed. In addition, FPRL-1 and TLR4 also play a role in SAA-induced COX-2 expression. These results suggested that the SAA effects on NF-ϞB and PPARↃ activation were regulated at least partially by FPRL-1 and TLR4. However, none of the inhibitors to FPRL-1, TLR2 and TLR4 could inhibit SAA-enhanced cholesterol efflux to HDL and apoA-I. Whether SAA-induced COX-2 expression, NF-ϞB and PPARↃ activation is mediated by Tanis or RAGE remains to be determined.

The scavenger receptor SR-BI is an HDL receptor that mediates the cellular uptake of cholesterol ester from HDL by selective lipid uptake [107, 108]. SR-BI-dependent selective lipid uptake in the liver plays an important role in HDL cholesterol clearance, thereby facilitating reverse cholesterol transport from the periphery to the liver. The receptor exhibits a broad ligand binging specificity and binds low density lipoprotein, very low density lipoprotein, and oxidized lipoproteins in addition to HDL [108]. SR-BI also associates with anionic phospholipids as well as the apolipoproteins A-I, A-II, C-III, and E, either as lipid-bound or as free apolipoproteins. In addition to mediating selective lipid uptake, SR-BI facilitates the efflux of cellular free cholesterol to HDL. Previous study had demonstrated that both lipid-free and lipid-bound SAA was bound and internalized by SR-BI and the SAA exerted its effect through the binding [109]. We examined the involvement of SR-BI in SAA-induced effects. Our data suggest that SAA promotes cellular cholesterol efflux through both SR-BI dependent and SR-BI independent pathway. However, unlike FPRL-1 and TLRs, SAA-induced COX-2 expression, NF-ϞB and PPARↃ activation were not affected by SR-BI inhibitor, BLT-1, indicating different functions of each receptor.

For the ligand selectivity of FPRL-1-mediated NF-ϟB and PPARↄ activation, we found that only SAA and not other FPRL-1 ligands examined (MMK-1, WKYMVM, HFYLPM and F-peptide) could activate these effects. A previous study had shown that SAA did not inhibit ^{125}I-labeled WKYMVm from binding FPRL-1 [115], suggesting that SAA and WKYMVm bind to FPRL-1 at different sites. Other studies also demonstrated that FPRL-1 could be differentially activated by distinct ligands in a ligand-specific manner [302, 303]. Thus, it is possible that SAA and other FPRL-1 ligands differentially stimulate FPRL-1 at different binding sites and subsequently induce different effects.

4.8 THE ESSENTIAL ROLE OF N-TERMINAL SAA IN PROTEIN EXPRESSION, SECRETION, CHOLESTEROL EFFLUX AND PPARↄ ACTIVATION

Most of the amyloid A peptides of the fibrils identified so far have variable C-termini but all retain the N-terminal region [67], this region was found to contribute to the amyloidogenic properties of the protein [31]. Using one-dimensional Fourier analysis of the amino acid sequence of human SAA1 together with sequence matching to known secondary structural motifs, Turnell et al. predicted an extremely hydrophobic lipid-binding N-terminus consisting of 11 amino acids residues (RSFFSFLGEAF), two helices and a putative calcium-binding motif [29]. The sequence between Ser-2 and Gly-8 forms two turns of a hydrophobic but weakly amphipathic helix. Previous data supported that this region played an important role in the lipid-binding property of SAA [31, 304]. In this study, the protein secretion and cholesterol-efflux properties of the 11 amino acids and the 8th residue at the N-terminal of SAA were investigated.

The data showed that the total yield of wild-type SAA was much higher than mutant SAA proteins. While the wild-type SAA expression was around 1400 ng/ml, the total yield of mutant SAA was between 100-650 ng/ml. Only 32-47% of the total yield of mutant SAA protein was secreted to the medium compared to 90% of wild-type SAA was secreted. The decrease in the total yield of mutant SAA proteins and lower percentage of the secreted SAA protein could be explained by a lower affinity for HDL in the serum. Previous study had shown that free SAA was degraded faster than SAA bound to HDL, as the half-live of SAA was markedly reduced to a few hours when fetal calf serum (FCS) was omitted from the culture medium, therefore HDL protects SAA from degradation [31]. Because the N-terminal mutant proteins have an impaired ability to bind to HDL, a higher rate of proteolytic degradation is likely. This might explain the lower levels of the mutant SAA protein in the culture medium shown by the ELISA. The deletion of 11 N-terminal residues or the substitution from non-polar to polar residue at the 8th amino acid in SAA, changing the charge and disrupting the tertiary structure of SAA, result in the signigicant decrease in the lipid-binding property of mutant SAA proteins. Other explanations could be that the mutant mRNAs are less stable, or translation and secretion of mutant proteins are less efficient, because mutant mRNA levels are the same as in the wild-type but the cytosolic concentration of mutant proteins are lower than that of wild-type SAA.

Previously, an 18 amino-acid signal peptide that is cleaved during SAA maturation was identified from sequencing SAA cDNA. As the amino acid sequence of this peptide is similar to the sequence of signal peptides found in other human secreted proteins, it is proposed to be required for SAA secretion [305]. The data obtained

supported this hypothesis because much less of mutSAA (NLS) could be detected in medium as compared to the wild-type SAA when the signal peptide was deleted (Table 5). However, the SAA secretion was not completely inhibited which implied that SAA could be secreted out of the cell by a pathway independent of the signal peptide.

The cholesterol efflux assay results demonstrated that endogenously expressed wild-type SAA increased the cholesterol efflux ~ 2 folds while the cholesterol efflux level remained at the basal level in cells expressing mutant SAA proteins (Fig. 27), which indicated the essential role of the N-terminal of SAA in promoting cholesterol efflux. There are severl explanations for that: 1) SAA was shown to be able to exert a synergistic effect with HDL in promoting cholesterol efflux [110]. The total yield and secretion percentage of wild-type SAA was much higher than mutant SAA, therefore, the cholesterol efflux activity was impaired in cells expressing mutant SAA proteins; 2) SAA was shown to be a cholesterol efflux acceptor. The N-terminal of SAA was suggested to be a lipid-binding domain. 11 N-terminal deletion or substitution from Glycine to Aspartic acid at the 8th residue may induce a conformational change of SAA and subsequently impair its lipid binding ability. Under this condition, the mutant SAA could not function as cholesterol efflux acceptor anymore; 3) In the results section, I have shown that SAA could indirectly induce cholesterol efflux through PPARↃ. The lower production of mutant SAA proteins makes this pathway impossible. Further experiments may be needed to prove these explanations.

The role of SAA N-terminal in PPARↃ activation was also evaluated with this system. The data showed that endogenously expressed wild-type SAA could activate PPARↃ, which is consistent with the recombinant SAA protein. The data that cells

expressing mutant SAA proteins could no longer activate PPARↄ indicated that the functional PPARↄ activating domain lies in the N-terminal of SAA.

CHAPTER V

CONCLUSIONS AND FUTURE WORK

5.1 MAIN FINDINGS

In summary, this study has investigated the effects of SAA on PPARↄ activation and the downstream cascades. The functional domain of SAA was also examined. Here are some of the main findings of this study.

- SAA was found to activate PPARↄ, induce ABCA1 and ABCG1 expression, and enhance cholesterol efflux.
- The SAA effects were mediated through ERK1/2 and NF-ʩB dependent COX-2 expression, which could increase the intracellular 15d-$PGJ_{2,}$ the natural ligand of PPARↄ.
- The receptors involved in this process include FPRL-1, TLR2 and TLR4.
- We also established that the N-terminal of SAA was indispensable in SAA protein expression, secretion, cholesterol efflux and PPARↄ activation. It remains to be determined whether the hydrophobic regions are critical for TLRs signaling by SAA.

5.2 SUMMARY OF MAJOR CONTRIBUTIONS OF THIS STUDY

- This study established a relationship between SAA and PPARↄ, which had not been shown previously. The macrophages signals induced by SAA may be part of the protective mechanisms to prevent progression of atherosclerosis.
- Our study provided a new insight into the role of SAA in cholesterol efflux.

5.3 SUGGESTIONS FOR FUTURE WORK

This study revealed evidence that SAA-induced PPARɔ activation was mediated by ERK1/2 and NF-ʢB-dependent COX-2 expression. Thus, several pathways that lead to the overexpression of COX-2 may also induce the activation of PPARɔ. It has been reported that CCAAT/enhancer-binding protein-ɓ (C/EBPɓ) and AP-1 are involved in transcriptional regulation of the COX-2 gene [306], and MAPK signaling pathways could regulate C/EBPɓ and AP-1 activity [307, 308]. Therefore, SAA-induced ERK1/2 activation may regulate the activity of C/EBPɓ and/or AP-1, thereby resulting in transcriptional activation of COX-2 gene. Further studies are needed to clarify the mechanisms by which SAA induces COX-2 expression.

SAA was shown to induce sustained ERK1/2 phosphorylation for up to 6 hours and the he phosphorylation level could be significantly reduced with the treatment of CHX, a protein biosynthesis inhibitor. CHX was also demonstrated to inhibit SAA-induced PPARɔ activation. These data suggested that other signaling molecule(s) might also contribute to the SAA-induced sustained ERK1/2 phosphorylation and PPARɔ activation. It would be important to determine the molecule(s) involved in these process.

This project provided clear evidences that SAA could lead to PPARɔ activation and induce cholesterol efflux in hepatocytes. However, because of the limitation of *in vitro* study, further investigations would be needed. Cultured cells in culture media are known to behave differently from intact cells and their interactions with the blood circulation, and in a larger context, the human body . As such, *in vivo* study of the effects of SAA on atherosclerosis will be useful. An assessment of the modulation of PPARɔ activation in animal models of atherosclerosis is now warranted to elucidate the

physiological relevance of SAA-induced PPARↃ activation in the progression of atherosclerosis. SAA transgenic mice, which overexpress SAA may be a useful candidate to investigate the *in vivo* atherogenesis of sustained SAA stimulation. Additionally, recombinant SAA should be injected into animals to determine its effect on PPARↃ. It is therefore now necessary to move from an *in vitro* to an *in vivo* approach to assess the role of SAA-induced PPARↃ activation in atherosclerosis. Only after a successful *in vivo* study with results consistent with the *in vitro* investigation can SAA be clearly shown to be involved in atherosclerosis through PPARↃ. Furthermore, peptides derived from SAA, which could induce the antiatherosclerotic effect while avoiding the atherogenic processes, will be a promising therapeutic target for CAD treatment.

CHAPTER VI

REFERENCES

1. Rosamond, W., et al., *Heart disease and stroke statistics--2008 update: a report from the American Heart Association Statistics Committee and Stroke Statistics Subcommittee.* Circulation, 2008. **117**(4): p. e25-146.
2. Ross, R. and L. Harker, *Hyperlipidemia and atherosclerosis.* Science, 1976. **193**(4258): p. 1094-100.
3. Ross, R., *Atherosclerosis--an inflammatory disease.* N Engl J Med, 1999. **340**(2): p. 115-26.
4. Lusis, A.J., *Atherosclerosis.* Nature, 2000. **407**(6801): p. 233-41.
5. Hansson, G.K. and K. Edfeldt, *Toll to be paid at the gateway to the vessel wall.* Arterioscler Thromb Vasc Biol, 2005. **25**(6): p. 1085-7.
6. Ross, R., *The pathogenesis of atherosclerosis: a perspective for the 1990s.* Nature, 1993. **362**(6423): p. 801-9.
7. Libby, P., *Inflammation in atherosclerosis.* Nature, 2002. **420**(6917): p. 868-74.
8. Willerson, J.T. and P.M. Ridker, *Inflammation as a cardiovascular risk factor.* Circulation, 2004. **109**(21 Suppl 1): p. II2-10.
9. Ridker, P.M., et al., *C-reactive protein and other markers of inflammation in the prediction of cardiovascular disease in women.* N Engl J Med, 2000. **342**(12): p. 836-43.
10. Ridker, P.M., *Role of inflammatory biomarkers in prediction of coronary heart disease.* Lancet, 2001. **358**(9286): p. 946-8.
11. Pasceri, V., J.T. Willerson, and E.T. Yeh, *Direct proinflammatory effect of C-reactive protein on human endothelial cells.* Circulation, 2000. **102**(18): p. 2165-8.
12. Pasceri, V., et al., *Modulation of C-reactive protein-mediated monocyte chemoattractant protein-1 induction in human endothelial cells by anti-atherosclerosis drugs.* Circulation, 2001. **103**(21): p. 2531-4.
13. Verma, S., et al., *A self-fulfilling prophecy: C-reactive protein attenuates nitric oxide production and inhibits angiogenesis.* Circulation, 2002. **106**(8): p. 913-9.
14. Cirillo, P., et al., *C-reactive protein induces tissue factor expression and promotes smooth muscle and endothelial cell proliferation.* Cardiovasc Res, 2005. **68**(1): p. 47-55.
15. Montero, I., et al., *C-reactive protein induces matrix metalloproteinase-1 and -10 in human endothelial cells: implications for clinical and subclinical atherosclerosis.* J Am Coll Cardiol, 2006. **47**(7): p. 1369-78.
16. Gabay, C. and I. Kushner, *Acute-phase proteins and other systemic responses to inflammation.* N Engl J Med, 1999. **340**(6): p. 448-54.
17. Kushner, I., *The phenomenon of the acute phase response.* Ann N Y Acad Sci, 1982. **389**: p. 39-48.
18. Hoffman, J.S. and E.P. Benditt, *Changes in high density lipoprotein content following endotoxin administration in the mouse. Formation of serum amyloid protein-rich subfractions.* J Biol Chem, 1982. **257**(17): p. 10510-7.
19. Marhaug, G., *Three assays for the characterization and quantitation of human serum amyloid A.* Scand J Immunol, 1983. **18**(4): p. 329-38.
20. Whitehead, A.S., et al., *Identification of novel members of the serum amyloid A protein superfamily as constitutive apolipoproteins of high density lipoprotein.* J Biol Chem, 1992. **267**(6): p. 3862-7.

21. de Beer, M.C., et al., *Mouse serum amyloid A protein (SAA5) structure and expression.* J Biol Chem, 1994. **269**(6): p. 4661-7.
22. Uhlar, C.M., et al., *Evolution of the serum amyloid A (SAA) protein superfamily.* Genomics, 1994. **19**(2): p. 228-35.
23. Uhlar, C.M., et al., *Wallaby serum amyloid A protein: cDNA cloning, sequence and evolutionary analysis.* Scand J Immunol, 1996. **43**(3): p. 271-6.
24. Jensen, L.E., et al., *Acute phase proteins in salmonids: evolutionary analyses and acute phase response.* J Immunol, 1997. **158**(1): p. 384-92.
25. Sipe, J., *Revised nomenclature for serum amyloid A (SAA). Nomenclature Committee of the International Society of Amyloidosis. Part 2.* Amyloid, 1999. **6**(1): p. 67-70.
26. Sellar, G.C., et al., *The human serum amyloid A protein (SAA) superfamily gene cluster: mapping to chromosome 11p15.1 by physical and genetic linkage analysis.* Genomics, 1994. **19**(2): p. 221-7.
27. Kluve-Beckerman, B., M.L. Drumm, and M.D. Benson, *Nonexpression of the human serum amyloid A three (SAA3) gene.* DNA Cell Biol, 1991. **10**(9): p. 651-61.
28. Steel, D.M. and A.S. Whitehead, *The major acute phase reactants: C-reactive protein, serum amyloid P component and serum amyloid A protein.* Immunol Today, 1994. **15**(2): p. 81-8.
29. Turnell, W., et al., *Secondary structure prediction of human SAA1. Presumptive identification of calcium and lipid binding sites.* Mol Biol Med, 1986. **3**(5): p. 387-407.
30. Westermark, G.T., U. Engstrom, and P. Westermark, *The N-terminal segment of protein AA determines its fibrillogenic property.* Biochem Biophys Res Commun, 1992. **182**(1): p. 27-33.
31. Patel, H., et al., *Expression of recombinant human serum amyloid A in mammalian cells and demonstration of the region necessary for high-density lipoprotein binding and amyloid fibril formation by site-directed mutagenesis.* Biochem J, 1996. **318 (Pt 3)**: p. 1041-9.
32. Preciado-Patt, L., et al., *Inhibition of cell adhesion to glycoproteins of the extracellular matrix by peptides corresponding to serum amyloid A. Toward understanding the physiological role of an enigmatic protein.* Eur J Biochem, 1994. **223**(1): p. 35-42.
33. Shainkin-Kestenbaum, R., et al., *Modulation of prostaglandin I2 production from bovine aortic endothelial cells by serum amyloid A and its N-terminal tetradecapeptide.* Biomed Pept Proteins Nucleic Acids, 1996. **2**(4): p. 101-6.
34. Preciado-Patt, L., M. Pras, and M. Fridkin, *Binding of human serum amyloid A (hSAA) and its high-density lipoprotein3 complex (hSAA-HDL3) to human neutrophils. Possible implication to the function of a protein of an unknown physiological role.* Int J Pept Protein Res, 1996. **48**(6): p. 503-13.
35. Uhlar, C.M. and A.S. Whitehead, *Serum amyloid A, the major vertebrate acute-phase reactant.* Eur J Biochem, 1999. **265**(2): p. 501-23.
36. Jensen, L.E. and A.S. Whitehead, *Regulation of serum amyloid A protein expression during the acute-phase response.* Biochem J, 1998. **334 (Pt 3)**: p. 489-503.

37. Meek, R.L., S. Urieli-Shoval, and E.P. Benditt, *Expression of apolipoprotein serum amyloid A mRNA in human atherosclerotic lesions and cultured vascular cells: implications for serum amyloid A function.* Proc Natl Acad Sci U S A, 1994. **91**(8): p. 3186-90.
38. Kumon, Y., et al., *Local expression of acute phase serum amyloid A mRNA in rheumatoid arthritis synovial tissue and cells.* J Rheumatol, 1999. **26**(4): p. 785-90.
39. Cunnane, G., *Amyloid precursors and amyloidosis in inflammatory arthritis.* Curr Opin Rheumatol, 2001. **13**(1): p. 67-73.
40. Rienhoff, H.Y., Jr., et al., *Molecular and cellular biology of serum amyloid A.* Mol Biol Med, 1990. **7**(3): p. 287-98.
41. Bausserman, L.L., et al., *Degradation of serum amyloid A by isolated perfused rat liver.* J Biol Chem, 1987. **262**(4): p. 1583-9.
42. Raynes, J.G. and E.H. Cooper, *Comparison of serum amyloid A protein and C-reactive protein concentrations in cancer and non-malignant disease.* J Clin Pathol, 1983. **36**(7): p. 798-803.
43. Herbert, P.N., et al., *High-density lipoprotein metabolism in runners and sedentary men.* JAMA, 1984. **252**(8): p. 1034-7.
44. Tape, C. and R. Kisilevsky, *Apolipoprotein A-I and apolipoprotein SAA half-lives during acute inflammation and amyloidogenesis.* Biochim Biophys Acta, 1990. **1043**(3): p. 295-300.
45. Gollaher, C.J. and L.L. Bausserman, *Hepatic catabolism of serum amyloid A during an acute phase response and chronic inflammation.* Proc Soc Exp Biol Med, 1990. **194**(3): p. 245-50.
46. Steel, D.M. and A.S. Whitehead, *Heterogeneous modulation of acute-phase-reactant mRNA levels by interleukin-1 beta and interleukin-6 in the human hepatoma cell line PLC/PRF/5.* Biochem J, 1991. **277 (Pt 2)**: p. 477-82.
47. Steel, D.M., et al., *Expression and regulation of constitutive and acute phase serum amyloid A mRNAs in hepatic and non-hepatic cell lines.* Scand J Immunol, 1996. **44**(5): p. 493-500.
48. Ganapathi, M.K., et al., *Effect of combinations of cytokines and hormones on synthesis of serum amyloid A and C-reactive protein in Hep 3B cells.* J Immunol, 1991. **147**(4): p. 1261-5.
49. Migita, K., et al., *Serum amyloid A protein induces production of matrix metalloproteinases by human synovial fibroblasts.* Lab Invest, 1998. **78**(5): p. 535-9.
50. Mitchell, T.I., C.I. Coon, and C.E. Brinckerhoff, *Serum amyloid A (SAA3) produced by rabbit synovial fibroblasts treated with phorbol esters or interleukin 1 induces synthesis of collagenase and is neutralized with specific antiserum.* J Clin Invest, 1991. **87**(4): p. 1177-85.
51. Strissel, K.J., et al., *Role of serum amyloid A as an intermediate in the IL-1 and PMA-stimulated signaling pathways regulating expression of rabbit fibroblast collagenase.* Exp Cell Res, 1997. **237**(2): p. 275-87.
52. Badolato, R., et al., *Serum amyloid A is a chemoattractant: induction of migration, adhesion, and tissue infiltration of monocytes and polymorphonuclear leukocytes.* J Exp Med, 1994. **180**(1): p. 203-9.

53. Xu, L., et al., *A novel biologic function of serum amyloid A. Induction of T lymphocyte migration and adhesion.* J Immunol, 1995. **155**(3): p. 1184-90.
54. Preciado-Patt, L., et al., *Serum amyloid A binds specific extracellular matrix glycoproteins and induces the adhesion of resting CD4+ T cells.* J Immunol, 1996. **156**(3): p. 1189-95.
55. Patel, H., et al., *Human serum amyloid A has cytokine-like properties.* Scand J Immunol, 1998. **48**(4): p. 410-8.
56. Olsson, N., A. Siegbahn, and G. Nilsson, *Serum amyloid A induces chemotaxis of human mast cells by activating a pertussis toxin-sensitive signal transduction pathway.* Biochem Biophys Res Commun, 1999. **254**(1): p. 143-6.
57. He, W., et al., *Adipose-specific peroxisome proliferator-activated receptor gamma knockout causes insulin resistance in fat and liver but not in muscle.* Proc Natl Acad Sci U S A, 2003. **100**(26): p. 15712-7.
58. Aldo-Benson, M.A. and M.D. Benson, *SAA suppression of immune response in vitro: evidence for an effect on T cell-macrophage interaction.* J Immunol, 1982. **128**(6): p. 2390-2.
59. Benson, M.D. and M. Aldo-Benson, *Effect of purified protein SAA on immune response in vitro: mechanisms of suppression.* J Immunol, 1979. **122**(5): p. 2077-82.
60. Benson, M.D. and M.A. Aldo-Benson, *SAA suppression of in vitro antibody response.* Ann N Y Acad Sci, 1982. **389**: p. 121-5.
61. Peristeris, P., et al., *Effects of serum amyloid A protein on lymphocytes, HeLa, and MRC5 cells in culture.* Biochem Cell Biol, 1989. **67**(7): p. 365-70.
62. Shainkin-Kestenbaum, R., et al., *Acute phase protein, serum amyloid A, inhibits IL-1- and TNF-induced fever and hypothalamic PGE2 in mice.* Scand J Immunol, 1991. **34**(2): p. 179-83.
63. Syversen, P.V., et al., *The effect of serum amyloid protein A fragment-SAA25-76 on blood platelet aggregation.* Thromb Res, 1994. **76**(3): p. 299-305.
64. Zimlichman, S., et al., *Serum amyloid A, an acute phase protein, inhibits platelet activation.* J Lab Clin Med, 1990. **116**(2): p. 180-6.
65. Gatt, M.E., et al., *Effect of serum amyloid A on selected in vitro functions of isolated human neutrophils.* J Lab Clin Med, 1998. **132**(5): p. 414-20.
66. Linke, R.P., et al., *Inhibition of the oxidative burst response of N-formyl peptide-stimulated neutrophils by serum amyloid-A protein.* Biochem Biophys Res Commun, 1991. **176**(3): p. 1100-5.
67. Husebekk, A., et al., *Transformation of amyloid precursor SAA to protein AA and incorporation in amyloid fibrils in vivo.* Scand J Immunol, 1985. **21**(3): p. 283-7.
68. Tape, C., et al., *Direct evidence for circulating apoSAA as the precursor of tissue AA amyloid deposits.* Scand J Immunol, 1988. **28**(3): p. 317-24.
69. Husby, G., *Classification of amyloidosis.* Baillieres Clin Rheumatol, 1994. **8**(3): p. 503-11.
70. Liepnieks, J.J., B. Kluve-Beckerman, and M.D. Benson, *Characterization of amyloid A protein in human secondary amyloidosis: the predominant deposition of serum amyloid A1.* Biochim Biophys Acta, 1995. **1270**(1): p. 81-6.

71. Parmelee, D.C., et al., *Amino acid sequence of amyloid-related apoprotein (apoSAA1) from human high-density lipoprotein.* Biochemistry, 1982. **21**(14): p. 3298-303.
72. Shiroo, M., et al., *Specific deposition of serum amyloid A protein 2 in the mouse.* Scand J Immunol, 1987. **26**(6): p. 709-16.
73. Westermark, G.T., et al., *AA-amyloidosis. Tissue component-specific association of various protein AA subspecies and evidence of a fourth SAA gene product.* Am J Pathol, 1990. **137**(2): p. 377-83.
74. Bausserman, L.L. and P.N. Herbert, *Degradation of serum amyloid A and apolipoproteins by serum proteases.* Biochemistry, 1984. **23**(10): p. 2241-5.
75. Elliott-Bryant, R., et al., *Catabolism of lipid-free recombinant apolipoprotein serum amyloid A by mouse macrophages in vitro results in removal of the amyloid fibril-forming amino terminus.* Scand J Immunol, 1998. **48**(3): p. 241-7.
76. Mitchell, T.I., et al., *The acute phase reactant serum amyloid A (SAA3) is a novel substrate for degradation by the metalloproteinases collagenase and stromelysin.* Biochim Biophys Acta, 1993. **1156**(3): p. 245-54.
77. Skogen, B. and J.B. Natvig, *Degradation of amyloid proteins by different serine proteases.* Scand J Immunol, 1981. **14**(4): p. 389-96.
78. Yamada, T., et al., *Accelerated amyloid deposition in mice treated with the aspartic protease inhibitor, pepstatin.* J Immunol, 1996. **157**(2): p. 901-7.
79. Yamada, T., et al., *Cathepsin B generates the most common form of amyloid A (76 residues) as a degradation product from serum amyloid A.* Scand J Immunol, 1995. **41**(1): p. 94-7.
80. Arai, K., et al., *Transformation from SAA2-fibrils to AA-fibrils in amyloid fibrillogenesis: in vivo observations in murine spleen using anti-SAA and anti-AA antibodies.* J Pathol, 1994. **173**(2): p. 127-34.
81. Ericsson, L.H., et al., *Primary structure of duck amyloid protein A. The form deposited in tissues may be identical to its serum precursor.* FEBS Lett, 1987. **218**(1): p. 11-6.
82. Westermark, P. and K. Sletten, *A serum AA-like protein as a common constituent of secondary amyloid fibrils.* Clin Exp Immunol, 1982. **49**(3): p. 725-31.
83. Yamada, T., et al., *Fibril formation from recombinant human serum amyloid A.* Biochim Biophys Acta, 1994. **1226**(3): p. 323-9.
84. Benditt, E.P., N. Eriksen, and R.H. Hanson, *Amyloid protein SAA is an apoprotein of mouse plasma high density lipoprotein.* Proc Natl Acad Sci U S A, 1979. **76**(8): p. 4092-6.
85. Van Lenten, B.J., et al., *Anti-inflammatory HDL becomes pro-inflammatory during the acute phase response. Loss of protective effect of HDL against LDL oxidation in aortic wall cell cocultures.* J Clin Invest, 1995. **96**(6): p. 2758-67.
86. Kisilevsky, R. and L. Subrahmanyan, *Serum amyloid A changes high density lipoprotein's cellular affinity. A clue to serum amyloid A's principal function.* Lab Invest, 1992. **66**(6): p. 778-85.
87. Rosenson, R.S., *Myocardial injury: the acute phase response and lipoprotein metabolism.* J Am Coll Cardiol, 1993. **22**(3): p. 933-40.
88. Steinmetz, A., et al., *Influence of serum amyloid A on cholesterol esterification in human plasma.* Biochim Biophys Acta, 1989. **1006**(2): p. 173-8.

89. Andersson, L.O., *Pharmacology of apolipoprotein A-I.* Curr Opin Lipidol, 1997. **8**(4): p. 225-8.
90. Coetzee, G.A., et al., *Serum amyloid A-containing human high density lipoprotein 3. Density, size, and apolipoprotein composition.* J Biol Chem, 1986. **261**(21): p. 9644-51.
91. Fielding, C.J., V.G. Shore, and P.E. Fielding, *A protein cofactor of lecithin:cholesterol acyltransferase.* Biochem Biophys Res Commun, 1972. **46**(4): p. 1493-8.
92. Vadas, P., et al., *Extracellular phospholipase A2 expression and inflammation: the relationship with associated disease states.* J Lipid Mediat, 1993. **8**(1): p. 1-30.
93. Menschikowski, M., et al., *Secretory group II phospholipase A2 in human atherosclerotic plaques.* Atherosclerosis, 1995. **118**(2): p. 173-81.
94. Pruzanski, W., et al., *Lipoproteins are substrates for human secretory group IIA phospholipase A2: preferential hydrolysis of acute phase HDL.* J Lipid Res, 1998. **39**(11): p. 2150-60.
95. Pruzanski, W., et al., *Serum amyloid A protein enhances the activity of secretory non-pancreatic phospholipase A2.* Biochem J, 1995. **309 (Pt 2)**: p. 461-4.
96. de Beer, F.C., et al., *Secretory non-pancreatic phospholipase A2: influence on lipoprotein metabolism.* J Lipid Res, 1997. **38**(11): p. 2232-9.
97. Banka, C.L., et al., *Serum amyloid A (SAA): influence on HDL-mediated cellular cholesterol efflux.* J Lipid Res, 1995. **36**(5): p. 1058-65.
98. Kisilevsky, R. and S.P. Tam, *Macrophage cholesterol efflux and the active domains of serum amyloid A 2.1.* J Lipid Res, 2003. **44**(12): p. 2257-69.
99. Tam, S.P., et al., *Promoting export of macrophage cholesterol: the physiological role of a major acute-phase protein, serum amyloid A 2.1.* J Lipid Res, 2002. **43**(9): p. 1410-20.
100. Macchia, T., et al., *Determination of membrane cholesterol in normal and pathological red blood cells.* Clin Chim Acta, 1991. **199**(1): p. 59-67.
101. Ely, S., et al., *The in-vitro influence of serum amyloid A isoforms on enzymes that regulate the balance between esterified and un-esterified cholesterol.* Amyloid, 2001. **8**(3): p. 169-81.
102. Lindhorst, E., et al., *Acute inflammation, acute phase serum amyloid A and cholesterol metabolism in the mouse.* Biochim Biophys Acta, 1997. **1339**(1): p. 143-54.
103. Stonik, J.A., et al., *Serum amyloid A promotes ABCA1-dependent and ABCA1-independent lipid efflux from cells.* Biochem Biophys Res Commun, 2004. **321**(4): p. 936-41.
104. Cavelier, C., et al., *Lipid efflux by the ATP-binding cassette transporters ABCA1 and ABCG1.* Biochim Biophys Acta, 2006. **1761**(7): p. 655-66.
105. Kluve-Beckerman, B., J. Manaloor, and J.J. Liepnieks, *Binding, trafficking and accumulation of serum amyloid A in peritoneal macrophages.* Scand J Immunol, 2001. **53**(4): p. 393-400.
106. Rocken, C. and R. Kisilevsky, *Comparison of the binding and endocytosis of high-density lipoprotein from healthy (HDL) and inflamed (HDL(SAA)) donors by*

murine macrophages of four different mouse strains. Virchows Arch, 1998. **432**(6): p. 547-55.
107. Connelly, M.A. and D.L. Williams, *Scavenger receptor BI: a scavenger receptor with a mission to transport high density lipoprotein lipids.* Curr Opin Lipidol, 2004. **15**(3): p. 287-95.
108. Rigotti, A., H.E. Miettinen, and M. Krieger, *The role of the high-density lipoprotein receptor SR-BI in the lipid metabolism of endocrine and other tissues.* Endocr Rev, 2003. **24**(3): p. 357-87.
109. Cai, L., et al., *Serum amyloid A is a ligand for scavenger receptor class B type I and inhibits high density lipoprotein binding and selective lipid uptake.* J Biol Chem, 2005. **280**(4): p. 2954-61.
110. van der Westhuyzen, D.R., et al., *Serum amyloid A promotes cholesterol efflux mediated by scavenger receptor B-I.* J Biol Chem, 2005. **280**(43): p. 35890-5.
111. Marsche, G., et al., *The lipidation status of acute-phase protein serum amyloid A determines cholesterol mobilization via scavenger receptor class B, type I.* Biochem J, 2007. **402**(1): p. 117-24.
112. Murphy, P.M., *The molecular biology of leukocyte chemoattractant receptors.* Annu Rev Immunol, 1994. **12**: p. 593-633.
113. Su, S.B., et al., *A seven-transmembrane, G protein-coupled receptor, FPRL1, mediates the chemotactic activity of serum amyloid A for human phagocytic cells.* J Exp Med, 1999. **189**(2): p. 395-402.
114. Badolato, R., et al., *Serum amyloid A induces calcium mobilization and chemotaxis of human monocytes by activating a pertussis toxin-sensitive signaling pathway.* J Immunol, 1995. **155**(8): p. 4004-10.
115. Lee, H.Y., et al., *Serum amyloid A stimulates matrix-metalloproteinase-9 upregulation via formyl peptide receptor like-1-mediated signaling in human monocytic cells.* Biochem Biophys Res Commun, 2005. **330**(3): p. 989-98.
116. Cai, H., et al., *Serum amyloid A induces monocyte tissue factor.* J Immunol, 2007. **178**(3): p. 1852-60.
117. Schmidt, A.M., et al., *The multiligand receptor RAGE as a progression factor amplifying immune and inflammatory responses.* J Clin Invest, 2001. **108**(7): p. 949-55.
118. Yan, S.D., et al., *Receptor-dependent cell stress and amyloid accumulation in systemic amyloidosis.* Nat Med, 2000. **6**(6): p. 643-51.
119. Sandri, S., et al., *Is serum amyloid A an endogenous TLR4 agonist?* J Leukoc Biol, 2008. **83**(5): p. 1174-80.
120. Cheng, N., et al., *Cutting edge: TLR2 is a functional receptor for acute-phase serum amyloid A.* J Immunol, 2008. **181**(1): p. 22-6.
121. He, R.L., et al., *Serum amyloid A induces G-CSF expression and neutrophilia via Toll-like receptor 2.* Blood, 2009. **113**(2): p. 429-37.
122. Walder, K., et al., *Tanis: a link between type 2 diabetes and inflammation?* Diabetes, 2002. **51**(6): p. 1859-66.
123. Bausserman, L.L., et al., *Time course of serum amyloid A response in myocardial infarction.* Clin Chim Acta, 1989. **184**(3): p. 297-305.
124. Liuzzo, G., et al., *The prognostic value of C-reactive protein and serum amyloid a protein in severe unstable angina.* N Engl J Med, 1994. **331**(7): p. 417-24.

125. Rosenthal, C.J. and E.C. Franklin, *Variation with age and disease of an amyloid A protein-related serum component.* J Clin Invest, 1975. **55**(4): p. 746-53.
126. Kisilevsky, R., S.P. Tam, and J.B. Ancsin, *The anti-atherogenic potential of serum amyloid A peptides.* Curr Opin Investig Drugs, 2008. **9**(3): p. 265-73.
127. von Eckardstein, A., M. Hersberger, and L. Rohrer, *Current understanding of the metabolism and biological actions of HDL.* Curr Opin Clin Nutr Metab Care, 2005. **8**(2): p. 147-52.
128. Braissant, O., et al., *Differential expression of peroxisome proliferator-activated receptors (PPARs): tissue distribution of PPAR-alpha, -beta, and -gamma in the adult rat.* Endocrinology, 1996. **137**(1): p. 354-66.
129. Kliewer, S.A., et al., *Differential expression and activation of a family of murine peroxisome proliferator-activated receptors.* Proc Natl Acad Sci U S A, 1994. **91**(15): p. 7355-9.
130. Lemberger, T., B. Desvergne, and W. Wahli, *Peroxisome proliferator-activated receptors: a nuclear receptor signaling pathway in lipid physiology.* Annu Rev Cell Dev Biol, 1996. **12**: p. 335-63.
131. Bordet, R., et al., *PPAR: a new pharmacological target for neuroprotection in stroke and neurodegenerative diseases.* Biochem Soc Trans, 2006. **34**(Pt 6): p. 1341-6.
132. Bishop-Bailey, D., *Peroxisome proliferator-activated receptors in the cardiovascular system.* Br J Pharmacol, 2000. **129**(5): p. 823-34.
133. Buchan, K.W. and D.G. Hassall, *PPAR agonists as direct modulators of the vessel wall in cardiovascular disease.* Med Res Rev, 2000. **20**(5): p. 350-66.
134. Berger, J.P., T.E. Akiyama, and P.T. Meinke, *PPARs: therapeutic targets for metabolic disease.* Trends Pharmacol Sci, 2005. **26**(5): p. 244-51.
135. Luquet, S., et al., *Roles of peroxisome proliferator-activated receptor delta (PPARdelta) in the control of fatty acid catabolism. A new target for the treatment of metabolic syndrome.* Biochimie, 2004. **86**(11): p. 833-7.
136. Forman, B.M., et al., *15-Deoxy-delta 12, 14-prostaglandin J2 is a ligand for the adipocyte determination factor PPAR gamma.* Cell, 1995. **83**(5): p. 803-12.
137. Kliewer, S.A., et al., *A prostaglandin J2 metabolite binds peroxisome proliferator-activated receptor gamma and promotes adipocyte differentiation.* Cell, 1995. **83**(5): p. 813-9.
138. Huang, J.T., et al., *Interleukin-4-dependent production of PPAR-gamma ligands in macrophages by 12/15-lipoxygenase.* Nature, 1999. **400**(6742): p. 378-82.
139. Nagy, L., et al., *Oxidized LDL regulates macrophage gene expression through ligand activation of PPARgamma.* Cell, 1998. **93**(2): p. 229-40.
140. Furnsinn, C. and W. Waldhausl, *Thiazolidinediones: metabolic actions in vitro.* Diabetologia, 2002. **45**(9): p. 1211-23.
141. Hu, X., et al., *Liver X receptors interact with corepressors to regulate gene expression.* Mol Endocrinol, 2003. **17**(6): p. 1019-26.
142. Krogsdam, A.M., et al., *Nuclear receptor corepressor-dependent repression of peroxisome-proliferator-activated receptor delta-mediated transactivation.* Biochem J, 2002. **363**(Pt 1): p. 157-65.

143. Shi, Y., M. Hon, and R.M. Evans, *The peroxisome proliferator-activated receptor delta, an integrator of transcriptional repression and nuclear receptor signaling.* Proc Natl Acad Sci U S A, 2002. **99**(5): p. 2613-8.
144. Wagner, B.L., et al., *Promoter-specific roles for liver X receptor/corepressor complexes in the regulation of ABCA1 and SREBP1 gene expression.* Mol Cell Biol, 2003. **23**(16): p. 5780-9.
145. Berger, J., et al., *Thiazolidinediones produce a conformational change in peroxisomal proliferator-activated receptor-gamma: binding and activation correlate with antidiabetic actions in db/db mice.* Endocrinology, 1996. **137**(10): p. 4189-95.
146. Zhu, Y., et al., *Cloning of a new member of the peroxisome proliferator-activated receptor gene family from mouse liver.* J Biol Chem, 1993. **268**(36): p. 26817-20.
147. Barak, Y., et al., *PPAR gamma is required for placental, cardiac, and adipose tissue development.* Mol Cell, 1999. **4**(4): p. 585-95.
148. Tontonoz, P., et al., *mPPAR gamma 2: tissue-specific regulator of an adipocyte enhancer.* Genes Dev, 1994. **8**(10): p. 1224-34.
149. Spiegelman, B.M. and J.S. Flier, *Adipogenesis and obesity: rounding out the big picture.* Cell, 1996. **87**(3): p. 377-89.
150. Fajas, L., J.C. Fruchart, and J. Auwerx, *Transcriptional control of adipogenesis.* Curr Opin Cell Biol, 1998. **10**(2): p. 165-73.
151. Kubota, N., et al., *PPAR gamma mediates high-fat diet-induced adipocyte hypertrophy and insulin resistance.* Mol Cell, 1999. **4**(4): p. 597-609.
152. Rosen, E.D., et al., *PPAR gamma is required for the differentiation of adipose tissue in vivo and in vitro.* Mol Cell, 1999. **4**(4): p. 611-7.
153. Agarwal, A.K. and A. Garg, *A novel heterozygous mutation in peroxisome proliferator-activated receptor-gamma gene in a patient with familial partial lipodystrophy.* J Clin Endocrinol Metab, 2002. **87**(1): p. 408-11.
154. Ristow, M., et al., *Obesity associated with a mutation in a genetic regulator of adipocyte differentiation.* N Engl J Med, 1998. **339**(14): p. 953-9.
155. Lehmann, J.M., et al., *An antidiabetic thiazolidinedione is a high affinity ligand for peroxisome proliferator-activated receptor gamma (PPAR gamma).* J Biol Chem, 1995. **270**(22): p. 12953-6.
156. Gurnell, M., et al., *The metabolic syndrome: peroxisome proliferator-activated receptor gamma and its therapeutic modulation.* J Clin Endocrinol Metab, 2003. **88**(6): p. 2412-21.
157. Gavrilova, O., et al., *Liver peroxisome proliferator-activated receptor gamma contributes to hepatic steatosis, triglyceride clearance, and regulation of body fat mass.* J Biol Chem, 2003. **278**(36): p. 34268-76.
158. Hevener, A.L., et al., *Muscle-specific Pparg deletion causes insulin resistance.* Nat Med, 2003. **9**(12): p. 1491-7.
159. Norris, A.W., et al., *Muscle-specific PPARgamma-deficient mice develop increased adiposity and insulin resistance but respond to thiazolidinediones.* J Clin Invest, 2003. **112**(4): p. 608-18.
160. Wu, Z., et al., *PPARgamma induces the insulin-dependent glucose transporter GLUT4 in the absence of C/EBPalpha during the conversion of 3T3 fibroblasts into adipocytes.* J Clin Invest, 1998. **101**(1): p. 22-32.

161. Lefebvre, A.M., et al., *Regulation of lipoprotein metabolism by thiazolidinediones occurs through a distinct but complementary mechanism relative to fibrates.* Arterioscler Thromb Vasc Biol, 1997. **17**(9): p. 1756-64.
162. Brun, R.P., et al., *Differential activation of adipogenesis by multiple PPAR isoforms.* Genes Dev, 1996. **10**(8): p. 974-84.
163. Maeda, N., et al., *PPARgamma ligands increase expression and plasma concentrations of adiponectin, an adipose-derived protein.* Diabetes, 2001. **50**(9): p. 2094-9.
164. Yamauchi, T., et al., *The mechanisms by which both heterozygous peroxisome proliferator-activated receptor gamma (PPARgamma) deficiency and PPARgamma agonist improve insulin resistance.* J Biol Chem, 2001. **276**(44): p. 41245-54.
165. Jiang, C., A.T. Ting, and B. Seed, *PPAR-gamma agonists inhibit production of monocyte inflammatory cytokines.* Nature, 1998. **391**(6662): p. 82-6.
166. Ricote, M., et al., *The peroxisome proliferator-activated receptor-gamma is a negative regulator of macrophage activation.* Nature, 1998. **391**(6662): p. 79-82.
167. Daynes, R.A. and D.C. Jones, *Emerging roles of PPARs in inflammation and immunity.* Nat Rev Immunol, 2002. **2**(10): p. 748-59.
168. Ricote, M., A.F. Valledor, and C.K. Glass, *Decoding transcriptional programs regulated by PPARs and LXRs in the macrophage: effects on lipid homeostasis, inflammation, and atherosclerosis.* Arterioscler Thromb Vasc Biol, 2004. **24**(2): p. 230-9.
169. Welch, J.S., et al., *PPARgamma and PPARdelta negatively regulate specific subsets of lipopolysaccharide and IFN-gamma target genes in macrophages.* Proc Natl Acad Sci U S A, 2003. **100**(11): p. 6712-7.
170. Tontonoz, P., et al., *PPARgamma promotes monocyte/macrophage differentiation and uptake of oxidized LDL.* Cell, 1998. **93**(2): p. 241-52.
171. Febbraio, M., D.P. Hajjar, and R.L. Silverstein, *CD36: a class B scavenger receptor involved in angiogenesis, atherosclerosis, inflammation, and lipid metabolism.* J Clin Invest, 2001. **108**(6): p. 785-91.
172. Chawla, A., et al., *A PPAR gamma-LXR-ABCA1 pathway in macrophages is involved in cholesterol efflux and atherogenesis.* Mol Cell, 2001. **7**(1): p. 161-71.
173. Chinetti, G., et al., *PPAR-alpha and PPAR-gamma activators induce cholesterol removal from human macrophage foam cells through stimulation of the ABCA1 pathway.* Nat Med, 2001. **7**(1): p. 53-8.
174. Li, A.C., et al., *Differential inhibition of macrophage foam-cell formation and atherosclerosis in mice by PPARalpha, beta/delta, and gamma.* J Clin Invest, 2004. **114**(11): p. 1564-76.
175. Szanto, A., et al., *Transcriptional regulation of human CYP27 integrates retinoid, peroxisome proliferator-activated receptor, and liver X receptor signaling in macrophages.* Mol Cell Biol, 2004. **24**(18): p. 8154-66.
176. Li, A.C. and C.K. Glass, *PPAR- and LXR-dependent pathways controlling lipid metabolism and the development of atherosclerosis.* J Lipid Res, 2004. **45**(12): p. 2161-73.

177. Minamikawa, J., et al., *Potent inhibitory effect of troglitazone on carotid arterial wall thickness in type 2 diabetes.* J Clin Endocrinol Metab, 1998. **83**(5): p. 1818-20.
178. Koshiyama, H., et al., *Rapid communication: inhibitory effect of pioglitazone on carotid arterial wall thickness in type 2 diabetes.* J Clin Endocrinol Metab, 2001. **86**(7): p. 3452-6.
179. Li, A.C., et al., *Peroxisome proliferator-activated receptor gamma ligands inhibit development of atherosclerosis in LDL receptor-deficient mice.* J Clin Invest, 2000. **106**(4): p. 523-31.
180. Collins, A.R., et al., *Troglitazone inhibits formation of early atherosclerotic lesions in diabetic and nondiabetic low density lipoprotein receptor-deficient mice.* Arterioscler Thromb Vasc Biol, 2001. **21**(3): p. 365-71.
181. Chen, Z., et al., *Troglitazone inhibits atherosclerosis in apolipoprotein E-knockout mice: pleiotropic effects on CD36 expression and HDL.* Arterioscler Thromb Vasc Biol, 2001. **21**(3): p. 372-7.
182. Johnson, G.L. and R. Lapadat, *Mitogen-activated protein kinase pathways mediated by ERK, JNK, and p38 protein kinases.* Science, 2002. **298**(5600): p. 1911-2.
183. Lee, J.D., R.J. Ulevitch, and J. Han, *Primary structure of BMK1: a new mammalian map kinase.* Biochem Biophys Res Commun, 1995. **213**(2): p. 715-24.
184. Zhou, G., Z.Q. Bao, and J.E. Dixon, *Components of a new human protein kinase signal transduction pathway.* J Biol Chem, 1995. **270**(21): p. 12665-9.
185. Abe, M.K., et al., *ERK8, a new member of the mitogen-activated protein kinase family.* J Biol Chem, 2002. **277**(19): p. 16733-43.
186. Boulton, T.G., et al., *ERKs: a family of protein-serine/threonine kinases that are activated and tyrosine phosphorylated in response to insulin and NGF.* Cell, 1991. **65**(4): p. 663-75.
187. Seger, R. and E.G. Krebs, *The MAPK signaling cascade.* FASEB J, 1995. **9**(9): p. 726-35.
188. Uhlik, M.T., et al., *Wiring diagrams of MAPK regulation by MEKK1, 2, and 3.* Biochem Cell Biol, 2004. **82**(6): p. 658-63.
189. Downward, J., *Targeting RAS signalling pathways in cancer therapy.* Nat Rev Cancer, 2003. **3**(1): p. 11-22.
190. Fong, C.W., et al., *Sprouty 2, an inhibitor of mitogen-activated protein kinase signaling, is down-regulated in hepatocellular carcinoma.* Cancer Res, 2006. **66**(4): p. 2048-58.
191. Miyoshi, K., et al., *The Sprouty-related protein, Spred, inhibits cell motility, metastasis, and Rho-mediated actin reorganization.* Oncogene, 2004. **23**(33): p. 5567-76.
192. Tsujita, E., et al., *Suppressed MKP-1 is an independent predictor of outcome in patients with hepatocellular carcinoma.* Oncology, 2005. **69**(4): p. 342-7.
193. Kennedy, N.J. and R.J. Davis, *Role of JNK in tumor development.* Cell Cycle, 2003. **2**(3): p. 199-201.

194. Smeal, T., et al., *Oncogenic and transcriptional cooperation with Ha-Ras requires phosphorylation of c-Jun on serines 63 and 73.* Nature, 1991. **354**(6353): p. 494-6.
195. Schreiber, M., et al., *Control of cell cycle progression by c-Jun is p53 dependent.* Genes Dev, 1999. **13**(5): p. 607-19.
196. Eferl, R., et al., *Liver tumor development. c-Jun antagonizes the proapoptotic activity of p53.* Cell, 2003. **112**(2): p. 181-92.
197. Iyoda, K., et al., *Involvement of the p38 mitogen-activated protein kinase cascade in hepatocellular carcinoma.* Cancer, 2003. **97**(12): p. 3017-26.
198. Lavoie, J.N., et al., *Cyclin D1 expression is regulated positively by the p42/p44MAPK and negatively by the p38/HOGMAPK pathway.* J Biol Chem, 1996. **271**(34): p. 20608-16.
199. Rousseau, D., et al., *Translation initiation of ornithine decarboxylase and nucleocytoplasmic transport of cyclin D1 mRNA are increased in cells overexpressing eukaryotic initiation factor 4E.* Proc Natl Acad Sci U S A, 1996. **93**(3): p. 1065-70.
200. Pelengaris, S., M. Khan, and G. Evan, *c-MYC: more than just a matter of life and death.* Nat Rev Cancer, 2002. **2**(10): p. 764-76.
201. Bouchard, C., et al., *Direct induction of cyclin D2 by Myc contributes to cell cycle progression and sequestration of p27.* EMBO J, 1999. **18**(19): p. 5321-33.
202. Coller, H.A., et al., *Expression analysis with oligonucleotide microarrays reveals that MYC regulates genes involved in growth, cell cycle, signaling, and adhesion.* Proc Natl Acad Sci U S A, 2000. **97**(7): p. 3260-5.
203. Adhikary, S. and M. Eilers, *Transcriptional regulation and transformation by Myc proteins.* Nat Rev Mol Cell Biol, 2005. **6**(8): p. 635-45.
204. Sears, R., et al., *Multiple Ras-dependent phosphorylation pathways regulate Myc protein stability.* Genes Dev, 2000. **14**(19): p. 2501-14.
205. Lutterbach, B. and S.R. Hann, *Hierarchical phosphorylation at N-terminal transformation-sensitive sites in c-Myc protein is regulated by mitogens and in mitosis.* Mol Cell Biol, 1994. **14**(8): p. 5510-22.
206. Yeh, E., et al., *A signalling pathway controlling c-Myc degradation that impacts oncogenic transformation of human cells.* Nat Cell Biol, 2004. **6**(4): p. 308-18.
207. Takenaka, K., T. Moriguchi, and E. Nishida, *Activation of the protein kinase p38 in the spindle assembly checkpoint and mitotic arrest.* Science, 1998. **280**(5363): p. 599-602.
208. Tikoo, K., S.S. Lau, and T.J. Monks, *Histone H3 phosphorylation is coupled to poly-(ADP-ribosylation) during reactive oxygen species-induced cell death in renal proximal tubular epithelial cells.* Mol Pharmacol, 2001. **60**(2): p. 394-402.
209. Chen, M., et al., *Activation of extracellular signal-regulated kinase mediates apoptosis induced by uropathogenic Escherichia coli toxins via nitric oxide synthase: protective role of heme oxygenase-1.* J Infect Dis, 2004. **190**(1): p. 127-35.
210. Matsunaga, Y., et al., *Involvement of activation of NADPH oxidase and extracellular signal-regulated kinase (ERK) in renal cell injury induced by zinc.* J Toxicol Sci, 2005. **30**(2): p. 135-44.

211. Sinha, D., et al., *Inhibition of ligand-independent ERK1/2 activity in kidney proximal tubular cells deprived of soluble survival factors up-regulates Akt and prevents apoptosis.* J Biol Chem, 2004. **279**(12): p. 10962-72.
212. Kanda, H. and M. Miura, *Regulatory roles of JNK in programmed cell death.* J Biochem, 2004. **136**(1): p. 1-6.
213. Fuchs, S.Y., et al., *JNK targets p53 ubiquitination and degradation in nonstressed cells.* Genes Dev, 1998. **12**(17): p. 2658-63.
214. Jijon, H.B., et al., *Serum amyloid A activates NF-kappaB and proinflammatory gene expression in human and murine intestinal epithelial cells.* Eur J Immunol, 2005. **35**(3): p. 718-26.
215. Baranova, I.N., et al., *Serum amyloid A binding to CLA-1 (CD36 and LIMPII analogous-1) mediates serum amyloid A protein-induced activation of ERK1/2 and p38 mitogen-activated protein kinases.* J Biol Chem, 2005. **280**(9): p. 8031-40.
216. Jo, S.H., et al., *Serum amyloid A induces WISH cell apoptosis.* Acta Pharmacol Sin, 2007. **28**(1): p. 73-80.
217. Zhao, Y., S. Zhou, and C.K. Heng, *Impact of serum amyloid A on tissue factor and tissue factor pathway inhibitor expression and activity in endothelial cells.* Arterioscler Thromb Vasc Biol, 2007. **27**(7): p. 1645-50.
218. He, R., et al., *Serum amyloid A is an endogenous ligand that differentially induces IL-12 and IL-23.* J Immunol, 2006. **177**(6): p. 4072-9.
219. Lee, H.Y., et al., *Serum amyloid A induces contrary immune responses via formyl peptide receptor-like 1 in human monocytes.* Mol Pharmacol, 2006. **70**(1): p. 241-8.
220. Koga, T., et al., *Serum amyloid A-induced IL-6 production by rheumatoid synoviocytes.* FEBS Lett, 2008. **582**(5): p. 579-85.
221. Ohashi, N., et al., *Role of p38 mitogen-activated protein kinase in neointimal hyperplasia after vascular injury.* Arterioscler Thromb Vasc Biol, 2000. **20**(12): p. 2521-6.
222. Zhang, G. and S. Ghosh, *Toll-like receptor-mediated NF-kappaB activation: a phylogenetically conserved paradigm in innate immunity.* J Clin Invest, 2001. **107**(1): p. 13-9.
223. O'Neill, L.A. and C.A. Dinarello, *The IL-1 receptor/toll-like receptor superfamily: crucial receptors for inflammation and host defense.* Immunol Today, 2000. **21**(5): p. 206-9.
224. Wallach, D., et al., *Tumor necrosis factor receptor and Fas signaling mechanisms.* Annu Rev Immunol, 1999. **17**: p. 331-67.
225. Girardin, S.E., J.P. Hugot, and P.J. Sansonetti, *Lessons from Nod2 studies: towards a link between Crohn's disease and bacterial sensing.* Trends Immunol, 2003. **24**(12): p. 652-8.
226. Feldmann, M. and R.N. Maini, *Anti-TNF alpha therapy of rheumatoid arthritis: what have we learned?* Annu Rev Immunol, 2001. **19**: p. 163-96.
227. Karin, M. and A. Lin, *NF-kappaB at the crossroads of life and death.* Nat Immunol, 2002. **3**(3): p. 221-7.
228. Karin, M., et al., *NF-kappaB in cancer: from innocent bystander to major culprit.* Nat Rev Cancer, 2002. **2**(4): p. 301-10.

229. Farrow, B. and B.M. Evers, *Inflammation and the development of pancreatic cancer.* Surg Oncol, 2002. **10**(4): p. 153-69.
230. Normark, S., et al., *Persistent infection with Helicobacter pylori and the development of gastric cancer.* Adv Cancer Res, 2003. **90**: p. 63-89.
231. Ghosh, S., M.J. May, and E.B. Kopp, *NF-kappa B and Rel proteins: evolutionarily conserved mediators of immune responses.* Annu Rev Immunol, 1998. **16**: p. 225-60.
232. Beinke, S. and S.C. Ley, *Functions of NF-kappaB1 and NF-kappaB2 in immune cell biology.* Biochem J, 2004. **382**(Pt 2): p. 393-409.
233. Lee, H.Y., et al., *Serum amyloid A induces CCL2 production via formyl peptide receptor-like 1-mediated signaling in human monocytes.* J Immunol, 2008. **181**(6): p. 4332-9.
234. Sullivan, C.P., et al., *Secretory phospholipase A2, group IIA is a novel serum amyloid A target gene: activation of smooth muscle cell expression by an interleukin-1 receptor-independent mechanism.* J Biol Chem. **285**(1): p. 565-75.
235. Mullan, R.H., et al., *Acute-phase serum amyloid A stimulation of angiogenesis, leukocyte recruitment, and matrix degradation in rheumatoid arthritis through an NF-kappaB-dependent signal transduction pathway.* Arthritis Rheum, 2006. **54**(1): p. 105-14.
236. Takeda, K., T. Kaisho, and S. Akira, *Toll-like receptors.* Annu Rev Immunol, 2003. **21**: p. 335-76.
237. Gordon, D.J. and B.M. Rifkind, *High-density lipoprotein--the clinical implications of recent studies.* N Engl J Med, 1989. **321**(19): p. 1311-6.
238. Linsel-Nitschke, P. and A.R. Tall, *HDL as a target in the treatment of atherosclerotic cardiovascular disease.* Nat Rev Drug Discov, 2005. **4**(3): p. 193-205.
239. Santamarina-Fojo, S., et al., *Complete genomic sequence of the human ABCA1 gene: analysis of the human and mouse ATP-binding cassette A promoter.* Proc Natl Acad Sci U S A, 2000. **97**(14): p. 7987-92.
240. Bodzioch, M., et al., *The gene encoding ATP-binding cassette transporter 1 is mutated in Tangier disease.* Nat Genet, 1999. **22**(4): p. 347-51.
241. Brooks-Wilson, A., et al., *Mutations in ABC1 in Tangier disease and familial high-density lipoprotein deficiency.* Nat Genet, 1999. **22**(4): p. 336-45.
242. Rust, S., et al., *Tangier disease is caused by mutations in the gene encoding ATP-binding cassette transporter 1.* Nat Genet, 1999. **22**(4): p. 352-5.
243. Costet, P., et al., *Sterol-dependent transactivation of the ABC1 promoter by the liver X receptor/retinoid X receptor.* J Biol Chem, 2000. **275**(36): p. 28240-5.
244. Sparrow, C.P., et al., *A potent synthetic LXR agonist is more effective than cholesterol loading at inducing ABCA1 mRNA and stimulating cholesterol efflux.* J Biol Chem, 2002. **277**(12): p. 10021-7.
245. Ide, T., et al., *Cross-talk between peroxisome proliferator-activated receptor (PPAR) alpha and liver X receptor (LXR) in nutritional regulation of fatty acid metabolism. II. LXRs suppress lipid degradation gene promoters through inhibition of PPAR signaling.* Mol Endocrinol, 2003. **17**(7): p. 1255-67.
246. Yoshikawa, T., et al., *Cross-talk between peroxisome proliferator-activated receptor (PPAR) alpha and liver X receptor (LXR) in nutritional regulation of*

fatty acid metabolism. I. PPARs suppress sterol regulatory element binding protein-1c promoter through inhibition of LXR signaling. Mol Endocrinol, 2003. **17**(7): p. 1240-54.
247. Vaisman, B.L., et al., *ABCA1 overexpression leads to hyperalphalipoproteinemia and increased biliary cholesterol excretion in transgenic mice.* J Clin Invest, 2001. **108**(2): p. 303-9.
248. Singaraja, R.R., et al., *Increased ABCA1 activity protects against atherosclerosis.* J Clin Invest, 2002. **110**(1): p. 35-42.
249. Timmins, J.M., et al., *Targeted inactivation of hepatic Abca1 causes profound hypoalphalipoproteinemia and kidney hypercatabolism of apoA-I.* J Clin Invest, 2005. **115**(5): p. 1333-42.
250. Haghpassand, M., et al., *Monocyte/macrophage expression of ABCA1 has minimal contribution to plasma HDL levels.* J Clin Invest, 2001. **108**(9): p. 1315-20.
251. Aiello, R.J., et al., *Increased atherosclerosis in hyperlipidemic mice with inactivation of ABCA1 in macrophages.* Arterioscler Thromb Vasc Biol, 2002. **22**(4): p. 630-7.
252. van Eck, M., et al., *Leukocyte ABCA1 controls susceptibility to atherosclerosis and macrophage recruitment into tissues.* Proc Natl Acad Sci U S A, 2002. **99**(9): p. 6298-303.
253. Kennedy, M.A., et al., *Characterization of the human ABCG1 gene: liver X receptor activates an internal promoter that produces a novel transcript encoding an alternative form of the protein.* J Biol Chem, 2001. **276**(42): p. 39438-47.
254. Nakamura, K., et al., *Expression and regulation of multiple murine ATP-binding cassette transporter G1 mRNAs/isoforms that stimulate cellular cholesterol efflux to high density lipoprotein.* J Biol Chem, 2004. **279**(44): p. 45980-9.
255. Wang, N., et al., *ATP-binding cassette transporters G1 and G4 mediate cellular cholesterol efflux to high-density lipoproteins.* Proc Natl Acad Sci U S A, 2004. **101**(26): p. 9774-9.
256. Vaughan, A.M. and J.F. Oram, *ABCG1 redistributes cell cholesterol to domains removable by high density lipoprotein but not by lipid-depleted apolipoproteins.* J Biol Chem, 2005. **280**(34): p. 30150-7.
257. Kliewer, S.A., et al., *Fatty acids and eicosanoids regulate gene expression through direct interactions with peroxisome proliferator-activated receptors alpha and gamma.* Proc Natl Acad Sci U S A, 1997. **94**(9): p. 4318-23.
258. Yang, M.S., et al., *Interleukin-13 enhances cyclooxygenase-2 expression in activated rat brain microglia: implications for death of activated microglia.* J Immunol, 2006. **177**(2): p. 1323-9.
259. Taketa, K., et al., *Oxidized low density lipoprotein activates peroxisome proliferator-activated receptor-alpha (PPARalpha) and PPARgamma through MAPK-dependent COX-2 expression in macrophages.* J Biol Chem, 2008. **283**(15): p. 9852-62.
260. Hwang, D., et al., *Expression of mitogen-inducible cyclooxygenase induced by lipopolysaccharide: mediation through both mitogen-activated protein kinase and NF-kappaB signaling pathways in macrophages.* Biochem Pharmacol, 1997. **54**(1): p. 87-96.

261. Newton, R., et al., *Superinduction of COX-2 mRNA by cycloheximide and interleukin-1beta involves increased transcription and correlates with increased NF-kappaB and JNK activation.* FEBS Lett, 1997. **418**(1-2): p. 135-8.
262. Guan, Z., et al., *Induction of cyclooxygenase-2 by the activated MEKK1 --> SEK1/MKK4 --> p38 mitogen-activated protein kinase pathway.* J Biol Chem, 1998. **273**(21): p. 12901-8.
263. Rothwarf, D.M. and M. Karin, *The NF-kappa B activation pathway: a paradigm in information transfer from membrane to nucleus.* Sci STKE, 1999. **1999**(5): p. RE1.
264. Bonizzi, G. and M. Karin, *The two NF-kappaB activation pathways and their role in innate and adaptive immunity.* Trends Immunol, 2004. **25**(6): p. 280-8.
265. Li, H., et al., *SAA Activates Peroxisome Proliferator-Activated Receptor gamma Through Extracellular-Regulated Kinase 1/2 and COX-2 Expression in Hepatocytes.* Biochemistry.
266. Kosaka, T., et al., *Characterization of the human gene (PTGS2) encoding prostaglandin-endoperoxide synthase 2.* Eur J Biochem, 1994. **221**(3): p. 889-97.
267. D'Acquisto, F., et al., *Involvement of NF-kappaB in the regulation of cyclooxygenase-2 protein expression in LPS-stimulated J774 macrophages.* FEBS Lett, 1997. **418**(1-2): p. 175-8.
268. Kojima, M., et al., *Lipopolysaccharide increases cyclo-oxygenase-2 expression in a colon carcinoma cell line through nuclear factor-kappa B activation.* Oncogene, 2000. **19**(9): p. 1225-31.
269. Klein, C., et al., *Identification of surrogate agonists for the human FPRL-1 receptor by autocrine selection in yeast.* Nat Biotechnol, 1998. **16**(13): p. 1334-7.
270. Baek, S.H., et al., *Identification of the peptides that stimulate the phosphoinositide hydrolysis in lymphocyte cell lines from peptide libraries.* J Biol Chem, 1996. **271**(14): p. 8170-5.
271. Bae, Y.S., et al., *Identification of novel chemoattractant peptides for human leukocytes.* Blood, 2001. **97**(9): p. 2854-62.
272. Deng, X., et al., *A synthetic peptide derived from human immunodeficiency virus type 1 gp120 downregulates the expression and function of chemokine receptors CCR5 and CXCR4 in monocytes by activating the 7-transmembrane G-protein-coupled receptor FPRL1/LXA4R.* Blood, 1999. **94**(4): p. 1165-73.
273. Bae, Y.S., et al., *Identification of peptides that antagonize formyl peptide receptor-like 1-mediated signaling.* J Immunol, 2004. **173**(1): p. 607-14.
274. Lee, G., et al., *T0070907, a selective ligand for peroxisome proliferator-activated receptor gamma, functions as an antagonist of biochemical and cellular activities.* J Biol Chem, 2002. **277**(22): p. 19649-57.
275. Chen, C.H., et al., *Serum amyloid A protein regulates the expression of porcine genes related to lipid metabolism.* J Nutr, 2008. **138**(4): p. 674-9.
276. Han, C.Y., et al., *Adipocyte-derived serum amyloid A3 and hyaluronan play a role in monocyte recruitment and adhesion.* Diabetes, 2007. **56**(9): p. 2260-73.
277. Kennedy, M.A., et al., *ABCG1 has a critical role in mediating cholesterol efflux to HDL and preventing cellular lipid accumulation.* Cell Metab, 2005. **1**(2): p. 121-31.

278. Gelissen, I.C., et al., *ABCA1 and ABCG1 synergize to mediate cholesterol export to apoA-I.* Arterioscler Thromb Vasc Biol, 2006. **26**(3): p. 534-40.
279. Cabana, V.G., et al., *Influence of apoA-I and apoE on the formation of serum amyloid A-containing lipoproteins in vivo and in vitro.* J Lipid Res, 2004. **45**(2): p. 317-25.
280. Morrow, J.F., et al., *Induction of hepatic synthesis of serum amyloid A protein and actin.* Proc Natl Acad Sci U S A, 1981. **78**(8): p. 4718-22.
281. Khovidhunkit, W., et al., *Effects of infection and inflammation on lipid and lipoprotein metabolism: mechanisms and consequences to the host.* J Lipid Res, 2004. **45**(7): p. 1169-96.
282. Hoffman, J.S. and E.P. Benditt, *Plasma clearance kinetics of the amyloid-related high density lipoprotein apoprotein, serum amyloid protein (apoSAA), in the mouse. Evidence for rapid apoSAA clearance.* J Clin Invest, 1983. **71**(4): p. 926-34.
283. Fielding, C.J. and P.E. Fielding, *Molecular physiology of reverse cholesterol transport.* J Lipid Res, 1995. **36**(2): p. 211-28.
284. Wellington, C.L., et al., *Alterations of plasma lipids in mice via adenoviral-mediated hepatic overexpression of human ABCA1.* J Lipid Res, 2003. **44**(8): p. 1470-80.
285. Farooqui, A.A., L.A. Horrocks, and T. Farooqui, *Modulation of inflammation in brain: a matter of fat.* J Neurochem, 2007. **101**(3): p. 577-99.
286. Bosetti, F., R. Langenbach, and G.R. Weerasinghe, *Prostaglandin E2 and microsomal prostaglandin E synthase-2 expression are decreased in the cyclooxygenase-2-deficient mouse brain despite compensatory induction of cyclooxygenase-1 and Ca2+-dependent phospholipase A2.* J Neurochem, 2004. **91**(6): p. 1389-97.
287. Murakami, M. and I. Kudo, *Recent advances in molecular biology and physiology of the prostaglandin E2-biosynthetic pathway.* Prog Lipid Res, 2004. **43**(1): p. 3-35.
288. Choi, S.H., R. Langenbach, and F. Bosetti, *Cyclooxygenase-1 and -2 enzymes differentially regulate the brain upstream NF-kappa B pathway and downstream enzymes involved in prostaglandin biosynthesis.* J Neurochem, 2006. **98**(3): p. 801-11.
289. Phillis, J.W., L.A. Horrocks, and A.A. Farooqui, *Cyclooxygenases, lipoxygenases, and epoxygenases in CNS: their role and involvement in neurological disorders.* Brain Res Rev, 2006. **52**(2): p. 201-43.
290. Fitzpatrick, F.A. and M.A. Wynalda, *Albumin-catalyzed metabolism of prostaglandin D2. Identification of products formed in vitro.* J Biol Chem, 1983. **258**(19): p. 11713-8.
291. Burleigh, M.E., et al., *Cyclooxygenase-2 promotes early atherosclerotic lesion formation in LDL receptor-deficient mice.* Circulation, 2002. **105**(15): p. 1816-23.
292. Fitzgerald, G.A., *Coxibs and cardiovascular disease.* N Engl J Med, 2004. **351**(17): p. 1709-11.
293. Furberg, C.D., B.M. Psaty, and G.A. FitzGerald, *Parecoxib, valdecoxib, and cardiovascular risk.* Circulation, 2005. **111**(3): p. 249.

294. Wang, D., et al., *Cardiovascular hazard and non-steroidal anti-inflammatory drugs.* Curr Opin Pharmacol, 2005. **5**(2): p. 204-10.
295. Yano, M., et al., *Statins activate peroxisome proliferator-activated receptor gamma through extracellular signal-regulated kinase 1/2 and p38 mitogen-activated protein kinase-dependent cyclooxygenase-2 expression in macrophages.* Circ Res, 2007. **100**(10): p. 1442-51.
296. Beg, A.A., *Endogenous ligands of Toll-like receptors: implications for regulating inflammatory and immune responses.* Trends Immunol, 2002. **23**(11): p. 509-12.
297. Lotze, M.T. and K.J. Tracey, *High-mobility group box 1 protein (HMGB1): nuclear weapon in the immune arsenal.* Nat Rev Immunol, 2005. **5**(4): p. 331-42.
298. Matzinger, P., *Friendly and dangerous signals: is the tissue in control?* Nat Immunol, 2007. **8**(1): p. 11-3.
299. Seong, S.Y. and P. Matzinger, *Hydrophobicity: an ancient damage-associated molecular pattern that initiates innate immune responses.* Nat Rev Immunol, 2004. **4**(6): p. 469-78.
300. Wang, L. and W. Colon, *The interaction between apolipoprotein serum amyloid A and high-density lipoprotein.* Biochem Biophys Res Commun, 2004. **317**(1): p. 157-61.
301. He, R., H. Sang, and R.D. Ye, *Serum amyloid A induces IL-8 secretion through a G protein-coupled receptor, FPRL1/LXA4R.* Blood, 2003. **101**(4): p. 1572-81.
302. Bae, Y.S., et al., *Differential activation of formyl peptide receptor-like 1 by peptide ligands.* J Immunol, 2003. **171**(12): p. 6807-13.
303. Bae, Y.S., et al., *Differential signaling of formyl peptide receptor-like 1 by Trp-Lys-Tyr-Met-Val-Met-CONH2 or lipoxin A4 in human neutrophils.* Mol Pharmacol, 2003. **64**(3): p. 721-30.
304. Husebekk, A., B. Skogen, and G. Husby, *Characterization of amyloid proteins AA and SAA as apolipoproteins of high density lipoprotein (HDL). Displacement of SAA from the HDL-SAA complex by apo AI and apo AII.* Scand J Immunol, 1987. **25**(4): p. 375-81.
305. Sipe, J.D., et al., *Human serum amyloid A (SAA): biosynthesis and postsynthetic processing of preSAA and structural variants defined by complementary DNA.* Biochemistry, 1985. **24**(12): p. 2931-6.
306. Wu, K.K., J.Y. Liou, and K. Cieslik, *Transcriptional Control of COX-2 via C/EBPbeta.* Arterioscler Thromb Vasc Biol, 2005. **25**(4): p. 679-85.
307. Karin, M., *The regulation of AP-1 activity by mitogen-activated protein kinases.* J Biol Chem, 1995. **270**(28): p. 16483-6.
308. Hu, J., et al., *ERK1 and ERK2 activate CCAAAT/enhancer-binding protein-beta-dependent gene transcription in response to interferon-gamma.* J Biol Chem, 2001. **276**(1): p. 287-97.